The Pennsylvania State University

The Graduate School

Department of Mathematics

ROBUST PRECONDITIONERS FOR $H(\mathbf{grad})$, $\mathbf{H}(\mathbf{curl})$ AND $\mathbf{H}(\mathrm{div})$ SYSTEMS WITH STRONGLY DISCONTINUOUS COEFFICIENTS

A Dissertation in

Mathematics

by

Yunrong Zhu

Submitted in Partial Fulfillment
of the Requirements
for the Degree of

Doctor of Philosophy

August 2008

The thesis of Yunrong Zhu was reviewed and approved* by the following:

Jinchao Xu
Distinguished Professor of Mathematics
Thesis Adviser
Chair of Committee

Victor Nistor
Professor of Mathematics

Francesco Costanzo
Associate Professor of Engineering Science and Mechanics

Ludmil Zikatanov
Associate Professor of Mathematics

Anna Mazzucato
Assistant Professor of Mathematics

John Roe
Professor of Mathematics
Head of Department of Mathematics

*Signatures are on file in the Graduate School.

Abstract

This dissertation is devoted to practical design and theoretical analysis of efficient and robust preconditioners for solving algebraic systems arising from the approximation of partial differential equations, with special emphasis on the problems with strongly discontinuous coefficients. The problems considered here include the standard second order elliptic equations ($H(\mathbf{grad})$ or H^1 equations), as well as the second order elliptic systems given in terms of curl and divergence operators ($\mathbf{H}(\mathbf{curl})$ and $\mathbf{H}(\mathrm{div})$ systems).

In regard to the H^1 equations with jump coefficients, we study both the multilevel and domain decomposition preconditioners. We analyze the eigenvalue distribution of the preconditioned systems, and prove that only a small number of eigenvalues may deteriorate with respect to coefficients and mesh size. We show that the other eigenvalues are bounded uniformly with respect to the coefficients of the PDE and bounded poly-logarithmically with respect to mesh size. As a result, the asymptotic convergence rate of the PCG algorithms is uniform with respect to the coefficients, and nearly uniform (up to a logarithmic factor) with respect to the mesh size. Various numerical experiments justify the theoretical results.

For $\mathbf{H}(\mathbf{curl})$ and $\mathbf{H}(\mathrm{div})$ systems, we give a comprehensive analysis of auxiliary space preconditioners, which rely on regular decompositions. Through such constructions, these preconditioners reduce $\mathbf{H}(\mathbf{curl})$ and $\mathbf{H}(\mathrm{div})$ systems to the solution of several $H(\mathbf{grad})$ equations, which are amenable by standard algebraic multigrid (AMG)

techniques. We also develop a preconditioner for $\mathbf{H}(\mathbf{curl})$ systems with jump coefficients. We show that the condition number of the preconditioned system is uniformly bounded with respect to coefficients and mesh size. Another class of preconditioners that we propose are the compatible AMG preconditioners for $\mathbf{H}(\mathbf{curl})$ and $\mathbf{H}(\mathrm{div})$ systems. This approach makes use of a compatible discretization framework. We reformulate the discrete systems into equivalent 2-by-2 block systems based on discrete Hodge decompositions on co-chains, and then construct the AMG preconditioners for the 2-by-2 block systems. As an important application, we present the augmented Lagrangian method for solving mixed formulations of elliptic boundary value problems, which reduces a saddle point problem to a nearly singular $\mathbf{H}(\mathrm{div})$ system.

Table of Contents

List of Tables

List of Figures

Acknowledgments

First and foremost, I am most grateful and indebted to my dissertation advisor, Professor Jinchao Xu, for his invaluable guidance, encouragement, and support. It was his guidance and deep insights that made this thesis a reality. I am also grateful to Professor Ludmil Zikatanov, for inspiration and enlightening discussions on a wide variety of topics, especially on the developing the codes.

I am also grateful to Sandia National Labs for supporting my internship in the summer 2006. Especially, I would like to thank Dr. Ray Tuminaro for providing this opportunity, as well as the helpful discussions during my visit at Sandia National Labs. Thanks also goes to Dr. Pavel Bochev and Dr. Chris Siefert for inspiration discussions.

I thank my other committee members, Professors Victor Nistor, Anna Mazzucato and Francesco Costanzo, for their kindness to serve as my committee and insightful comments on my work.

Last but not least, I would like to thank my dear wife, Qingqin. Without her support, this work would not have been possible. This work is dedicated to her.

Chapter 1

Introduction

1.1 Foreword

Multilevel and domain decomposition methods are primarily developed for solving algebraic systems arising from the discretizations of partial differential equations. By effectively using the underlying multilevel structure of the discretizations, these algorithms are proven to be among the most efficient methods for solving the resulting large scale algebraic systems.

For elliptic equations with smooth coefficients, multilevel and domain decomposition methods have been well studied in the literature (see the monographs [56, 22, 104] and the surveys [119, 38, 126]). How these methods behave for elliptic equations with strongly discontinuous coefficients, however, has remained an open problem. One of the main contributions of this dissertation is to answer this question by proving the *robustness* of the preconditioned conjugate gradient (PCG) algorithms with the multilevel and domain decomposition methods as preconditioners. By "robust", we mean that the resulting condition number of the preconditioned system is not only independent on the coefficients of the equation, but also independent, or only weakly dependent, on the underlying mesh size. This leads to a (nearly) uniformly convergent PCG algorithm.

Studying efficient solvers for second order elliptic boundary value problems is not only fundamentally important for its own sake, but it is also important in the design

of efficient solvers for the elliptic systems involving curl and divergence operators. Applications of the robust preconditioners for $\mathbf{H}(\mathrm{div})$ systems arise naturally in solving the mixed formulations and the first order least-squares formulations of second order elliptic equations (cf. [4, 116]). Applications of efficient and robust preconditioners for $\mathbf{H}(\mathbf{curl})$ systems arise in various contexts in electromagnetism; for example, in the time-discretizations of Maxwell's equations (cf. [63, 85]). Such solvers also have applications for some formulations of the Navier-Stokes equations, as discussed in [53].

Another goal of this dissertation is to design efficient algebraic solvers for elliptic systems involving curl and divergence operators. We refer to these systems as $\mathbf{H}(\mathbf{curl})$ and $\mathbf{H}(\mathrm{div})$ systems respectively. Research on multilevel methods for the $\mathbf{H}(\mathbf{curl})$ and $\mathbf{H}(\mathrm{div})$ systems has been very active in recent years (see [60, 4, 61, 62, 116, 5, 67, 68, 69]; see also [11, 96, 13, 16] for other related works). The principal challenge in designing an efficient solver for finite element discretization of the $\mathbf{H}(\mathbf{curl})$ and $\mathbf{H}(\mathrm{div})$ systems is the presence of kernels of large dimensions in the discrete problems. The guideline of construction of efficient solvers is to convert discrete $\mathbf{H}(\mathbf{curl})$ and $\mathbf{H}(\mathrm{div})$ systems into discrete H^1 systems in certain ways such that some standard preconditioners or AMG techniques can be applied. Our results also hold for problems with strongly discontinuous coefficients.

1.2 Overview

1.2.1 Robust Preconditioners for $H(\mathbf{grad})$ Equations with Discontinuous Coefficients

Second order elliptic equations with discontinuous coefficients are relevant to many applications, such as groundwater flow (cf. [1, 74]), fluid pressure prediction (cf. [110]), electromagnetics (cf. [58]), semiconductor modeling (cf. [42, 84, 73, 82]), electrical power network (cf. [70]), and fuel cell modeling (cf. [114, 111]), where the coefficients have large discontinuities across interfaces between regions with different material properties.

In our work, we assume that the physical domain Ω contains M fixed subdomains Ω_m, $m = 1, \cdots, M$. We assume that, without loss of generality, the coefficients $\omega_m > 0$ are constant but may have large variations across the interfaces. More precise assumptions are given in Chapter 2.

It is well known that the conditioning of finite element discretization will depend on both the coefficients and also the mesh size (see [126]). There has been a lot of interest in the development of iterative methods, such as domain decomposition and multigrid methods, whose convergence rates are robust with respect to the variations of the size of coefficients and that of meshes (see [24, 100, 47, 83, 126, 37] and the references cited therein). In two dimensions it is not difficult to see that both domain decomposition (cf. [23, 113, 89, 40]) and multigrid (cf. [25, 119, 126]) methods lead to robust iterative methods. In three dimensions, some non-overlapping domain decomposition methods have been shown to be robust with respect to the size of both the coefficients and the

meshes (see [80, 113, 83, 101, 126]). As was pointed out in [120, Remark 6.3], the deterioration is not significantly severe in certain cases. In fact, if the interface has no cross points, or if every subdomain touches part of the Dirichlet boundary (so called "exceptional" or "edge-type" in [93, 112]), or if the coefficients satisfy the quasi-monotonicity (cf. [46, 45]), then using the estimates related to weighted L^2-inner products in [27], it can be proved that $\kappa(BA) \leq C|\log h|^2$ in these cases when $d = 3$. In general, however, the condition number of overlapping domain decomposition methods or multilevel methods preconditioned systems depends not only on the mesh size but also on the variation of the coefficients. In particular, when $d = 3$, for the multigrid V-cycle, the best we can do is to bound the convergence rate by $1 - \frac{c}{\omega(h)}$ and bound the condition number by $\kappa(BA) \leq C\omega(h)$, where $\omega(h) = \min\left\{\frac{\max_m \omega_m}{\min_m \omega_m}, \frac{1}{h}\right\}$ (see [117, 128, 126]). Numerical experiments in Section 2.4 show that this convergence rate is sharp. For the BPX preconditioner, a similar condition number estimate was obtained by Oswald [93], and the sharpness was shown rigorously. Technically, the difficulty is due to the lack of uniform or nearly uniform error and stability estimates for weighted L^2-projection, as demonstrated in [118, 93].

Although the resulting condition numbers can deteriorate, as mentioned above, we will show that both the multilevel and domain decomposition preconditioners will lead to nearly uniformly convergent PCG methods. Our work is related to the work of Graham and Hagger [55]. In their work, they proved that a simple diagonal scaling would lead to a preconditioned system that only has a finite number of small eigenvalues, which are severely infected by the discontinuous jumps. More precisely, they proved that the ratio of the extreme values of the remaining eigenvalues, known as *effective condition number*,

can be bounded by Ch^{-2}, where C is a constant independent of jumps in coefficients and mesh size.

The goal of Chapter 2 is to improve the effective condition number bound from Ch^{-2} for diagonal scaling to $C|\log h|^2$ for multilevel and domain decomposition preconditioners. To this end, the first key step is an analytic proof that we are able to obtain for the aforementioned result in [55] that was originally proved by a purely algebraic approach. Using this new technique and various other estimates in [27, 125], we analyze the eigenvalue distribution of the preconditioned systems and prove that, except for a few "bad" eigenvalues, the effective condition number is bounded uniformly with respect to the coefficients and poly-logarithmically with respect to the mesh size. Thanks to a standard theory for PCG methods (see [57, 55, 10, 123]), these small eigenvalues will not have significant impact on the convergence rate. More precisely, the convergence rate of the PCG methods can be bounded by $1 - \frac{2}{C|\log h|+1}$, where C is a generic constant independent of the discontinuous coefficients and mesh size.

1.2.2 HX-Preconditioner for H(curl) and H(div) Systems

It is well known that the standard point smoothers for the H^1-equations (see Chapter 2) do not yield effective multilevel iterations when applied to the finite element discretizations of $\mathbf{H}(\mathbf{curl})$ and $\mathbf{H}(\mathrm{div})$ systems (see [34, 61, 63, 131]). The reason is that the kernel of **curl** (or div) contains all vector fields in the range of **grad** (or **curl**). Special smoothers and relevant convergence results of the multilevel methods have been discussed in many works (see for example [48, 109, 49, 4, 61, 63, 6]). Most of these aforementioned works made use of the Helmholtz decomposition of an arbitrary vector field

into irrotational and solenoidal components, and its discrete versions. The irrotational component is, in general, not $\mathbf{H}^1$-regular; for example, when the underlying domain Ω is not convex, many estimates fail in this case (see [66]).

Recently, Hiptmair and Xu [68] proposed an innovative approach to solve $\mathbf{H}(\mathbf{curl})$ and $\mathbf{H}(\mathrm{div})$ systems, known as HX preconditioners. One of the main theoretical tools of this approach is *regular decomposition*. In this work, we give a detailed discussion of the regular decomposition for vector fields in the Hilbert spaces $\mathbf{H}(\mathbf{curl})$ ([12, 44, 94]) and $\mathbf{H}(\mathrm{div})$ ([64, 36]). These results were built on the spaces with pure Dirichlet or pure Neumann boundary conditions. However, in some practical applications, the problems may have more general boundary conditions, for example mixed boundary conditions. We prove the regular decompositions for the $\mathbf{H}(\mathbf{curl})$ systems with several general boundary conditions. These results are of fundamental importance and are of significant use in many applications, such as the analysis of multigrid and domain decomposition methods (cf.[66, 94, 65]), the convergence analysis of the adaptive algorithms (cf. [36, 39]), and the construction of preconditioners for $\mathbf{H}(\mathbf{curl})$ and $\mathbf{H}(\mathrm{div})$ systems (cf. [68]).

The regular decompositions link the vector fields in $\mathbf{H}(\mathbf{curl})$ and $\mathbf{H}(\mathrm{div})$ and their norms directly with functions in $H(\mathbf{grad})$ and the relevant H^1 norm. Specifically, given a vector field $\mathbf{v}$ in $\mathbf{H}(D)$ with $D = \mathbf{curl}$ or div, the regular decomposition asserts that $\mathbf{v}$ can be decomposed in a stable fashion as a vector field in $\mathbf{H}(\mathbf{grad})$ plus a function in the kernel of D. Therefore, on the complement of the kernel of D, we can treat it as a (vector) $\mathbf{H}(\mathbf{grad})$ system that is amenable to standard preconditioning techniques (see Chapter 2 for an example). However, using a discrete $\mathbf{H}(\mathbf{grad})$ system as preconditioner is not immediately possible because it does not fit the **curl**- and div-conforming finite

element spaces. For this reason, we need the auxiliary space preconditioning technique [121] to link the finite element discretization of $\mathbf{H}(\mathbf{curl})$ and $\mathbf{H}(\mathrm{div})$ systems and the vectorial $\mathbf{H}(\mathbf{grad})$-conforming finite elements. By using this framework, the evaluation of the preconditioner for $\mathbf{H}(\mathbf{curl})$ and $\mathbf{H}(\mathrm{div})$ systems is reduced to several second-order elliptic operators approximately. Hence, the standard robust preconditioners for the $H(\mathbf{grad})$ equations can be applied for the $\mathbf{H}(\mathbf{curl})$ and $\mathbf{H}(\mathrm{div})$ systems. For instance, for the space $\mathbf{H}_0(\mathbf{curl})$ we have the stable splitting

$$\mathbf{H}_0(\mathbf{curl}) := \mathbf{H}_0^1(\Omega) + \mathbf{grad}\, H_0^1(\Omega).$$

This suggests that a preconditioner for the $\mathbf{H}_0(\mathbf{curl})$ system can be based on solving one vector $\mathbf{H}_0^1(\Omega)$ system and one $H_0^1(\Omega)$ equation.

Some other generalizations of the auxiliary space techniques on unstructured grids for $\mathbf{H}(\mathbf{curl})$ problems are discussed in some recent works (see [67, 78]). From another aspect, the compatible AMG preconditioners proposed in [16] are very similar to the HX preconditioners. Namely, both of these two approaches try to reduce the original discrete $\mathbf{H}(\mathbf{curl})$ and $\mathbf{H}(\mathrm{div})$ systems to solving some discrete H^1 linear systems.

1.2.3 Compatible Gauge AMG Approach for $\mathbf{H}(\mathbf{curl})$ and $\mathbf{H}(\mathrm{div})$ Systems

In Chapter 4, we develop some efficient multilevel preconditioners for $\mathbf{H}(\mathbf{curl})$ and $\mathbf{H}(\mathrm{div})$ systems from a different point of view. Motivated by the recent work [16] for $\mathbf{H}(\mathbf{curl})$ systems, we develop multilevel preconditioners for the $\mathbf{H}(\mathrm{div})$ system by using *compatible discretization* framework.

Compatible discretization is a general framework, which unifies the standard finite element, finite difference, or finite volume methods using the techniques from differential geometry. Due to the pioneering work of Bossavit [18], it is well known that the stable and accurate numerical schemes for $\mathbf{H}(\mathbf{curl})$ and $\mathbf{H}(\mathrm{div})$ systems can be achieved by using discrete spaces from a finite-dimensional analog of the differential De Rham complex (see [19, 64, 7, 17] and the references cited therein). Given the triangulation, such discretizations of the problems are constructed in special ways to mimic the abstract structure revealed by differential forms. Numerical methods that are based on such discretizations are referred to as compatible (or mimetic) methods.

To design multilevel preconditioners for $\mathbf{H}(\mathrm{div})$ systems, we first give a compatible finite element discretization for the $\mathbf{H}(\mathrm{div})$ system. Based on this discretization, we propose an algebraic reformulation of the discrete $\mathbf{H}(\mathrm{div})$ system along with a new AMG technique for this reformulated problem. The reformulation process takes advantage of a discrete Hodge decomposition on co-chains to replace the discrete $\mathbf{H}(\mathrm{div})$ system by an equivalent 2×2 block linear system whose diagonal blocks are discrete Hodge Laplace operators acting on 2-cochains and 1-cochains respectively. The new AMG algorithm we will develop makes use of the Hiptmair smoother (see [61] for example) on the fine mesh, uses the canonical interpolations Π_h^{div} and $\Pi_h^{\mathbf{curl}}$ on $\mathbf{H}(\mathrm{div})$ and $\mathbf{H}(\mathbf{curl})$ to construct the grid-transfer operators, and then uses the standard AMG methods for Laplace-type problems on the coarse meshes.

The $\mathbf{H}(\mathrm{div})$ systems arise naturally in the solution of second order elliptic partial differential equations (PDE) by first order least-square methods or by mixed methods with augmented Lagrangians (see [109, 4, 61, 116] and the references cited therein). In

order to show the efficiency and robustness of the $\mathbf{H}(\mathrm{div})$ preconditioner, as an example, we consider the augmented Lagrange method to solve the mixed formulations of second order elliptic equations (cf. [51, 81]). The key step is to solve a nearly singular $\mathbf{H}(\mathrm{div})$ system. Using the $\mathbf{H}(\mathrm{div})$ preconditioner proposed in this work, we can solve this nearly singular system very efficiently. The numerical experiments in Section 4.4 justify the robustness of this preconditioner and the convergence rate of the augmented Lagrange algorithm.

1.3 Outline of This Dissertation

The rest of this work is organized as follows. Chapter 2 discusses robust preconditioners for H^1-systems with strongly discontinuous coefficients. Chapter 3 then examines the auxiliary space preconditioners for $\mathbf{H}(\mathbf{curl})$ and $\mathbf{H}(\mathrm{div})$ systems. Chapter 4 describes the compatible discretization and AMG approaches for the $\mathbf{H}(\mathbf{curl})$ and $\mathbf{H}(\mathrm{div})$ systems. An example of applications of $\mathbf{H}(\mathrm{div})$ solvers to the mixed formulation of second order elliptic equations is discussed there. Finally, we summarize the dissertation by some conclusion remarks and future works in Chapter 5.

Parts of the work reported in this dissertation summarize some joint work with my dissertation advisor Professor Jinchao Xu [124, 130]. Also, part of the work has been done jointly with Dr. Ray Tuminaro during my internship in Sandia national labs [16].

Chapter 2

Robust Preconditioners for H^1 Equations

The focus of this chapter is on the behavior of multilevel and domain decomposition preconditioners for second order elliptic boundary value problems with strongly discontinuous coefficients:

$$\begin{cases} -\nabla \cdot (\omega \nabla u) = f & \text{in } \Omega \\ u = g_D & \text{on } \Gamma_D \\ \omega \frac{\partial u}{\partial n} = g_N & \text{on } \Gamma_N \end{cases} . \tag{2.0.1}$$

Here, $\Omega \subset \mathbb{R}^d$ is a polygonal ($d = 2$) or polyhedral ($d = 3$) domain with Dirichlet boundary Γ_D and Neumann boundary Γ_N. The coefficient $\omega = \omega(x)$ is a positive and piecewise constant function. More precisely, we assume that there are M open disjointed polygonal or polyhedral subdomains Ω_m ($m = 1, \cdots, M$), satisfying $\cup_{m=1}^{M} \overline{\Omega}_m = \overline{\Omega}$ with

$$\omega|_{\Omega_m} = \omega_m, \quad m = 1, \ldots, M$$

where $\omega_m > 0$ is a constant for each m. Our analysis can be easily generalized to the case when $\omega(x)$ varies moderately in each subdomain. Here we assume that the regions $\{\Omega_m : \ m = 1, \cdots, M\}$ are given and fixed but may possibly have complicated geometry.

This chapter is organized as follows. In Section 2.1, we give the basic notation, a short review of the convergence of the PCG algorithm, and an analysis of the eigenvalue distribution of Jacobi/symmetric Gauss-Siedel preconditioners. In Section 2.2, we give a review of the approximation and stability properties of the weighted L^2-projection, which is the theoretical foundation of the multilevel and domain decomposition analysis. In Section 2.3, we discuss the eigenvalue distributions of the multilevel preconditioned systems and the convergence rate of the corresponding PCG algorithms. The numerical justifications of these results are given in Section 2.4. In Section 2.5, we prove the robustness of an overlapping domain decomposition preconditioner. Finally, we discuss some relationships between the operator and algebraic representations of the preconditioners in Section 2.6.

2.1 Preliminaries

In this section, we introduce some basic notation and analyze the convergence rate of PCG methods with Jacobi and symmetric Gauss-Seidel preconditioners. For Jacobi preconditioner, we refer to [55, 110] for similar results. However, our analysis here is of independent interest, and moreover, we also give the behavior of the symmetric Gauss-Seidel preconditioner.

2.1.1 Notation

We introduce the bilinear form

$$a(u,v) = \sum_{m=1}^{M} \omega_m (\nabla u, \nabla v)_{L^2(\Omega_m)}, \quad \forall\, u, v \in H^1_D(\Omega),$$

where $H^1_D(\Omega) = \{v \in H^1(\Omega) : \ v|_{\Gamma_D} = 0\}$; and introduce the H^1 semi-norm and H^1-norm with respect to any subdomain Ω_m by

$$|u|_{1,\Omega_m} = \|\nabla u\|_{0,\Omega_m}, \quad \|u\|_{1,\Omega_m} = \left(\|u\|^2_{0,\Omega_m} + |u|^2_{1,\Omega_m}\right)^{\frac{1}{2}}.$$

We denote $|\cdot|_{1,\omega}$ as the weighted H^1 semi-norm defined by

$$|u|^2_{1,\omega} := a(u,u) = \sum_{m=1}^{M} \omega_m |u|^2_{1,\Omega_m}.$$

We define the weighted L^2-inner product

$$(u,v)_{0,\omega} := \sum_{m=1}^{M} \omega_m (u,v)_{L^2(\Omega_m)}$$

and the weighted L^2- and H^1-norms

$$\|u\|_{0,\omega} := (u,u)^{\frac{1}{2}}_{0,\omega}, \quad \|u\|_{1,\omega} := \left(\|u\|^2_{0,\omega} + |u|^2_{1,\omega}\right)^{\frac{1}{2}}$$

corresponding to ω. For any subset $G \subset \Omega$, we denote $|u|_{1,\omega,G}$ and $\|u\|_{0,\omega,G}$ to be the restrictions of $|u|_{1,\omega}$ and $\|u\|_{0,\omega}$ on the subset G, respectively.

Notation. The letters C and c, with or without subscript, denote generic constants that may not be the same at their different occurrences. To avoid writing these constants repeatedly, following [120], by $x \lesssim y$ we mean that there exists a constant C such that $x \leq Cy$. We also define $x \gtrsim y$ as $y \lesssim x$, and $x \eqsim y$ as $x \lesssim y$ and $x \gtrsim y$.

All constants hidden in this notation do not depend on the interested parameters of the problem, such as the coefficients of the equation, and the mesh size of the triangulation.

2.1.2 The Discrete System

Given a quasi-uniform triangulation $\mathcal{T}_h$, let

$$\mathcal{V}_h = \left\{ v \in \overset{1}{H_D}(\Omega) : v|_\tau \in \mathcal{P}_1(\tau),\ \forall \tau \in \mathcal{T}_h \right\}$$

be the piecewise continuous linear finite element space, where $\mathcal{P}_1$ denotes the set of linear polynomials. The finite element approximation of (2.0.1) is the function $u \in \mathcal{V}_h$, such that

$$a(u, v) = (f, v) + \int_{\Gamma_N} g_N v, \quad \forall v \in \mathcal{V}_h.$$

We define a linear symmetric positive definite (SPD) operator $A : \mathcal{V}_h \to \mathcal{V}_h$ by

$$(Au, v)_{0,\omega} = a(u, v).$$

The related inner product and the induced energy norm are denoted by

$$(\cdot, \cdot)_A = a(\cdot, \cdot), \qquad \| \cdot \|_A = \sqrt{a(\cdot, \cdot)}.$$

Then we have the following operator equation,

$$Au = F, \tag{2.1.1}$$

where $F \in L^2(\Omega)$ such that $(F, v)_{0,\omega} = (f, v) + \int_{\Gamma_N} g_N v, \ \ \forall v \in \mathcal{V}_h$.

The space $\mathcal{V}_h$ has a natural nodal basis $\{\phi_i\}_{i=1}^n$ such that $\phi_i(x_j) = \delta_{ij}$ for each non-Dirichlet boundary node x_j. By means of these nodal basis functions, (2.1.1) can be reduced to the following system of linear algebraic equations

$$\mathcal{A}\mu = b \tag{2.1.2}$$

where $\mathcal{A} = \left(a_{ij}\right)_{n\times n}$ with $a_{ij} = a\left(\phi_j, \phi_i\right) = \int_\Omega \omega \nabla\phi_j \cdot \nabla\phi_i$, is the stiffness matrix; and $b = \left(b_1, \cdots, b_n\right) \in \mathbb{R}^n$ is such that $b_i = \left(f, \phi_i\right) + \int_{\Gamma_N} g_N \phi_i$. We introduce the discrete weighted ℓ^2 inner product as follows: let $\mu, \nu \in \mathbb{R}^n$ be the vector representation of $u, v \in \mathcal{V}_h$ respectively, i.e., $u = \sum_{i=1}^n \mu_i \phi_i$ and $v = \sum_{i=1}^n \nu_i \phi_i$. Define

$$(\mu, \nu)_{\ell^2,\omega} = \sum_{i=1}^n \bar{\omega}_i \mu_i \nu_i,$$

where $\bar{\omega}_j = \int_{o_j} \omega / \left|o_j\right|$ is the average of the coefficient ω on $o_j = \text{supp}\left(\phi_j\right)$. By definition and quasi-uniformity of the mesh, we have the following result.

Lemma 2.1.1. *Let $u = \sum_{i=1}^n \mu_i \phi_i \in \mathcal{V}_h$. Then the weighted L^2 norm and the discrete weighted ℓ^2 norm satisfy*

$$h^d (\mu, \mu)_{\ell^2,\omega} \eqsim \|u\|_{0,\omega}^2.$$

Proof. Since $u \in \mathcal{V}_h$ is a piecewise linear function, by numerical quadrature and quasi-uniformity it is obvious that

$$\int_\Omega \omega(x) u^2 dx \lesssim h^d \sum_{i=1}^n \bar{\omega}_i \mu_i^2.$$

On the other hand, noticing that $\bar{\omega}_i$ is the average of ω over the macro-element associated with the node x_i, there exists a $\tau_i \in \mathcal{T}_h$ such that $x_i \in \tau_i$ and $\omega|_{\tau_i} \geq \omega|_\tau$ for any $\tau \in \mathcal{T}_h$ containing x_i. By inverse inequality,

$$h^d \bar{\omega}_i \mu_i^2 \leq h^d \omega|_{\tau_i} \|u\|^2_{\infty,\tau_i} \lesssim \int_{\tau_i} \omega(x) u^2 dx \leq \int_{o_i} \omega(x) u^2 dx.$$

Summing the above inequality over all the nodes yields the inequality

$$h^d \sum_{i=1}^n \bar{\omega}_i \mu_i^2 \lesssim \int_\Omega \omega(x) u^2 dx.$$

This completes the proof. □

Let $\kappa(A)$ be the condition number of A, i.e., the ratio between the largest and the smallest eigenvalues. According to [126], it is known that

$$\kappa(A) = \kappa(\mathcal{A}) \eqsim h^{-2} \mathcal{J}(\omega), \quad \text{with } \mathcal{J}(\omega) = \frac{\max_m \omega_m}{\min_m \omega_m}.$$

In other words, the condition number of A is large when $\mathcal{J}(\omega)$ is large or the mesh size h is small. Therefore, we need to introduce preconditioning techniques.

2.1.3 Preconditioned Conjugate Gradient (PCG) Methods

Conjugate gradient method is the basis of many of the solution techniques to be studied in this work. PCG method can be viewed as a conjugate gradient method applied to the preconditioned system

$$BAu = Bf.$$

Here, B is an SPD operator, known as a preconditioner of A. Note that BA is SPD with respect to the inner product $(\cdot,\cdot)_{B^{-1}}$ (or $(\cdot,\cdot)_A$). For the implementation of PCG algorithm, see [75, 97] for example.

Let $u_k,\ k = 0, 1, 2, \cdots$, be the solution sequence of PCG algorithm. It is well known that

$$\left\|u - u_k\right\|_A \leq 2\left(\frac{\sqrt{\kappa(BA)} - 1}{\sqrt{\kappa(BA)} + 1}\right)^k \left\|u - u_0\right\|_A \tag{2.1.3}$$

which implies that PCG method will generally converge faster with a smaller condition number $\kappa(BA)$.

Even though the estimate given in (2.1.3) is sufficient for many applications, it is not sharp in general. One way to improve the estimate is to look at the eigenvalue distribution of BA (see [57, 55, 10, 123]). More specifically, suppose that the spectrum of BA, $\sigma(BA)$ is the union of two sets $\sigma_0(BA)$ and $\sigma_1(BA)$, where σ_0 consists of all "bad" eigenvalues and σ_1 contains remaining eigenvalues which are bounded above and below, then we have the following theorem.

Theorem 2.1.2 ([57, 55, 10, 123]). *Suppose that* $\sigma(BA) = \sigma_0(BA) \cup \sigma_1(BA)$ *such that there are* m *elements in* $\sigma_0(BA)$ *and* $\lambda \in [a, b]$ *for each* $\lambda \in \sigma_1(BA)$. *Then*

$$\left\|u - u_k\right\|_A \leq 2K \left(\frac{\sqrt{b/a} - 1}{\sqrt{b/a} + 1}\right)^{k-m} \left\|u - u_0\right\|_A \tag{2.1.4}$$

where

$$K = \max_{\lambda \in \sigma_1(BA)} \prod_{\mu \in \sigma_0(BA)} \left|1 - \frac{\lambda}{\mu}\right|.$$

Especially, if there are only m small eigenvalues in σ_0, say

$$0 < \lambda_1 \leq \lambda_2 \cdots \leq \lambda_m \ll \lambda_{m+1} \leq \cdots \leq \lambda_n,$$

then

$$K \leq \prod_{i=1}^{m} \left|1 - \frac{\lambda_n}{\lambda_i}\right| \leq \left(\frac{\lambda_n}{\lambda_1} - 1\right)^m = (\kappa(BA) - 1)^m.$$

In this case, the convergence rate estimate (2.1.4) becomes

$$\frac{\left\|u - u_k\right\|_A}{\left\|u - u_0\right\|_A} \leq 2\,(\kappa(BA) - 1)^m \left(\frac{\sqrt{b/a} - 1}{\sqrt{b/a} + 1}\right)^{k-m}. \tag{2.1.5}$$

Based on this estimate, given a tolerance $\epsilon < 1$, the number of iterations of the PCG algorithm needed for $\frac{\left\|u-u_k\right\|_A}{\left\|u-u_0\right\|_A} \leq \epsilon$ is given by

$$k \geq m + \left(\log\left(\frac{2}{\epsilon}\right) + m \log\left(\kappa(BA) - 1\right)\right) / c_0 \tag{2.1.6}$$

where $c_0 = \log \frac{\sqrt{b/a}+1}{\sqrt{b/a}-1}$. More details on the iteration number of PCG methods can be found in [9, 10].

Observing the convergence estimate (2.1.5), if there are only a few small eigenvalues of BA in $\sigma_0(BA)$, then the convergent rate of the PCG methods will be dominated by the factor $\frac{\sqrt{b/a}-1}{\sqrt{b/a}+1}$, i.e., by b/a where $b = \lambda_n(BA)$ and $a = \lambda_{m+1}(BA)$. We define this quantity as "effective condition number."

Definition 2.1.3. *Let $\mathcal{V}$ be a finite dimensional Hilbert space, and $A : \mathcal{V} \to \mathcal{V}$ be a bounded linear operator with the eigenvalues $0 < \lambda_1 \leq \lambda_2 \leq \cdots \leq \lambda_n$. The* m-th effective condition number *of A is defined by*

$$\kappa_m(A) = \frac{\lambda_n}{\lambda_{m+1}}.$$

When $m = 0$, then $\kappa_0(A) = \frac{\lambda_n}{\lambda_1}$ is the usual condition number $\kappa(A)$.

In order to estimate the effective condition number, we need to estimate $\lambda_{m+1}(A)$. A basic tool is the *Courant-Fisher "minimax" principle* (see e.g., [54]):

Lemma 2.1.4. *Let $\mathcal{V}$ be a finite dimensional Hilbert space and $A : \mathcal{V} \to \mathcal{V}$ is an SPD operator on $\mathcal{V}$. Suppose $\lambda_1 \leq \lambda_2 \leq \cdots \leq \lambda_n$ are the eigenvalues of A, then*

$$\lambda_{m+1}(A) = \max_{dim(S)=m} \min_{0 \neq v \in S^{\perp}} \frac{(Av, v)}{(v, v)}$$

for $m = 1, 2, \cdots, n$. *Especially, for any subspace* $\mathcal{V}_0 \subset \mathcal{V}$ *with* $\dim(\mathcal{V}_0) = n - m$, *the following estimate of* $\lambda_{m+1}(A)$ *holds:*

$$\lambda_{m+1}(A) \geq \min_{0 \neq v \in \mathcal{V}_0} \frac{(Av, v)}{(v, v)}. \tag{2.1.7}$$

Inequality (2.1.7) is the starting point for our analysis of the eigenvalue distribution. It enables us to obtain a lower bound of every eigenvalue if we can estimate $\min_{0 \neq v \in \mathcal{V}_0} \frac{(Av, v)}{(v, v)}$ for some suitable subspace $\mathcal{V}_0$. As a simple example, in the following subsection we analyze the behavior of the Jacobi and symmetric Gauss-Seidel preconditioners for the equation (2.1.2).

2.1.4 Jacobi and Symmetric Gauss-Seidel Preconditioners

In [55, 110], it was proved that there are only a few small eigenvalues that are infected by the coefficients for the diagonally scaled system $\mathcal{D}^{-1}\mathcal{A}$. Their proofs, which are based on a perturbation theory and careful analysis of the entries of $\mathcal{D}^{-1}\mathcal{A}$, are purely algebraic, and difficult to generalize to other preconditioners. In this subsection, we present an entirely different and more analytic proof of this result, and extend this result to the symmetric Gauss-Seidel preconditioner. Such an analytic proof plays a key role in our analysis and seems to be more concise and more insightful.

First, we introduce a special subspace $\widetilde{\mathcal{V}}_h \subset \mathcal{V}_h$. Let

$$I = \left\{ m : \text{meas}\left(\partial\Omega_m \cap \Gamma_D\right) = 0 \right\}$$

be the index set of all the subdomains except for those whose boundaries contain a non-trivial subset of the Dirichlet boundary Γ_D. Here meas$(\cdot)$ denotes the $d-1$ dimensional measure. Define

$$\widetilde{\mathcal{V}}_h = \left\{ v \in \mathcal{V}_h : \int_{\Omega_m} v = 0, \;\; m \in I \right\}.$$

Suppose that $m_0 := \#I$, the cardinality of I. Then it is clear that

(1) $m_0 \leq M$,

(2) $\dim\left(\widetilde{\mathcal{V}}_h\right) = \dim\left(\mathcal{V}_h\right) - m_0 = n - m_0$, where $n = \dim\mathcal{V}_h$,

(3) On $\widetilde{\mathcal{V}}_h$, the following Poincaré-Friedrichs inequality holds:

$$c_0 \left\|v\right\|_{0,\omega} \leq \left\|\nabla v\right\|_{0,\omega}, \;\; \forall v \in \widetilde{\mathcal{V}}_h. \tag{2.1.8}$$

We emphasize that m_0 is a fixed number which depends only on the distribution of the coefficients on the domain.

Remark 2.1.5. *The condition $\int_{\Omega_m} v = 0$ is not essential. The key idea is to introduce a subspace such that the Poincaré-Friedrichs inequality* (2.1.8) *holds. For this purpose, it can be replaced by some other conditions. For example, we can use*

$$\int_{F_m} v = 0, \;\; F_m \subset \partial\Omega_m \text{ and } \text{meas}\left(F_m\right) > 0$$

for each Ω_m such that $m \in I$. In this case, the Poincaré-Friedrichs inequality (2.1.8) *is still true. When $d = 3$, we may also assume that $\int_{E_m} v = 0$, where E_m is an edge of*

Ω_m. *In this case, the Poincaré-Friedrichs inequality* (2.1.8) *becomes*

$$\|v\|_{0,\omega} \lesssim |\log h|^{\frac{1}{2}} |v|_{1,\omega}, \tag{2.1.9}$$

which deteriorates slightly (see [47, 126] for more details).

In what follows, we denote $\mathcal{A} = \mathcal{D} - \mathcal{L} - \mathcal{L}^t$ where $\mathcal{D}, \mathcal{L}, \mathcal{L}^t$ are the diagonal, strictly lower and upper triangular part of $\mathcal{A}$ respectively. We have the following norm equivalent Lemma.

Lemma 2.1.6. *Let $v \in \mathcal{V}_h$ and $\nu \in \mathbb{R}^n$ be the vector representation of v. Then*

$$\nu^t \mathcal{D} \nu \eqsim h^{-2} \|v\|^2_{0,\omega} \equiv \sum_{\tau \in \mathcal{T}_h} h^{-2} \|v\|^2_{0,\omega,\tau}.$$

Proof. Since each ϕ_i is a piecewise linear function with a local support $o_i \subset \Omega$, each diagonal entry a_{ii} of $\mathcal{A}$ satisfies

$$a_{ii} = \int_\Omega \omega \left|\nabla \phi_i\right|^2 = \left|\nabla \phi_i\right|^2 \int_{o_i} \omega = \bar{\omega}_i \int_{o_i} \left|\nabla \phi_i\right|^2 \eqsim \bar{\omega}_i h^{d-2}.$$

Therefore, by Lemma 2.1.1 we have

$$\nu^t \mathcal{D} \nu \eqsim h^{d-2} (\nu, \nu)_{\ell^2,\omega} \eqsim h^{-2} \|v\|^2_{0,\omega}.$$

This completes the proof. □

From Lemma 2.1.6, the Poincaré-Friedrichs inequality (2.1.8), and the minimax Lemma 2.1.4, we have the following result regarding the condition number and the effective condition number for Jacobi preconditioner.

Theorem 2.1.7. *Assume that the triangulation $\mathcal{T}_h$ is quasi-uniform, then we have*

$$h^2 \mathcal{J}(\omega)^{-1} \nu^t \mathcal{D}\nu \lesssim \nu^t \mathcal{A}\nu \lesssim \nu^t \mathcal{D}\nu, \ \forall \nu \in \mathbb{R}^n, \tag{2.1.10}$$

where $\mathcal{J}(\omega) = \frac{\max_m \omega_m}{\min_m \omega_m}$. *Moreover, for any* $v \in \widetilde{\mathcal{V}}_h$ *with* $v = \sum_{i=1}^n \nu_i \phi_i$ *we have*

$$h^2 \nu^t \mathcal{D}\nu \lesssim \nu^t \mathcal{A}\nu. \tag{2.1.11}$$

Consequently,

$$\kappa\left(\mathcal{D}^{-1}\mathcal{A}\right) \lesssim \mathcal{J}(\omega) h^{-2}, \quad \textit{and} \quad \kappa_{m_0}\left(\mathcal{D}^{-1}\mathcal{A}\right) \lesssim h^{-2}. \tag{2.1.12}$$

Proof. Given ν, let $v = \sum_i \nu_i \phi_i \in \mathcal{V}_h$. Then

$$\nu^t \mathcal{A}\nu \ = \ a(v,v) = \sum_{\tau \in \mathcal{T}_h} |v|^2_{1,\omega,\tau} \lesssim \sum_{\tau \in \mathcal{T}_h} h^{-2} \|v\|^2_{0,\omega,\tau}.$$

In the last step, we used the inverse inequality $|v|_{1,\tau} \lesssim h^{-1} \|v\|_{0,\tau}$. The upper bound of the inequality (2.1.10) follows from Lemma 2.5.2. The lower bound of (2.1.10) follows from the observation:

$$a(v,v) \geq \min_m\{\omega_m\} |v|^2_{1,\Omega} \gtrsim \min_m\{\omega_m\} \|v\|^2_{0,\Omega} \geq \frac{\min_m\{\omega_m\}}{\max_m\{\omega_m\}} h^2 \left(h^{-2} \|v\|^2_{0,\omega}\right).$$

In the second step, we used Poincaré-Friedrichs inequality $\|v\|_{0,\Omega} \lesssim |v|_{1,\Omega}$.

Given any $v \in \widetilde{\mathcal{V}}_h$, let $\nu \in \mathbb{R}^n$ such that $v = \sum_{i=1}^{n} \nu_i \phi_i$. Then by Lemma 2.5.2 we have

$$\begin{aligned} \nu^t \mathcal{D} \nu &\lesssim \sum_{\tau \in \mathcal{T}_h} h^{-2} \|v\|^2_{0,\omega,\tau} = h^{-2} \sum_{m=1}^{M} \omega_m \|v\|^2_{0,\Omega_m} \\ &\lesssim h^{-2} |v|^2_{1,\omega} = h^{-2} \nu^t \mathcal{A} \nu. \end{aligned}$$

In the last inequality, we have used the inequality (2.1.8), since $v \in \widetilde{\mathcal{V}}_h$.

The upper bound of inequality (2.1.10) implies that $\lambda_{\max}\left(\mathcal{D}^{-1}\mathcal{A}\right) \lesssim 1$, and the lower bound of (2.1.10) implies that $\lambda_1\left(\mathcal{D}^{-1}\mathcal{A}\right) \gtrsim h^2 \mathcal{J}(\omega)^{-1}$. Thus, we get

$$\kappa\left(\mathcal{D}^{-1}\mathcal{A}\right) \lesssim \mathcal{J}(\omega) h^{-2}.$$

By inequality (2.1.11) and the minimax Lemma 2.1.4, we have $\lambda_{m_0+1}\left(\mathcal{D}^{-1}\mathcal{A}\right) \gtrsim h^2$. Therefore, we have the estimate for the effective condition number

$$\kappa_{m_0}\left(\mathcal{D}^{-1}\mathcal{A}\right) \lesssim h^{-2}.$$

This completes the proof. □

Now let us consider symmetric Gauss-Seidel preconditioner defined by

$$\mathcal{B} = \left(\mathcal{D} - \mathcal{L}^t\right)^{-1} \mathcal{D} \left(\mathcal{D} - \mathcal{L}\right)^{-1}. \tag{2.1.13}$$

We have the following relationship between symmetric Gauss-Seidel preconditioner and Jacobi preconditioner. A proof can be found in [131].

Lemma 2.1.8. *For the symmetric Gauss-Seidel preconditioner $\mathcal{B}$ defined in* (2.1.13)*, we have*

$$\frac{1}{4}\nu^t\mathcal{D}\nu \leq \nu^t\mathcal{B}^{-1}\nu \lesssim \nu^t\mathcal{D}\nu, \ \ \forall \nu \in \mathbb{R}^n.$$

Lemma 2.1.8 actually states that there is certain equivalence between symmetric Gauss-Seidel method and Jacobi method. As a direct consequence of Lemma 2.1.8 and Theorem 2.1.7, we have the same results for symmetric Gauss-Seidel preconditioner.

Theorem 2.1.9. *For the symmetric Gauss-Seidel preconditioner $\mathcal{B}$ defined in* (2.1.13)*, we have*

$$\lambda_{\min}(\mathcal{B}\mathcal{A}) \geq \mathcal{J}(\omega)^{-1}h^2, \ \ \lambda_{\max}(\mathcal{B}\mathcal{A}) \lesssim 1, \quad \textit{and} \quad \lambda_{m_0+1}(\mathcal{B}\mathcal{A}) \gtrsim h^2.$$

Moreover, the condition number and the m_0-th effective condition number for symmetric Gauss-Seidel preconditioner satisfy:

$$\kappa(\mathcal{B}\mathcal{A}) \leq C_0\mathcal{J}(\omega)h^{-2}, \quad \kappa_{m_0}(\mathcal{B}\mathcal{A}) \leq C_1^2h^{-2}.$$

By Theorem 2.1.7, Theorem 2.1.9 and Theorem 2.1.2, we have

Theorem 2.1.10. *For Jacobi or symmetric Gauss-Seidel PCG, we have the following convergence rate estimate*

$$\frac{\left\|u-u_k\right\|_A}{\left\|u-u_0\right\|_A} \leq 2\left(C_0\mathcal{J}(\omega)h^{-2}-1\right)^{m_0}\left(1-\frac{2}{1+C_1h^{-1}}\right)^{k-m_0}, \quad k \geq m_0.$$

From this theorem, it is obvious that for Jacobi or symmetric Gauss-Seidel PCG algorithms, the asymptotic convergence rate is of $1-Ch$ which approaches to 1 as the mesh size $h \to 0$. On the other hand, the influence of the large condition number $\kappa(BA)$ is not negligible. Actually, the inequality (2.1.6) shows that we may need a lot of PCG iterations to converge to the solution. This deterioration of the condition number, due to the variation in the coefficients, was also observed numerically for incomplete Cholesky preconditioner in [110].

2.2 L^2 and Weighted L^2-projections

This section is devoted to the approximation and stability properties of the L^2-projection $Q_H : L^2(\Omega) \to \mathcal{V}_H$ and weighted L^2-projections $Q_H^\omega : L^2(\Omega) \to \mathcal{V}_H$ defined by

$$\begin{aligned}\left(Q_Hu, v_H\right) &= \left(u, v_H\right), \ \forall v_H \in \mathcal{V}_H,\\ \left(Q_H^\omega u, v_H\right)_{0,\omega} &= \left(u, v_H\right)_{0,\omega}, \ \forall v_H \in \mathcal{V}_H.\end{aligned}$$

These properties play an essential role in multilevel analysis.

It is well known that the standard L^2-projection satisfies the simultaneous approximation property

$$\left\|u - Q_H u\right\|_{0,\Omega} + H\left\|u - Q_H u\right\|_{1,\Omega} \lesssim H\|u\|_{1,\Omega},\ \forall u \in H_0^1(\Omega). \tag{2.2.1}$$

For a proof of this estimate, we refer to [27]. In their proof, they used the local L^2 projections $Q_\tau : L^2(\tau) \to \mathcal{P}_1(\tau)$ for any $\tau \in \mathcal{T}_H$, defined by

$$\left(Q_\tau u, \phi\right)_{0,\tau} := (u, \phi)_{0,\tau}\ \ \forall \phi \in \mathcal{P}_1(\tau).$$

These locally defined operators satisfy the following approximation and stability properties.

Lemma 2.2.1 ([27, Lemma 3.3])**.** *For any $\tau \in \mathcal{T}_H$ and $u \in H^1(\tau)$, we have*

$$\left\|u - Q_\tau u\right\|_{0,\tau} \lesssim H|u|_{1,\tau}\ \ \textit{and}\ \ \left|Q_\tau u\right|_{1,\tau} \lesssim |u|_{1,\tau}.$$

For the weighted L^2-projection, the following properties are well known.

Lemma 2.2.2 ([27, Theorem 4.5])**.** *Let $\mathcal{V}_H \subset \mathcal{V}_h$ be two nested linear finite element spaces. Then for any $u \in \mathcal{V}_h$, there holds,*

$$\left\|\left(I - Q_H^\omega\right) u\right\|_{0,\omega} \leq c_d(h, H) H|u|_{1,\omega}, \tag{2.2.2}$$

and

$$\left|Q_H^\omega u\right|_{1,\omega} \lesssim c_d(h, H)|u|_{1,\omega}, \tag{2.2.3}$$

$$\text{where } c_d(h,H) = C \cdot \begin{cases} 1, & \text{if } d = 1 \\ \left(\log \frac{H}{h}\right)^{\frac{1}{2}}, & \text{if } d = 2 \\ \left(\frac{H}{h}\right)^{\frac{1}{2}}, & \text{if } d = 3. \end{cases}$$

The proof of this lemma is based on the properties of standard interpolation operator and Sobolev imbedding theorem (see [27] for the details). For a general $H^1(\Omega)$ function, this lemma is not necessarily true. But if we use the full weighted H^1 norm, then we have

Lemma 2.2.3 ([27, Lemma 4.6])**.** *For all $u \in H^1_D(\Omega)$, we have*

$$\left\| \left(I - Q^{\omega}_{H} \right) u \right\|_{0,\omega} \lesssim H \left| \log H \right|^{\frac{1}{2}} \left\| u \right\|_{1,\omega}.$$

In general, we can not replace $\|u\|_{1,\omega}$ by the semi-norm $|u|_{1,\omega}$ in the above lemma (see [118, 93] for counter-examples). Since we need the estimate with the energy norm $|\cdot|_{1,\omega}$ in the right hand side, we need to impose certain conditions on $u \in H^1_D(\Omega)$. Similar to $\widetilde{\mathcal{V}}_h$ introduced in Section 2.1.4, we introduce a subspace $\widetilde{H}^1_D(\Omega)$ of $H^1_D(\Omega)$ as follows:

$$\widetilde{H}^1_D(\Omega) = \left\{ u \in H^1_D(\Omega) : \int_{\Omega_m} u dx = 0, \forall m \in I \right\}.$$

Recall that I is the index set of all the subdomains, except for those whose boundaries have nontrivial intersections with the Dirichlet boundary Γ_D. A distinct feature of this subspace is that the following Poincaré-Friedrichs inequality holds:

$$c_0 \left\| v \right\|_{0,\omega} \leq \left\| \nabla v \right\|_{0,\omega}, \quad \forall v \in \widetilde{H}^1_D(\Omega). \tag{2.2.4}$$

Thanks to inequality (2.2.4), we have the following estimates for the weighted L^2-projection:

Lemma 2.2.4. *For any $v \in \widetilde{H}^1_D(\Omega)$ we have*

$$\left\| \left(I - Q^{\omega}_{H} \right) v \right\|_{0,\omega} \lesssim H \left| \log H \right|^{\frac{1}{2}} |v|_{1,\omega} \tag{2.2.5}$$

and

$$\left| Q^{\omega}_{H} v \right|_{1,\omega} \lesssim \left| \log H \right|^{\frac{1}{2}} |v|_{1,\omega} . \tag{2.2.6}$$

Proof. By assumption, v satisfies Poincaré-Friedrichs inequality (2.2.4). The inequality (2.2.5) then follows by Lemma 2.2.3.

The proof of inequality (2.2.6) relies on (2.2.5) and Lemma 2.2.1. On each element $\tau \in \mathcal{T}_H$, we have

$$\begin{aligned}
\left| Q^{\omega}_{H} v \right|^2_{1,\tau} &\lesssim \left| Q^{\omega}_{H} v - Q_{\tau} v \right|^2_{1,\tau} + \left| Q_{\tau} v \right|^2_{1,\tau} \\
&\lesssim H^{-2} \left\| Q^{\omega}_{H} v - Q_{\tau} v \right\|^2_{0,\tau} + \left| Q_{\tau} v \right|^2_{1,\tau} \\
&\lesssim H^{-2} \left(\left\| v - Q^{\omega}_{H} v \right\|^2_{0,\tau} + \left\| v - Q_{\tau} v \right\|^2_{0,\tau} \right) + \left| Q_{\tau} v \right|^2_{1,\tau} \\
&\lesssim H^{-2} \left\| v - Q^{\omega}_{H} v \right\|^2_{0,\tau} + |v|^2_{1,\tau} .
\end{aligned}$$

In the last inequality, we used Lemma 2.2.1. Multiplying by suitably chosen weights and summing up over all $\tau \in \mathcal{T}_H$ on both sides, we get

$$\left|Q_H^{\omega} v\right|_{1,\omega}^2 \lesssim H^{-2} \left\|v - Q_H^{\omega} v\right\|_{0,\omega}^2 + |v|_{1,\omega}^2 \lesssim |\log H|\, |v|_{1,\omega}^2 .$$

In the last step, we used inequality (2.2.5). □

Although Lemma 2.2.4 is true for $d = 1,\ 2$ or 3, it is of interest only when $d = 3$. When $d = 1$ or 2, Lemma 2.2.2 is sufficient for our future use. From Lemma 2.2.4, the approximation and stability of the weighted L^2-projection will deteriorate by $|\log H|$. A sharper estimate can be obtained if we assume that each subregion Ω_m is a polyhedral domain with each edge of length H_0.

Lemma 2.2.5 ([27])**.** *Assume that G is a polyhedral domain in $\mathbb{R}^3$. Then*

$$\|v\|_{0,E} \lesssim |\log H|^{\frac{1}{2}} \|v\|_{1,G}, \quad \forall v \in \mathcal{V}_H(G),$$

where E is any edge of G.

By Poincaré-Friedrichs inequality (2.2.4), for each $v \in \widetilde{H}_D^1(\Omega)$, we have

$$\|v\|_{1,\Omega_m} \lesssim |v|_{1,\Omega_m} \quad \text{for all } \Omega_m (m = 1, \cdots, M).$$

Therefore, if Ω_m is a polyhedral domain with the boundary edges satisfying length$(E) \eqsim H_0$, then by Lemma 2.2.5 and a standard scaling argument, we have

$$\|v\|_{0,E} \lesssim \left(\log \frac{H_0}{H}\right)^{\frac{1}{2}} |v|_{1,\Omega_m}, \quad \forall v \in \mathcal{V}_H\left(\Omega_m\right) \cap \widetilde{H}^1_D(\Omega). \tag{2.2.7}$$

In this case, we have the following approximation and stability properties for the weighted L^2-projection:

Lemma 2.2.6. *In $\mathbb{R}^3$, assume that each subregion Ω_m satisfies $H_0 \eqsim$ length(E) for any edge E of Ω_m. Then for all $v \in \widetilde{H}^1_D(\Omega)$, we have*

$$\left\| \left(I - Q^{\omega}_H\right) v \right\|_{0,\omega} \lesssim H \left(\log \frac{H_0}{H}\right)^{\frac{1}{2}} |v|_{1,\omega} \tag{2.2.8}$$

and

$$\left| Q^{\omega}_H v \right|_{1,\omega} \lesssim \left(\log \frac{H_0}{H}\right)^{\frac{1}{2}} |v|_{1,\omega}. \tag{2.2.9}$$

Proof. The idea follows Bramble and Xu [27, Lemma 4.6]. Define $w \in \mathcal{V}_H$ by

$$w = \begin{cases} w_m, & \text{at the nodes inside } \Omega_m, \\ Q_F u, & \text{at the nodes inside } F \subset \partial\Omega_m, \\ 0, & \text{at the nodes elsewhere,} \end{cases}$$

where $w_m = Q_H v$ is the standard L^2-projection of v, $F \subset \partial\Omega_m$ is any face of Ω_m, and $Q_F : L^2(F) \to \mathcal{V}_H(F)$ is the orthogonal $L^2(F)$ projection. Then

$$\begin{aligned}
\left\|w - w_m\right\|^2_{0,\Omega_m} &\lesssim H^3 \sum_{x\in\partial\Omega_m} \left(w - w_m\right)^2(x) \\
&\lesssim H^3 \sum_{F\subset\partial\Omega_m} \sum_{x\in F} \left(w - w_m\right)^2(x) \\
&\lesssim H^3 \sum_{F\subset\partial\Omega_m} \left(\sum_{x\in F} \left(w_m - Q_F u\right)^2(x) + \sum_{x\in\partial F} w_m^2(x) \right) \\
&\lesssim \sum_{F\subset\partial\Omega_m} \left(H \left\|w_m - Q_F u\right\|^2_{0,F} + H^2 \left\|w_m\right\|^2_{0,\partial F} \right).
\end{aligned}$$

We need to bound two terms appearing in the last expression. For the first term, we have

$$\begin{aligned}
\sum_{F\subset\partial\Omega_m} H \left\|w_m - Q_F u\right\|^2_{0,F} &\lesssim H \left\|u - w_m\right\|^2_{0,\partial\Omega_m} \\
&\lesssim \left\|u - w_m\right\|^2_{0,\Omega_m} + H^2 \left\|u - w_m\right\|^2_{1,\Omega_m} \\
&\lesssim H^2 \|u\|^2_{1,\Omega_m}.
\end{aligned}$$

In the second step, we used inequality

$$\|v\|_{L^2\left(\partial\Omega_m\right)} \lesssim \epsilon^{-1} \|v\|_{0,\Omega_m} + \epsilon \|v\|_{1,\Omega_m}. \tag{2.2.10}$$

The second term can be bounded by using the inequality (2.2.7)

$$\sum_{F\subset\partial\Omega_m} H^2 \left\|w_m\right\|^2_{0,\partial F} \lesssim H^2 \left(\log\frac{H_0}{H}\right) \left|w_m\right|^2_{1,\Omega_m} \lesssim H^2 \left(\log\frac{H_0}{H}\right) |u|^2_{1,\Omega_m}.$$

In the last step, we used the stability of Q_H: $\left|w_m\right|_{1,\Omega_m} = \left|Q_H u\right|_{1,\Omega_m} \lesssim |u|_{1,\Omega_m}$. Consequently,

$$\left\|w - w_m\right\|_{0,\Omega_m} \lesssim H \left(\log\frac{H_0}{H}\right)^{\frac{1}{2}} |u|_{1,\Omega_m}.$$

This proves (2.2.8). The proof of the stability (2.2.9) is the same as in Lemma 2.2.4. □

Remark 2.2.7. *In addition to the conditions in Lemma 2.2.6, if $H \eqsim H_0$ then for all $v \in \widetilde{H}^1_D(\Omega)$, we have*

$$\left\|\left(I - Q^{\omega}_H\right) v\right\|_{0,\omega} \lesssim H\,|v|_{1,\omega}, \tag{2.2.11}$$

$$\left|Q^{\omega}_H v\right|_{1,\omega} \lesssim |v|_{1,\omega}. \tag{2.2.12}$$

In fact, in this case, by norm equivalent in $\mathcal{V}_H(\Omega_m)$, inequality (2.2.7) *becomes*

$$\|v\|_{L^2(E)} \lesssim |v|_{1,\Omega_m}, \quad \forall v \in \mathcal{V}_H\left(\Omega_m\right) \cap \widetilde{H}^1_D(\Omega). \tag{2.2.13}$$

Then inequalities (2.2.11) *and* (2.2.12) *follow by the same proof as Lemma 2.2.6.*

2.3 Multilevel Preconditioners

As we have seen from Theorem 2.1.7 and Theorem 2.1.9, the Jacobi and symmetric Gauss-Seidel preconditioned systems have a condition number $\kappa(BA) \lesssim \mathcal{J}(\omega)h^{-2}$, and the effective condition number $\kappa_{m_0}(BA) \lesssim h^{-2}$. In order to obtain a condition number that is (nearly) uniform with respect to the mesh size, we use multilevel techniques. In this section, we analyze the eigenvalue distribution of the multilevel preconditioners, and prove that the BPX and multigrid V-cycle preconditioners have robust effective condition numbers.

We construct a sequence of quasi-uniform triangulations $\mathcal{T}_l,\ l = 0, 1, \cdots, L$ by a successive uniform refinement process. More precisely, $\left\{\mathcal{T}_l,\ l = 0, 1, \cdots, L\right\}$ is a nested sequence of quasi-uniform triangulations, i.e., $\mathcal{T}_l$ consists of simplices $\left\{\tau_i^l\right\}$ of size h_l such that $\Omega = \cup_i \tau_i^l$ for which the quasi-uniformity constants are independent of l, and each simplex $\tau_i^{l-1} \in \mathcal{T}_{l-1}$ is a union of simplices in $\mathcal{T}_l$. We further assume that there is a constant $\gamma \in (0, 1)$, independent of l, such that h_l is proportional to γ^{2l}. Here, we assume that the coarsest mesh $\mathcal{T}_0$ aligns with the discontinuity in ω; namely, the restriction of $\mathcal{T}_0$ on each Ω_m is also a triangulation of Ω_m itself. We denote that $h := h_L$, and note that $L = O(|\log h|)$.

Corresponding to each triangulation $\mathcal{T}_l$, a linear finite element space $\mathcal{V}_l$ is defined by

$$\mathcal{V}_l = \left\{ v \in H_D^1(\Omega) : v|_\tau \in \mathcal{P}_1(\tau)\ \ \tau \in \mathcal{T}_l \right\}.$$

Obviously, the following inclusion relation holds:

$$\mathcal{V}_0 \subset \mathcal{V}_1 \subset \cdots \subset \mathcal{V}_L := \mathcal{V}.$$

This gives a natural space decomposition $\mathcal{V} = \sum_{l=0}^{L} \mathcal{V}_l$. As before, we introduce a subspace $\widetilde{\mathcal{V}}$ of $\mathcal{V}$ defined by

$$\widetilde{\mathcal{V}} = \left\{ v \in \mathcal{V} : \int_{\Omega_m} v = 0, \text{ for } m \in I \right\}.$$

We emphasize here that $\dim\left(\mathcal{V}^{\perp}\right) = m_0$ and the Poincaré-Friedrichs inequality (2.1.8) holds in $\widetilde{\mathcal{V}}$.

For each level $l = 0, 1, \ldots, L$, we define the projections $P_l,\ Q_l^{\omega} : \mathcal{V} \to \mathcal{V}_l$ by

$$a\left(P_l u, v_l\right) = a\left(u, v_l\right), \quad \left(Q_l^{\omega} u, v_l\right)_{0,\omega} = \left(u, v_l\right)_{0,\omega}, \quad \forall v_l \in \mathcal{V}_l;$$

and define operators $A_l : \mathcal{V}_l \to \mathcal{V}_l$ by

$$\left(A_l u_l, v_l\right)_{0,\omega} = a\left(u_l, v_l\right), \quad \forall u_l, v_l \in \mathcal{V}_l.$$

For convenience, we denote $A = A_L,\ Q_{-1}^{\omega} = 0$. It follows from the definitions that $Q_l^{\omega} A = A_l P_l$, and $Q_l^{\omega} Q_k^{\omega} = Q_k^{\omega} Q_l^{\omega} = Q_k^{\omega}$ for $k \leq l$.

On each subspace $\mathcal{V}_l$, we introduce an SPD operator $R_l : \mathcal{V}_l \to \mathcal{V}_l$ that represents an approximation inverse of A_l, such that

$$\left(R_l u_l, u_l\right)_{0,\omega} \eqsim h_l^2 \left(u_l, u_l\right)_{0,\omega} \quad \forall u_l \in \mathcal{V}_l. \tag{2.3.1}$$

According to Lemma 2.1.6 and Lemma 2.1.8, both of Jacobi and symmetric Gauss-Seidel smoothers satisfy the above assumption. On the coarsest level, i.e., when $l = 0$, we choose the exact solver $R_0 = A_0^{-1}$.

2.3.1 The BPX Preconditioner

The BPX preconditioner $B : \mathcal{V} \to \mathcal{V}$ is an additive multilevel preconditioner which was first proposed in [26]. It can be defined as:

$$B = \sum_{l=0}^{L} R_l Q_l^{\omega}. \tag{2.3.2}$$

The following identity for BPX preconditioner is well known in the literature [115, 120, 125]. We refer to [125] for a concise proof.

Lemma 2.3.1. *The operator B defined by* (2.3.2) *is SPD on $\mathcal{V}$, and*

$$\left(B^{-1} v, v\right)_{0,\omega} = \inf_{\sum_{l=0}^{L} v_l = v} \sum_{l=0}^{L} \left(R_l^{-1} v_l, v_l\right)_{0,\omega}. \tag{2.3.3}$$

Thus, based on the assumption on R_l, we have the following:

$$\left(B^{-1}v,v\right)_{0,\omega} \eqsim \inf_{\sum_{l=0}^{L} v_l = v} \left(a\left(v_0,v_0\right) + \sum_{l=1}^{L} h_l^{-2} \left\|v_l\right\|_{0,\omega}^2 \right), \ \forall v \in \mathcal{V}. \tag{2.3.4}$$

Based on (2.3.4), we have the main result of this subsection.

Lemma 2.3.2. *For the BPX preconditioner* (2.3.2)*, we have*

$$\frac{1}{\min\left\{c_d^2(h), \mathcal{J}(\omega)\right\}} \left(B^{-1}v,v\right)_{0,\omega} \lesssim (Av,v)_{0,\omega} \lesssim \left(B^{-1}v,v\right)_{0,\omega}, \ \ \forall\, v \in \mathcal{V} \tag{2.3.5}$$

where $c_d(h) = C \cdot \begin{cases} 1, & d=1 \\ |\log h|, & d=2 \\ h^{-\frac{1}{2}}, & d=3 \end{cases}$ *and* $\mathcal{J}(\omega) = \frac{\max_m \omega_m}{\min_m \omega_m}$*. Moreover,*

$$\left(B^{-1}v,v\right)_{0,\omega} \lesssim |\log h|^2 (Av,v)_{0,\omega}, \ \ \forall v \in \widetilde{\mathcal{V}}. \tag{2.3.6}$$

Consequently, the condition number $\kappa(BA)$ *and the* m_0*-th effective condition number* $\kappa_{m_0}(BA)$ *satisfy*

$$\kappa(BA) \le C_0 \min\left\{c_d^2(h), \mathcal{J}(\omega)\right\}, \quad \kappa_{m_0}(BA) \le C_1^2 |\log h|^2.$$

Proof. The proof of (2.3.5) is standard (see for example [93]). For completeness, we include the proof here. For the upper bound of (2.3.5), we have for each $v \in \mathcal{V}$,

$$\begin{aligned} a(v,v) &\lesssim \inf_{v_0 \in \mathcal{V}_0} \left(a\left(v_0, v_0\right) + \sum_{m=1}^{M} \omega_m \left| v - v_0 \right|_{1,\Omega_m}^2 \right) \\ &\lesssim \inf_{v_0 \in \mathcal{V}_0} \left(a\left(v_0, v_0\right) + \sum_{m=1}^{M} \omega_m \inf_{v-v_0|_{\Omega_m} = \sum_{l=1}^{L} v_{l,\Omega_m}} \sum_{l=1}^{L} h_l^{-2} \left\| v_{l,\Omega_m} \right\|_{0,\Omega_m}^2 \right) \\ &\lesssim \inf_{v = v_0 + \sum_{l=1}^{L} v_l} \left(a\left(v_0, v_0\right) + \sum_{l=1}^{L} h_l^{-2} \left\| v_l \right\|_{0,\omega}^2 \right) \\ &\eqsim \left(B^{-1} v, v \right)_{0,\omega}. \end{aligned}$$

In the second inequality, we used the standard norm equivalency (see [92, 93]):

$$|u|_{1,\Omega_m}^2 \eqsim \inf_{\sum_{l=1}^{L} u_l = u} \sum_{l=1}^{L} h_l^{-2} \left\| u_l \right\|_{0,\Omega_m}^2$$

on each subdomain Ω_m.

On the other hand, notice that from (2.3.4), for any decomposition $v = \sum_{l=0}^{L} v_l$, we have

$$\left(B^{-1} v, v \right)_{0,\omega} \lesssim \left| v_0 \right|_{1,\omega}^2 + \sum_{l=1}^{L} h_l^{-2} \left\| v_l \right\|_{0,\omega}^2.$$

If we choose $v_l = \left(Q_l^{\omega} - Q_{l-1}^{\omega} \right) v$ for $l = 0, 1, \cdots, L$ then

$$\left(B^{-1} v, v \right)_{0,\omega} \lesssim \left| Q_0^{\omega} v \right|_{1,\omega}^2 + \sum_{l=1}^{L} h_l^{-2} \left\| \left(Q_l^{\omega} - Q_{l-1}^{\omega} \right) v \right\|_{0,\omega}^2. \tag{2.3.7}$$

By Lemma 2.2.2, it is easy to see that $\left(B^{-1}v,v\right)_{0,\omega} \lesssim c_d^2(h)a(v,v)$. Moreover, the trivial estimate $\left(B^{-1}v,v\right)_{0,\omega} \lesssim \mathcal{J}(\omega)a(v,v)$ can be obtained by switching to the case of constant weight and by using the approximation property (2.2.1) of the standard L^2 projections (see also [26]). This proves the lower bound of inequality (2.3.5).

To prove (2.3.6), we consider for any $v \in \widetilde{\mathcal{V}}$, and apply Lemma 2.2.4 to (2.3.7). Then we have

$$\left|Q_0^{\omega}v\right|_{1,\omega}^2 + \sum_{l=1}^{L} h_l^{-2}\left\|\left(Q_l^{\omega}-Q_{l-1}^{\omega}\right)v\right\|_{0,\omega}^2 \lesssim \sum_{l=0}^{L}\left|\log h_l\right||v|_{1,\omega}^2 \lesssim |\log h|^2 a(v,v).$$

From inequality (2.3.5), it follows that

$$\lambda_{\max}(BA) \lesssim 1 \ \text{ and } \ \lambda_{\min}(BA) \gtrsim \frac{1}{\min\left\{c_d(h),\mathcal{J}(\omega)\right\}}.$$

Besides, (2.3.6) and the minimax Lemma 2.1.4 implies that

$$\lambda_{m_0+1}(BA) \gtrsim |\log h|^{-2}.$$

This completes the proof. □

Remark 2.3.3. *From the above proof, the approximation and stability properties of the weighted L^2-projection play crucial roles. Based on the theory of weighted L^2-projection in Section 2.2 (see also [27]), we summarize the bounds of the condition number of the BPX preconditioned system for different cases.*

(1) If $\mathcal{J}(\omega) \leq C$, which means the coefficients are mild, then $\kappa(BA) \leq C$. In this case, by (2.1.3) *the BPX PCG algorithm converges uniformly.*

(2) If $d = 1$, or if the interface has no internal cross point (e.g. [27]), or if the coefficients satisfy the "quasi-monotonicity" (e.g. [45]), then $\kappa(BA) \leq C$. In these cases, by (2.1.3)*, the BPX PCG algorithm is also uniformly convergent.*

(3) For general case in $d = 2$, or if the coefficients are of "edge-type" in $d = 3$ (e.g. [93]), then $\kappa(BA) \leq C^2|\log h|^2$. Another interesting case is when all subdomains contain nontrivial subset of the Dirichlet boundary (for $d = 2, 3$, see [112] for example). By the definition of the subspace $\widetilde{\mathcal{V}}$, we have $m_0 \equiv 0$. Thus by Lemma 2.3.2, the effective condition number $\kappa_{m_0}(BA) = \kappa(BA) \leq C^2|\log h|^2$. In these cases, by (2.1.3) *the convergence rate of the BPX PCG algorithm can be bounded by $1 - \frac{2}{C|\log h|+1}$, which is also quite robust.*

(4) For the worst case when $d = 3$, it was proved in [93] that the condition number estimate of Lemma 2.3.2 is sharp. Specifically, $\kappa(BA) \eqsim Ch^{-1}$ which deteriorates rapidly as $h \to 0$. According to (2.1.3)*, the convergence rate of the BPX PCG algorithm can be bounded by $1 - \frac{2C}{h}$. The following theorem states that the BPX PCG algorithm behaves much better than this estimate.*

Theorem 2.3.4. *Let $u \in \mathcal{V}$ be the exact solution to equation* (2.1.1) *and u_k, $k = 0, 1, 2, \ldots$ be the solution sequence of the BPX PCG algorithm. Then we have*

$$\frac{\left\|u - u_k\right\|_A}{\left\|u - u_0\right\|_A} \leq 2\left(\frac{C_0}{h} - 1\right)^{m_0}\left(1 - \frac{2}{C_1|\log h| + 1}\right)^{k-m_0} \quad \text{for } k \geq m_0,$$

where C_0 *and* C_1 *are constants independent of jumps of coefficients and mesh size. Moreover, given a tolerance* $\epsilon < 1$*, the number of iterations needed for* $\frac{\left\|u-u_k\right\|_A}{\left\|u-u_0\right\|_A} \leq \epsilon$ *satisfies*

$$k \geq m_0 + \left(\log\left(\frac{2}{\epsilon}\right) + m_0 \log\left(\frac{C_0}{h} - 1\right)\right) / c_0(h),$$

where $c_0(h) = \log\left(\frac{C_l|\log h|+1}{C_l|\log h|-1}\right)$.

Proof. The conclusion follows directly by Lemma 2.3.2, inequality (2.1.5) and (2.1.6). □

From Theorem 2.3.4, although the convergence rate of the PCG algorithm is still depends on the condition number $\kappa(BA)$, since m_0 is a fixed number, the asymptotic convergence rate is bounded by $1 - \frac{C}{|\log h|}$, which is independent of the variations in the coefficients and nearly uniform with respect to the mesh size. Moreover, in comparison to Theorem 2.1.10, the estimate in Theorem 2.3.4 is not only significantly better asymptotically, it is also independent of the jump $\mathcal{J}(\omega)$.

2.3.2 Multigrid V-cycle Preconditioner

In this section, we discuss the convergence behavior of multigrid V-cycle. We also discuss multigrid V-cycle as a preconditioner B in PCG algorithm. We would like to point out that using multigrid V-cycle as a preconditioner for conjugate gradient method is not a new approach. Actually, it is known as MGCG algorithm in the literature (see some related references, for example [76, 21, 127, 103, 102]).

It is clear that the convergence of multigrid W-cycle is a consequence of the convergence of multigrid V-cycle. Thus, all the analysis here can be carried through to the

W-cycle case; the main results in this section also hold true for W-cycle preconditioned MGCG algorithms. Although we will refer to MGCG algorithm in the following discussion, we clarify that MGCG algorithm is not a single method or even a family of methods. In this section, we restrict ourself to the case of multigrid V-cycle preconditioner, that is, when we say "the MGCG algorithm", we refer to multigrid V-cycle PCG algorithm. The analysis of this section relies on the following X-Z identity.

Lemma 2.3.5 (X-Z identity,[125]). *Let $\mathcal{V}$ be a Hilbert space and $\mathcal{V}_l \subset \mathcal{V}$ for $l = 1, \cdots, L$ be a number of closed subspaces satisfying $\mathcal{V} = \sum_{l=1}^{L} \mathcal{V}_l$. Let $P_l : \mathcal{V} \to \mathcal{V}_l$ be the orthogonal projection with respect to the inner product $(\cdot, \cdot)$ of $\mathcal{V}$. Denote $\|\cdot\|$ as the induced norm of this inner product in $\mathcal{V}$. Then*

$$\left\| \left(I - P_L\right) \cdots \left(I - P_1\right) \right\|^2_{\mathcal{L}(\mathcal{V})} = 1 - \frac{1}{1 + c_0},$$

where

$$c_0 = \sup_{\|v\|=1} \inf_{v = \sum_{l=1}^{L} v_l} \sum_{l=1}^{L} \left\| P_l \left(\sum_{j=l+1}^{L} v_j \right) \right\|^2.$$

To define the V-cycle preconditioner, we use point Gauss-Seidel as the smoother. For $l = 1, \cdots, L$ and $i = 1, \cdots, n_l$, let $P_i^l : \mathcal{V} \to \text{span}\left\{\phi_i^l\right\} := \mathcal{V}_i^l$ be defined by

$$a\left(P_i^l u, \phi_i^l\right) = a\left(u, \phi_i^l\right), \quad \forall u \in \mathcal{V}.$$

Then the point Gauss-Seidel smoothing operators $R_l : \mathcal{V}_l \to \mathcal{V}_l$ are defined by

$$R_l = \left(I - \prod_{i=1}^{n_l} \left(I - P_i^l \right) \right) A_l^{-1}.$$

The standard multigrid V-cycle algorithm solves (2.1.1) by the iterative method

$$u_l \leftarrow u_l + B_l \left(f_l - A_l u_l \right).$$

The operators $B_l : \mathcal{V}_l \to \mathcal{V}_l$ are recursively defined as follows:

Algorithm 2.3.1 (V-cycle)**.** *Let* $B_0 = A_0^{-1}$, *for* $l > 0$ *and* $g \in \mathcal{V}_l$, *define* $B_l g = w_3$.

(1) Presmoothing : $w_1 = R_l g$;

(2) Correction: $w_2 = w_1 + B_{l-1} Q_{l-1} \left(g - A_l w_1 \right)$;

(3) Postsmoothing: $w_3 = w_2 + R_l^* \left(g - A_l w_2 \right)$.

It is well known (see [22, 125, 123] for example) that multigrid V-cycle operator $B := B_L$ in the algorithm has the representation

$$I - BA = \left(\left(I - P_0 \right) \prod_{l=1}^{L} \prod_{i=1}^{n_l} \left(I - P_i^l \right) \right)^* \left(\left(I - P_0 \right) \prod_{l=1}^{L} \prod_{i=1}^{n_l} \left(I - P_i^l \right) \right).$$

Obviously, for any $v \in \mathcal{V}$ we have

$$a \left(\left(\left(I - P_0 \right) \prod_{l=1}^{L} \prod_{i=1}^{n_l} \left(I - P_i^l \right) \right) v, \left(\left(I - P_0 \right) \prod_{l=1}^{L} \prod_{i=1}^{n_l} \left(I - P_i^l \right) \right) v \right) \geq 0.$$

Therefore, $a(BAv, v) \leq a(v, v)$, which implies that

$$\lambda_{\max}(BA) \leq 1. \tag{2.3.8}$$

On the other hand, notice that $I - BA$ is self-adjoint with respect to the inner product $a(\cdot, \cdot)$, so we have

$$\|I - BA\|_A = \left\| \left(I - P_0\right) \prod_{l=1}^{L} \prod_{i=1}^{n_l} \left(I - P_i^l\right) \right\|_A^2 .$$

From Lemma 2.3.5, we deduce that

$$\|I - BA\|_A = \frac{c_0}{1 + c_0}, \quad \text{with} \quad c_0 = \sup_{|v|_{1,\omega}=1} \inf_{v=v_0+\sum_{l=1}^{L}\sum_{i=1}^{n_l} v_i^l} c(v)$$

where

$$c(v) = \left| P_0 \left(v - v_0\right) \right|_{1,\omega}^2 + \sum_{l=1}^{L} \sum_{i=1}^{n_l} \left| P_i^l \sum_{(k,j)>(l,i)} v_j^k \right|_{1,\omega}^2 .$$

From this identity, it is obvious that

$$\lambda_{\min}(BA) = \inf_{0 \neq v \in \mathcal{V}} \frac{a(BAv, v)}{a(v, v)} \geq \frac{1}{1 + c_0}. \tag{2.3.9}$$

In other words, by estimating an upper bound of c_0 we get a convergence rate estimate of multigrid V-cycle, and also a lower bound of minimum eigenvalue of BA. For this purpose, we introduce the following lemma to give an upper bound of $c(v)$.

Lemma 2.3.6. *Given $v \in \mathcal{V}$, for the decomposition $v = \sum_{l=0}^{L} \left(Q_l^\omega - Q_{l-1}^\omega\right) v$ we have*

$$c(v) \lesssim \sum_{l=0}^{L} \left| P_l v - Q_l^\omega v \right|_{1,\omega}^2 + \sum_{l=1}^{L} h_l^{-2} \left\| \left(Q_l^\omega - Q_{l-1}^\omega\right) v \right\|_{0,\omega}^2 . \tag{2.3.10}$$

Proof. Denote $v = \sum_{l=0}^{L} v_l = v_0 + \sum_{l=1}^{L} \sum_{i=1}^{n_l} v_i^l$ with $v_l = \left(Q_l^\omega - Q_{l-1}^\omega\right) v$. Let $\Omega_{l,i} := \mathrm{supp}(\phi_i^l)$ and notice

$$\sum_{(k,j)>(l,i)} v_j^k = \left(v - Q_l^\omega v\right) + \sum_{j=i+1}^{n_l} v_j^l .$$

Then we have,

$$\begin{aligned}
\sum_{l=1}^{L} \sum_{i=1}^{n_l} \left| P_i^l \sum_{(k,j)>(l,i)} v_j^k \right|_{1,\omega}^2 &= \sum_{l=1}^{L} \sum_{i=1}^{n_l} \left| P_i^l \sum_{(k,j)>(l,i)} v_j^k \right|_{1,\omega,\Omega_{l,i}}^2 \\
&\le 2 \sum_{l=1}^{L} \sum_{i=1}^{n_l} \left(\left| P_i^l \left(v - Q_l^\omega v\right) \right|_{1,\omega,\Omega_{l,i}}^2 + \left| P_i^l \sum_{j=i+1}^{n_l} v_j^l \right|_{1,\omega,\Omega_{l,i}}^2 \right) \\
&\le 2 \sum_{l=1}^{L} \sum_{i=1}^{n_l} \left(\left| P_i^l \left(v - Q_l^\omega v\right) \right|_{1,\omega,\Omega_{l,i}}^2 + \left| \sum_{j=i+1}^{n_l} v_j^l \right|_{1,\omega,\Omega_{l,i}}^2 \right).
\end{aligned}$$

By quasi-uniformity of the triangulations, it is easy to see that

$$\sum_{i=1}^{n_l} \left| P_i^l \left(v - Q_l^\omega v\right) \right|_{1,\omega,\Omega_{l,i}}^2 \lesssim \left| P_l v - Q_l^\omega v \right|_{1,\omega}^2 ,$$

and by inverse inequality and quasi-uniformity of the triangulations

$$\begin{aligned}\sum_{i=1}^{n_l}\left|\sum_{j=i+1}^{n_l} v_j^l\right|_{1,\omega,\Omega_{l,i}}^2 &\lesssim \sum_{i=1}^{n_l}\sum_{j=i+1}^{n_l} h_l^{-2}\left\|v_j^l\right\|_{0,\omega,\Omega_{l,i}}^2 \lesssim h_l^{-2}\left\|v_l\right\|_{0,\omega}^2 \\ &= h_l^{-2}\left\|\left(Q_l^\omega - Q_{l-1}^\omega\right)v\right\|_{0,\omega}^2.\end{aligned}$$

Therefore, we get

$$c(v) \lesssim \sum_{l=0}^{L}\left|P_l v - Q_l^\omega v\right|_{1,\omega}^2 + \sum_{l=1}^{L} h_l^{-2}\left\|\left(Q_l^\omega - Q_{l-1}^\omega\right)v\right\|_{0,\omega}^2.$$

This completes the proof. □

From this lemma, in order to estimate the convergence rate of multigrid algorithm we only need the stability and approximation properties of the weighted L^2-projection Q_l^ω. According to Lemma 2.2.2, we have the following convergence result.

Lemma 2.3.7. *For the V-cycle algorithm defined above, we have the following convergence rate estimate:*

$$\left\|\left(I - P_0\right)\prod_{l=1}^{L}\prod_{i=1}^{n_l}\left(I - P_i^l\right)\right\|_A^2 = \frac{c_0}{1+c_0},$$

with

$$c_0 = \sup_{v\in\mathcal{V}}\inf_{v=v_0+\sum_{l=1}^{L}\sum_{i=1}^{n_l} v_i^l} c(v) \lesssim \min\left\{c_d(h)^2, \mathcal{J}(\omega)\right\}$$

where $c_{d}(h) = C \cdot \begin{cases} 1, & d = 1 \\ |\log h|, & d = 2 \\ h^{-\frac{1}{2}}, & d = 3 \end{cases}$ *and* $\mathcal{J}(\omega) = \frac{\max_m \omega_m}{\min_m \omega_m}$. *Consequently,*

$$\kappa(BA) \leq C_{0} \min\left\{c_{d}(h)^{2}, \mathcal{J}(\omega)\right\}.$$

Proof. To estimate c_{0}, for any $v \in \mathcal{V}$, we need to estimate the right hand side of (2.3.10). For the first term, by the stability inequality (2.2.3) of Q_{l}^{ω} we have

$$\begin{aligned} \left|P_{l}v - Q_{l}^{\omega}v\right|_{1,\omega} &\leq \left|P_{l}v\right|_{1,\omega} + \left|Q_{l}^{\omega}v\right|_{1,\omega} \\ &\lesssim |v|_{1,\omega} + c_{d}\left(h, h_{l}\right)|v|_{1,\omega} \\ &\lesssim c_{d}\left(h, h_{l}\right)|v|_{1,\omega}, \end{aligned}$$

that is,

$$\sum_{l=0}^{L}\left|P_{l}v - Q_{l}^{\omega}v\right|_{1,\omega}^{2} \lesssim \left(\sum_{l=0}^{L} c_{d}^{2}\left(h, h_{l}\right)\right)|v|_{1,\omega}^{2} \lesssim c_{d}(h)^{2}|v|_{1,\omega}^{2}.$$

For the second term, by the approximation inequality (2.2.2) of Q_{l-1}^{ω} ($l = 1, \cdots, L$),

$$\left\|Q_{l}^{\omega}v - Q_{l-1}^{\omega}v\right\|_{0,\omega} \leq \left\|v - Q_{l-1}^{\omega}v\right\|_{0,\omega} \lesssim h_{l-1}c_{d}\left(h, h_{l-1}\right)|v|_{1,\omega}.$$

Hence we have

$$\sum_{l=1}^{L} h_l^{-2} \left\| \left(Q_l^{\omega} - Q_{l-1}^{\omega} \right) v \right\|_{0,\omega}^2 \lesssim \left(\sum_{l=1}^{L} c_d^2 \left(h, h_{l-1} \right) \right) |v|_{1,\omega}^2 \lesssim c_d^2(h) \, |v|_{1,\omega}^2 .$$

Therefore, by the X-Z identity, we have $c_0 \lesssim c_d^2(h)$.

On the other hand, the estimate $c_0 \lesssim \mathcal{J}(\omega)$ can be obtained by switching to the case of constant weight and using the standard L^2 estimates in the above proof. This proves the convergence rate of multigrid V-cycle:

$$\rho \leq 1 - \frac{1}{1 + c_0}, \text{ with } c_0 \lesssim \min\{c_d(h)^2, \mathcal{J}(\omega)\}.$$

Finally, the estimate for $\kappa(BA)$ follows by the inequality (2.3.9):

$$\kappa(BA) \lesssim \min\left\{ c_d(h)^2, \mathcal{J}(\omega) \right\}.$$

This completes the proof. □

Remark 2.3.8. *When $d = 2$, the same result as Lemma 2.3.7 was proved in [25], and when $d = 3$, another proof of this lemma can be found in [117]. As we can see from Lemma 2.3.7, for $d = 3$, the convergence rate grows rapidly as $h \to 0$. The numerical results in Section 2.4 indicate that this convergence rate estimate is sharp.*

Alternatively, if we apply Lemma 2.2.4 in the subspace $\widetilde{\mathcal{V}}$, then by X-Z identity restricted on $\widetilde{\mathcal{V}}$ we can get an estimate on $\|I - BA\|_{A,\widetilde{\mathcal{V}}}$, which is the main result in this section.

Lemma 2.3.9. *In the subspace $\widetilde{\mathcal{V}}$, we have*

$$\|I - BA\|_{A,\widetilde{\mathcal{V}}} = \left\| \left(I - P_0\right) \prod_{l=1}^{L} \prod_{i=1}^{n_l} \left(I - P_i^l\right) \right\|_{A,\widetilde{\mathcal{V}}}^2 = \frac{\tilde{c}_0}{1+\tilde{c}_0},$$

with

$$\tilde{c}_0 = \sup_{v \in \widetilde{\mathcal{V}}} \inf_{v = v_0 + \sum_{l=1}^{L} \sum_{i=1}^{n_l} v_i^l} c(v) \lesssim |\log h|^2.$$

Consequently,

$$\kappa_{m_0}(BA) \leq C_1^2 |\log h|^2.$$

Proof. The proof is similar to that of Lemma 2.3.7. For any $v \in \widetilde{\mathcal{V}}$, we estimate the upper bound of $\tilde{c}_0$ as in (2.3.10). For the first term in (2.3.10), by the stability inequality (2.2.6) of Q_l^ω we have

$$\left| P_l v - Q_l^\omega v \right|_{1,\omega} \leq |v|_{1,\omega} + \left| Q_l^\omega v \right|_{1,\omega} \lesssim \left(1 + \left|\log h_l\right|^{\frac{1}{2}}\right) |v|_{1,\omega},$$

that is,

$$\sum_{l=0}^{L} \left| P_l v - Q_l^\omega v \right|_{1,\omega}^2 \lesssim \left(\sum_{l=0}^{L} \left|\log h_l\right| \right) |v|_{1,\omega}^2 \lesssim |\log h|^2 |v|_{1,\omega}^2.$$

For the second term in (2.3.10), by the approximation property (2.2.5) of Q_{l-1}^ω ($l = 1, \cdots, L$),

$$\left\| Q_l^\omega v - Q_{l-1}^\omega v \right\|_{0,\omega} \leq \left\| v - Q_{l-1}^\omega v \right\|_{0,\omega} \lesssim h_{l-1} \left|\log h_{l-1}\right|^{\frac{1}{2}} |v|_{1,\omega}.$$

Hence we have

$$\sum_{l=1}^{L} h_l^{-2} \left\| \left(Q_l^{\omega} - Q_{l-1}^{\omega} \right) v \right\|_{0,\omega}^2 \lesssim \left(\sum_{l=1}^{L} \left| \log h_{l-1} \right| \right) |v|_{1,\omega}^2 \lesssim |\log h|^2 |v|_{1,\omega}^2 .$$

By the X-Z identity, we obtain $\tilde{c}_0 \lesssim |\log h|^2$.

Then by minimax Lemma 2.1.4, we obtain

$$\lambda_{m_0+1}(BA) \geq \min_{0 \neq v \in \widetilde{\mathcal{V}}} \frac{a(BAv, v)}{a(v, v)} \geq \frac{1}{1 + \tilde{c}_0} \gtrsim |\log h|^{-2}.$$

Thus we get the estimate on the effective condition number of BA:

$$\kappa_{m_0}(BA) \lesssim |\log h|^2.$$

This completes the proof. □

Remark 2.3.10. *Similar to the BPX preconditioner, from Lemma 2.3.6, the approximation and stability properties of the weighted L^2-projection are essential. We summarize the convergence of multigrid V-cycle and the bounds of the condition number of the MGCG algorithm for different cases.*

(1) If the coefficients are mild, i.e., $\mathcal{J}(\omega) \leq C$, then multigrid V-cycle has a convergence rate of $\rho \leq 1 - \frac{1}{C+1}$ and the MGCG algorithm has a condition number $\kappa(BA) \leq C$, which are uniformly bounded with respect to jumps in coefficients and mesh size. Hence, both multigrid V-cycle and the MGCG algorithm converge uniformly.

(2) *If* $d = 1$, *or if the interface has no internal cross point (e.g. [27]), or if the coefficients satisfy the "quasi-monotonicity" (e.g. [45]), then multigrid* V*-cycle and the MGCG algorithm are also uniformly convergent.*

(3) *For the general case in* $d = 2$, *or if the coefficients are of "edge-type" in* $d = 3$ *(e.g. [93]), then* $\kappa(BA) \leq C^2 |\log h|^2$. *Another interesting case is when all subdomains contain nontrivial subset of the Dirichlet boundary (for* $d = 2, 3$, *see [112] for example). By the definition of the subspace* $\widetilde{\mathcal{V}}$, *we have* $m_0 \equiv 0$. *Thus, by Lemma 2.3.9, the effective condition number* $\kappa_{m_0}(BA) \equiv \kappa(BA) \leq C^2 |\log h|^2$. *In these cases, by* (2.1.3) *the convergence rate of the MGCG algorithm can be bounded by* $1 - \frac{2}{C|\log h|+1}$*; and according to Lemma 2.3.7, the convergence rate of multigrid* V*-cycle is bounded by* $\rho \leq 1 - \frac{1}{C|\log h|^2+1}$. *We observe that the convergence rate of the MGCG algorithm is a little better than multigrid* V*-cycle algorithm in this case.*

(4) *For the worst case, when* $d = 3$, *we have* $\kappa(BA) \lesssim h^{-1}$, *which grows rapidly when* $h \to 0$. *The convergence rate* ρ *of multigrid* V*-cycle can be bounded by* $\rho \leq 1 - \frac{1}{1+Ch^{-1}}$. *In terms of the number of levels* L, *since* $h \eqsim 2^{-L}$, *we have* $\rho \leq 1 - \frac{1}{1+C2^L}$. *This convergence rate shows that multigrid* V*-cycle converges* uniformly, *provided that the number of levels* L *is fixed. We also notice that these estimates are independent of the coefficients. The numerical justification is given in Section 2.4.*

On the other hand, because ρ *approaches to 1 rapidly as* $h \to 0$, *a small increment of* L *could cause multigrid method to converge extremely slowly. Therefore, we*

consider the MGCG algorithm, and we show that it behaves identically to the BPX PCG in the following theorem.

Theorem 2.3.11. *Let $u \in \mathcal{V}$ be the exact solution to equation (2.1.1) and $u_k \in \mathcal{V}$, $k = 0, 1, 2, \ldots$ be the solution sequence of the MGCG algorithm. Then we have*

$$\frac{\left\|u - u_k\right\|_A}{\left\|u - u_0\right\|_A} \leq 2\left(\frac{C_0}{h} - 1\right)^{m_0}\left(1 - \frac{2}{C_1|\log h| + 1}\right)^{k-m_0}, \quad \text{for } k \geq m_0$$

where C_0 and C_1 are constants independent of coefficients and mesh. Moreover, given a tolerance $\epsilon < 1$, the number of iterations needed for $\frac{\left\|u-u_k\right\|_A}{\left\|u-u_0\right\|_A} \leq \epsilon$ satisfies

$$k \geq m_0 + \left(\log\left(\frac{2}{\epsilon}\right) + m_0 \log\left(\frac{C_0}{h} - 1\right)\right)/c_0(h)$$

where $c_0(h) = \log\left(\frac{C_l|\log h|+1}{C_l|\log h|-1}\right)$.

Proof. By Lemma 2.3.7, we have $\kappa(BA) \leq c_d(h)$. The conclusion then follows directly from Lemma 2.3.9 and inequality (2.1.5). □

Same as the BPX PCG algorithm, the asymptotic convergence rate of the MGCG algorithm is $1 - \frac{C}{|\log h|}$, which is independent of the coefficients and robust with respect to the mesh size. Moreover, in comparison to Theorem 2.1.10, the estimate in Theorem 2.3.4 and 2.3.11 is not only significantly better asymptotically, it is also independent of the jump $\mathcal{J}(\omega)$.

2.4 Numerical Results

In this section, we present some numerical experiments to demonstrate the theoretical results in the previous sections. The implementation of the BPX preconditioner and multigrid methods are standard, and can be found in a lot of literature (for example [56, 122, 33]). Also, the implementation of the PCG algorithm can be found in many textbooks (for example [75, 54, 97, 91]).

According to Lemma 2.3.2 and 2.3.7, and inspired by [118, 93], we consider solving the model equation (2.0.1) on the unit cube $\Omega = (0,1)^3$ with homogeneous Dirichlet boundary conditions. Let the coefficient ω to be constants $\omega_1 = \omega_2 = 1$ and $\omega_3 = \epsilon$ on the three subdomains Ω_1, Ω_2 and Ω_3 respectively (see Figure 2.1), where

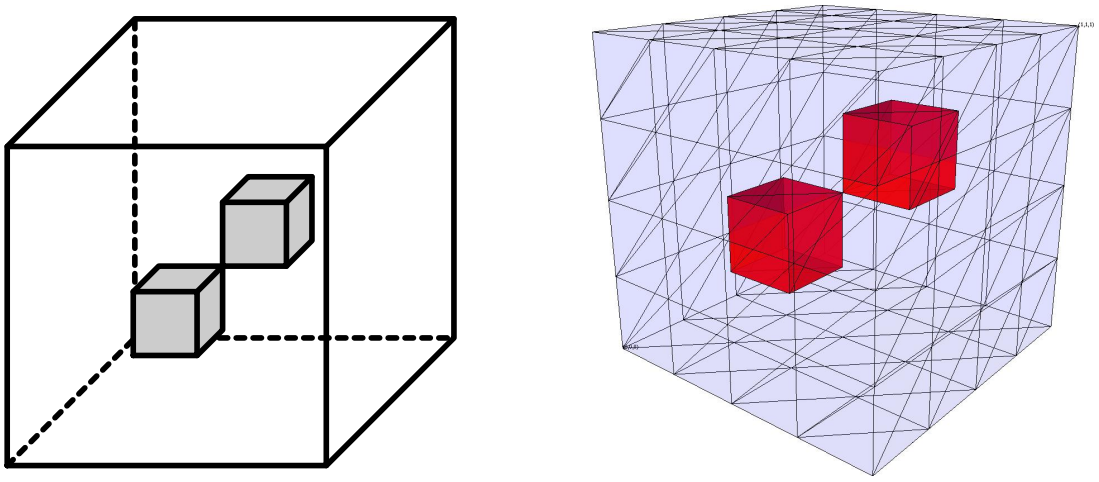

Fig. 2.1. Jump domains and the triangulation

$$\Omega_1 = (0.25, 0.5) \times (0.25, 0.5) \times (0.25, 0.5),$$

$$\Omega_2 = (0.5, 0.75) \times (0.5, 0.75) \times (0.5, 0.75),$$

and $\Omega_3 = \Omega \setminus (\overline{\Omega}_1 \cup \overline{\Omega}_2)$. Thus, the jump of coefficients is $\mathcal{J}(\omega) = \epsilon^{-1}$. The domain Ω is triangulated by uniform refinements, with the initial mesh size $h_0 \approx 2^{-2}$. The numerical experiments are performed by using the stopping criteria $\frac{\|r_k\|}{\|r_0\|} < 10^{-12}$, where r_k is the residual of k-th iteration. For multigrid V-cycle and W-cycle, we use one step point Gauss-Seidel as the pre-smoother and the post-smoother on each fine level, and use exact solver on the coarsest level. For BPX preconditioner, we use one step symmetric Gauss-Seidel iteration as the smoother, and use exact solver on the coarsest level.

According to Lemma 2.3.7, the asymptotic convergence rate ρ of multigrid method is $1 - Ch$. Table 2.1 shows the estimated convergence rate ρ of multigrid V-cycle and W-cycle when $\epsilon = 10^{-8}$. From Table 2.1, we observe that the convergence rate ρ of multi-

Levels	0	1	2	3	4	5	6
h	2^{-2}	2^{-3}	2^{-4}	2^{-5}	2^{-6}	2^{-7}	2^{-8}
V-cycle	0	0.714	0.876	0.945	0.974	0.988	0.994
W-cycle	0	0.714	0.822	0.873	0.901	0.917	0.926

Table 2.1. Convergence rate ρ of multigrid V-cycle and W-cycle ($\epsilon = 10^{-8}$)

grid methods is deteriorated by the number of levels. Figure 2.2 shows the relationship between the convergence rate ρ and the mesh size h of multigrid V-cycle. Theoretically,

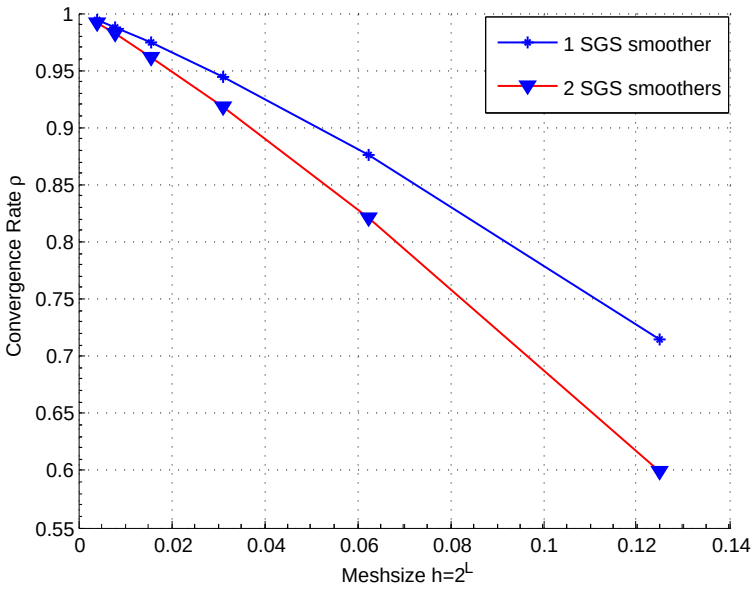

Fig. 2.2. Convergence rate ρ of multigrid V-cycle

we expect that $1 - \rho \propto h$. As we can see from Figure 2.2, ρ approaches to 1 almost linearly as $h \to 0$, which indicates that the convergence rate estimate in Lemma 2.3.7 is sharp. Therefore, the estimate on the condition number $\kappa(BA)$ is also sharp. The comparison of multigrid V-cycle and the W-cycle in Table 2.1 shows that the convergence rate of multigrid W-cycle has no substantial improvement. Thus in the following numerical experiments of the MGCG algorithm, we list the results for multigrid V-cycle preconditioner only. One can expect that multigrid W-cycle has similar behavior.

Table 2.2 shows the estimated convergence rate of multigrid V-cycle with re-

		i (such that $\epsilon = 10^{-i}$)					
Levels	h	0	2	4	6	8	10
1	2^{-3}	0.346	0.667	0.714	0.714	0.714	0.714
2	2^{-4}	0.438	0.807	0.875	0.876	0.876	0.876
3	2^{-5}	0.467	0.867	0.944	0.945	0.945	0.945
4	2^{-6}	0.470	0.895	0.973	0.974	0.974	0.974
5	2^{-7}	0.477	0.908	0.987	0.988	0.988	0.988
6	2^{-8}	0.477	0.915	0.993	0.994	0.994	0.994

Table 2.2. Multigrid V-cycle convergence rate v.s. jump and level

spect to different coefficients $\epsilon = 10^{-i}$, $i = 0, 2, \cdots, 10$ (rows) and different levels $L = 1, 2, \cdots, 6$ (columns). The last four numbers for each row in this table are almost identical. This demonstrates that for a fixed number of levels, the convergence rate ρ is a constant (independent of jump). Moreover we can see that, the convergence rate

of multigrid V-cycle deteriorates rapidly with respect to the jump coefficients. Actually, when $\epsilon \leq 10^{-2}$ i.e. $i \geq 2$, multigrid V-cycle is unfavorable.

Table 2.3 shows the number of iterations of conjugate gradient method with the Jacobi, BPX, multigrid V-cycle preconditioners (MGCG) when $\epsilon = 10^{-8}$. For Jacobi

Levels	0	1	2	3	4	5	6
h	2^{-2}	2^{-3}	2^{-4}	2^{-5}	2^{-6}	2^{-7}	2^{-8}
Jacobi PCG	13	46	151	319	639	> 1000	> 1000
BPX PCG	2	25	39	44	58	64	70
MGCG	2	15	18	21	25	25	25

Table 2.3. Iterations of PCG algorithms

PCG algorithm, the iteration number doubles, which coincides with Theorem 2.1.7. Comparing Table 2.3 with Table 2.1, we observe that BPX PCG algorithm or MGCG algorithm is much faster and more robust than multigrid solver itself in the presence of a large jump.

Concerning the eigenvalue distribution of the preconditioned system BA, we estimate the eigenvalues from the conjugate gradient coefficients (see Saad [97]). Figure 2.3 shows the eigenvalue distribution of the BPX and multigrid V-cycle preconditioned systems for mesh size $h = 2^{-5}$ when $\epsilon = 10^{-8}$. We observe that there is only one small eigenvalue, which coincides with the theoretical result that there are at most two small eigenvalues. Table 2.4 shows the condition number and the effective condition number for the BPX and multigrid V-cycle preconditioned systems. These results shows

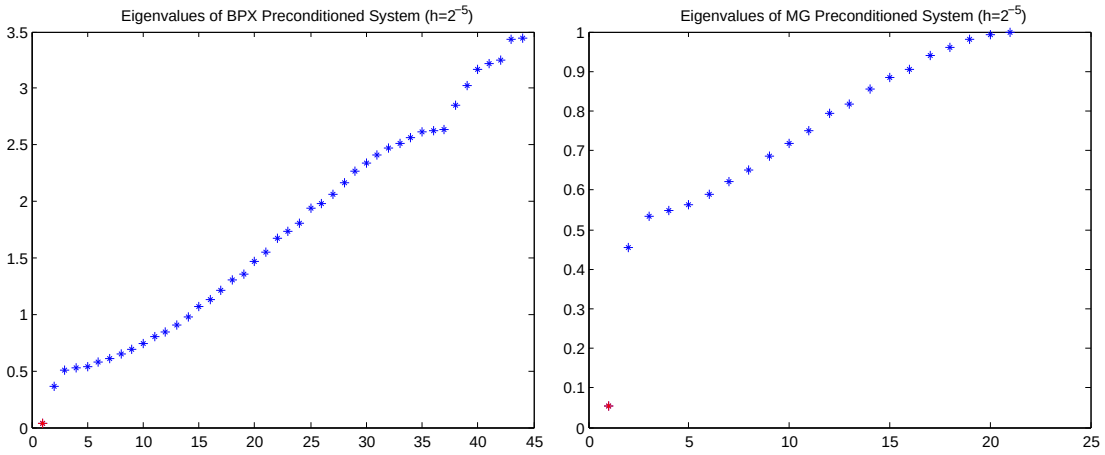

Fig. 2.3. Eigenvalue distributions

Levels	h	BPX		MG	
0	2^{-2}	$\kappa(BA)$	$\kappa_2(BA)$	$\kappa(BA)$	$\kappa_2(BA)$
1	2^{-3}	9.3502	4.4277	3.4981	1.6794
2	2^{-4}	31.2900	7.2766	8.0547	2.0200
3	2^{-5}	85.9480	9.5111	18.0130	2.2029
4	2^{-6}	210.8800	11.1127	39.0490	2.3036
5	2^{-7}	482.7100	12.2524	82.3490	2.4690
6	2^{-8}	1056.8000	13.6131	170.4500	2.7796

Table 2.4. The condition number $\kappa(BA)$ and effective condition number $\kappa_2(BA)$

that although the condition number $\kappa(BA)$ may deteriorate rapidly, the effective condition number $\kappa_2(BA)$ is quite robust, which coincides with the theoretical results of Lemma 2.3.2 and Lemma 2.3.7-2.3.9. Figure 2.4 shows the effective condition number versus number of levels of the BPX and multigrid V-cycle preconditioned systems.

For a fixed mesh size h, Table 2.5 shows the number of iterations of different methods with respect to the variation of ϵ. Here, we fix the mesh size to be $h = 2^{-6}$, and

i	0	2	4	6	8	10
MG	31	140	336	342	342	342
Jacobi PCG	99	143	173	283	329	414
BPX PCG	37	46	51	54	58	66
MGCG	16	19	21	21	21	21

Table 2.5. Number of iterations vs. jumps

vary the coefficient $\epsilon = 10^{-i}$ for $i = 0, 2, 4, \cdots, 10$. When the jump is not severe, that is, when i is small, the number of iterations of multigrid V-cycle grows with respect to the jump size. While at some point, when jump size is large, say $i > 4$, the convergence rate of multigrid is $1 - \frac{C}{\min\left\{c_d(h), \mathcal{J}(\omega)\right\}} = 1 - \frac{C}{c_d(h)}$ which is a constant for the fixed mesh size. This explains why the numbers of iterations of MG are the same when $i = 6, 8$ and 10. The number of iterations of Jacobi PCG algorithm grows with respect to the jump size. This confirms the deterioration of $\kappa\left(\mathcal{D}^{-1}\mathcal{A}\right) \lesssim \mathcal{J}(\omega)h^{-2}$ where $\mathcal{J}(\omega) = \epsilon^{-1} = 10^{i}$ grows rapidly with respect to i. On the other hand, the BPX PCG and the MGCG algorithms are very robust with respect to the growth of the jump.

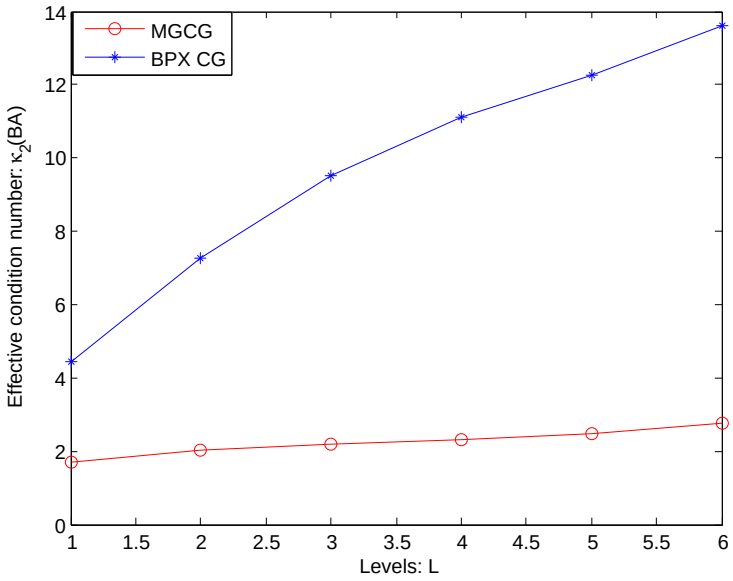

Fig. 2.4. Effective condition number $\kappa_2(BA)$

2.5 Overlapping Domain Decomposition Preconditioner

In this section, we consider a two level overlapping domain decomposition method. Specifically, the domain Ω is triangulated by a fine grid $\mathcal{T}_h$ with mesh size h, and also a coarse grid $\mathcal{T}_H$ with mesh size H. For simplicity, we assume that each element in $\mathcal{T}_H$ is a union of some elements in $\mathcal{T}_h$, and we also assume that $\mathcal{T}_H$ is aligned with the interfaces. Let $\mathcal{V} := \mathcal{V}_h$ and $\mathcal{V}_0 := \mathcal{V}_H$ be the piecewise linear continuous finite element spaces on $\mathcal{T}_h$ and $\mathcal{T}_H$, respectively.

We partition the domain Ω into L nonoverlapping subdomains Ω_l^0 $(l = 1, \ldots, L)$, such that $\overline{\Omega} = \cup_{l=1}^{L} \overline{\Omega}_l^0$. Enlarge each subdomain Ω_l^0 to Ω_l' in such a way that the restriction of triangulation $\mathcal{T}_h$ on Ω_l' is also a triangulation of Ω_l' itself, and Ω_l' consists of all points in Ω within a distance of CH from Ω_l^0. Here, we make no assumption on the relationship between this partition and the jump regions Ω_m $(m = 1, \ldots, M)$. Based on this partition, a natural decomposition of the finite element space $\mathcal{V}$ is

$$\mathcal{V} = \sum_{l=1}^{L} \mathcal{V}_l, \quad \text{where } \mathcal{V}_l := \left\{ v \in \mathcal{V} : v = 0 \text{ in } \Omega \setminus \Omega_l' \right\}.$$

The coarse space $\mathcal{V}_0$ provides the global coupling between subdomains. Obviously, we have the space decomposition

$$\mathcal{V} = \sum_{l=0}^{L} \mathcal{V}_l.$$

As in Section 2.3, for each $l = 0, 1, \ldots, L$, we define the projections P_l, $Q_l^\omega : \mathcal{V} \to \mathcal{V}_l$ by

$$a\left(P_l u, v_l\right) = a\left(u, v_l\right), \quad \left(Q_l^\omega u, v_l\right)_{0,\omega} = \left(u, v_l\right)_{0,\omega}, \quad \forall v_l \in \mathcal{V}_l,$$

and define the operator $A_l : \mathcal{V}_l \to \mathcal{V}_l$ by

$$\left(A_l u_l, v_l\right)_{0,\omega} = a\left(u_l, v_l\right), \ \ \forall u_l, v_l \in \mathcal{V}_l.$$

For convenience, we denote $A = A_L$ and $Q^{\omega}_{-1} = 0$. It follows from the definitions that

$$Q^{\omega}_{l} A = A_l P_l, \text{ and } Q^{\omega}_{l} Q^{\omega}_{k} = Q^{\omega}_{k} Q^{\omega}_{l} = Q^{\omega}_{k} \text{ for } k \leq l.$$

The additive Schwarz preconditioner is defined by

$$B = \sum_{l=0}^{L} A_l^{-1} Q^{\omega}_{l}. \tag{2.5.1}$$

Obviously, we have

$$BA = \sum_{l=0}^{L} A_l^{-1} Q^{\omega}_{l} A = \sum_{l=0}^{L} P_l.$$

Relation between additive Schwarz and diagonal scaling In [55], it was proved that the additive Schwarz preconditioner and diagonal scaling (Jacobi preconditioner) have the following relationship:

Proposition 2.5.1 ([55]). *There exist constants $C_1 \geq 1$ and $C_2 > 0$ which depend only on the connectivity of the mesh such that, for all $k = 1, \cdots, n$,*

$$\lambda_k\left(D^{-1} A\right) \leq C_1 \lambda_k(BA) \leq C_2.$$

By using this proposition, we can bound the

$$\lambda_{m_0+1}(BA) \geq \lambda_{m_0+1}\left(D^{-1}A\right) \gtrsim h^2.$$

From this relationship, as a result of Theorem 2.1.7, we obtain that the m_0-th effective condition number $\kappa_{m_0}(BA) \lesssim h^{-2}$ is independent of the coefficients. However, this estimate is too rough. It was pointed out that $\lambda_{m_0+1}(BA)$ could be much better than this estimate, but no rigorous proof was given in [55]. In the following subsection, we analyze the eigenvalue distribution of BA and prove the robustness of the additive Schwarz preconditioner (2.5.1).

Eigenvalue analysis of BA By a standard coloring technique [38, 104] , we can easily prove $\lambda_{\max}(BA) \leq C$, where C is independent of the mesh and coefficients. The analysis of the lower bound of eigenvalues relies on certain stable decomposition.

Recall that $\widetilde{\mathcal{V}} \subset \mathcal{V}$ is a subspace of dimension $\dim\left(\widetilde{\mathcal{V}}\right) = \dim(\mathcal{V}) - m_0$ on which the Poincaré-Friedrichs inequality (2.2.4) holds for any $v \in \widetilde{\mathcal{V}}$. Then we have the following stable decomposition result.

Lemma 2.5.2. *For any $v \in \mathcal{V}$, there exist $v_l \in \mathcal{V}_l$ such that $v = \sum_{l=0}^{L} v_l$ and*

$$\sum_{l=0}^{L} a\left(v_l, v_l\right) \lesssim c_d(h, H)^2 a(v, v). \tag{2.5.2}$$

For any $v \in \widetilde{\mathcal{V}}$, *there are* $v_l \in \mathcal{V}_l$ *that satisfy* $v = \sum_{l=0}^{L} v_l$ *and*

$$\sum_{l=0}^{L} a\left(v_l, v_l\right) \lesssim |\log H| a(v, v). \tag{2.5.3}$$

Furthermore, if each subdomain Ω_m *satisfies length*$(E) \eqsim H_0$ *for any edge* E *of* Ω_m, *then for any* $v \in \widetilde{\mathcal{V}}$, *there are* $v_l \in \mathcal{V}_l$ *that satisfy* $v = \sum_{l=0}^{L} v_l$ *and*

$$\sum_{l=0}^{L} a\left(v_l, v_l\right) \lesssim \left(1 + \log \frac{H_0}{H}\right) a(v, v). \tag{2.5.4}$$

Especially, if $H \eqsim H_0$ *then* $\sum_{l=0}^{L} a\left(v_l, v_l\right) \lesssim a(v, v)$.

Proof. The ideas to prove inequality (2.5.2)-(2.5.4) are the same. The main difference is that we use different properties of weighted L^2-projection in Section 2.2. Here, we follow the idea from [120].

Let $\{\theta_l\}_{l=1}^{L}$ be a partition of unity defined on Ω satisfying $\sum_{l=1}^{L} \theta_l = 1$, and for $l = 1, 2, \cdots, L$

$$\text{supp}\theta_l \subset \Omega_l' \cup \partial\Omega, \;\; 0 \leq \theta_l \leq 1, \;\; \left\|\nabla\theta_l\right\|_{\infty, \Omega_l^0} \leq CH^{-1},$$

where $\|\cdot\|_{\infty,O}$ denote the L^∞ norm of a function defined on a subdomain O. The construction of such a partition of unity is standard. A partition $v = \sum_{l=0}^{L} v_l$ for $v_l \in \mathcal{V}_l$ can then be obtained by taking $v_0 = Q_0^\omega v$ and

$$v_l = I_h\left(\theta_l\left(v - Q_0^\omega v\right)\right) \in \mathcal{V}_l, \; l = 1, \cdots, L,$$

where I_h is the nodal value interpolant on $\mathcal{V}$.

From this decomposition, we prove that the inequalities (2.5.2) and (2.5.3) hold. For any $\tau \in \mathcal{T}_h$, note that

$$\left\|\theta_l - \overline{\theta}_{l,\tau}\right\|_{L^\infty(\tau)} \lesssim h \left\|\nabla\theta_l\right\|_{L^\infty(\tau)} \lesssim \frac{h}{H}.$$

Let $w = v - Q_0^\omega v$, and by inverse inequality

$$\begin{aligned} \left|v_l\right|_{1,\tau} &\leq \left|\overline{\theta}_{l,\tau} w\right|_{1,\tau} + \left|I_h\left(\theta_l - \overline{\theta}_{l,\tau}\right) w\right|_{1,\tau} \\ &\lesssim |w|_{1,\tau} + h^{-1}\left\|I_h\left(\theta_l - \overline{\theta}_{l,\tau}\right) w\right\|_{0,\tau}. \end{aligned}$$

It is easy to show that

$$\left\|I_h\left(\theta_l - \overline{\theta}_{l,\tau}\right) w\right\|_{0,\tau} \lesssim \frac{h}{H}\|w\|_{0,\tau}.$$

Consequently,

$$\left|v_l\right|_{1,\tau}^2 \lesssim |w|_{1,\tau}^2 + \frac{1}{H^2}\|w\|_{0,\tau}^2.$$

Summing over all $\tau \in \mathcal{T}_h \cap \Omega_l^0$ with appropriate weights yields

$$\left|v_l\right|_{1,\omega}^2 = \left|v_l\right|_{1,\omega,\Omega_l^0}^2 \lesssim |w|_{1,\omega,\Omega_l^0}^2 + \frac{1}{H^2}\|w\|_{0,\omega,\Omega_l^0}^2,$$

and

$$\begin{aligned}\sum_{l=1}^{L} a\left(v_l, v_l\right) &\lesssim \sum_{l=1}^{L} \left|v_l\right|^2_{1,\omega,\Omega_l} \lesssim \sum_{l=1}^{L} \left(|w|^2_{1,\omega,\Omega_l^0} + \frac{1}{H^2}\|w\|^2_{0,\omega,\Omega_l^0} \right) \\ &\lesssim \left(\left| v - Q_0^{\omega} v \right|^2_{1,\omega} + \frac{1}{H^2} \left\| v - Q_0^{\omega} v \right\|^2_{0,\omega} \right).\end{aligned}$$

From this inequality, for any $v \in \mathcal{V}$, applying Lemma 2.2.2 we obtain inequality (2.5.2). Applying Lemma 2.2.4 for $v \in \widetilde{\mathcal{V}}$ gives us inequality (2.5.3), and applying Lemma 2.2.6 for any $v \in \widetilde{\mathcal{V}}$ gives inequality (2.5.4). This completes the proof. □

Based on this lemma, we obtain the following eigenvalue distribution of BA.

Theorem 2.5.3. *For the additive Schwarz preconditioner B defined by* (2.5.1)*, the eigenvalues of BA satisfy*

$$\lambda_{\min}(BA) \geq c_d(h,H)^{-2}, \ \ \lambda_{m_0+1}(BA) \geq C|\log H|^{-1}, \ \ \textit{and} \ \ \lambda_{\max}(BA) \leq C.$$

Furthermore, when $d = 3$ and if each subregion Ω_m is a polyhedral domain with each edge of length H_0, then

$$\lambda_{m_0+1}(BA) \geq C\left(1 + \log\frac{H_0}{H}\right)^{-1}.$$

Especially, if $H \eqsim H_0$ then $\lambda_{m_0+1}(BA) \geq C$.

Proof. Noticing that $BA = \sum_{l=0}^{L} P_l$, by a standard coloring argument (see [38, 104] for example), we have

$$\lambda_{\max}(BA) \leq C.$$

For the minimum eigenvalue, for any $v \in \mathcal{V}$, we consider the decomposition $v = \sum_{l=0}^{L} v_l$ as in Lemma 2.5.2. By the Schwarz inequality, we obtain

$$\begin{aligned} a(v,v) &= \sum_{l=0}^{L} a\left(v_l, v\right) = \sum_{l=0}^{L} a\left(v_l, P_l v\right) \\ &\leq \left(\sum_{l=0}^{L} a\left(v_l, v_l\right)\right)^{\frac{1}{2}} \left(\sum_{l=0}^{L} a\left(P_l v, P_l v\right)\right)^{\frac{1}{2}} \\ &= \left(\sum_{l=0}^{L} a\left(v_l, v_l\right)\right)^{\frac{1}{2}} \left(a\left(BAv, v\right)\right)^{\frac{1}{2}}. \end{aligned}$$

Applying inequality (2.5.2), we get

$$a(v,v) \leq c_d(h,H) a(v,v)^{\frac{1}{2}} a\left(BAv, v\right)^{\frac{1}{2}}, \quad \forall v \in \mathcal{V}.$$

This implies

$$\lambda_{\min}(BA) \geq c_d(h,H)^{-2}.$$

On the other hand, by (2.5.3), we have

$$a(v,v) \lesssim |\log H|^{\frac{1}{2}} a(v,v)^{\frac{1}{2}} a\left(BAv, v\right)^{\frac{1}{2}}, \forall v \in \widetilde{\mathcal{V}}.$$

By minimax Lemma 2.1.4, and noticing that $\dim\left(\widetilde{\mathcal{V}}^{\perp}\right) = m_0$, we obtain

$$\lambda_{m_0+1}(BA) \gtrsim |\log H|^{-1}.$$

Similarly, from (2.5.4) and minimax Lemma 2.1.4,

$$\lambda_{m_0+1}(BA) \geq C\left(1+\log\frac{H_0}{H}\right)^{-1}$$

when each edge of the subregions satisfies $\text{length}(E) \eqsim H_0$. This completes the proof. □

Remark 2.5.4. *Theorem 2.5.3 gives a direct proof of the robustness of overlapping domain decomposition preconditioner for the variable coefficient problem* (2.0.1)*. That is, the preconditioned system BA has only m_0 small eigenvalues, and the effective condition number of BA is bounded by $C|\log H|$, or $C\left(1+\log\frac{H_0}{H}\right)$ if each subregion is a polyhedral domain whose boundary edges have length $\eqsim H_0$. Especially, when $H_0 \eqsim H$, the effective condition number is bounded uniformly.*

The estimates of the maximum and minimum eigenvalues of BA are standard, and can be found in many references (see for example [38, 46, 104]). From the above theorem, we know that when $d = 2$, $\kappa(BA) \leq C\left(1+\log\frac{H}{h}\right)$ which is also quite robust. But, for the worst case in $d = 3$, we have $\kappa(BA) \leq C\frac{H}{h}$, which grows rapidly as $h \to 0$. In this case, we have the following convergence estimate for the PCG algorithm.

Theorem 2.5.5. *In $\mathbb{R}^3$, assume that each subregion Ω_m $(m = 1, \cdots, M)$ is a polyhedral domain with each edge of length H_0. Let $u \in \mathcal{V}$ be the exact solution to equation* (2.1.1)

and $\left\{u_k : k = 0, 1, 2, \ldots\right\}$ *be the solution sequence of the PCG algorithm. Then we have*

$$\frac{\left\|u - u_k\right\|_A}{\left\|u - u_0\right\|_A} \leq 2\left(\frac{C_0 H}{h} - 1\right)^{m_0} \rho^{k-m_0} \quad \text{for } k \geq m_0, \tag{2.5.5}$$

where $\rho = 1 - \frac{2}{C\sqrt{1+\log\frac{H_0}{H}}+1} < 1$ *and* C_0, C *are constants independent of coefficients and mesh size. Moreover, given a tolerance* $0 < \epsilon < 1$*, the number of iterations needed for* $\frac{\left\|u-u_k\right\|_A}{\left\|u-u_0\right\|_A} \leq \epsilon$ *satisfies*

$$k \geq m_0 + \left(\log\left(\frac{2}{\epsilon}\right) + m_0 \log\left(\frac{C_0 H}{h} - 1\right)\right) / |\log(\rho)|.$$

Especially, if $H \eqsim H_0$ *then the asymptotic convergence rate* ρ *of the PCG algorithm is uniformly bounded with respect to both jumps in coefficients and mesh size.*

Proof. Theorem 2.5.5 is a direct consequence of inequalities (2.1.5), (2.1.6) and Theorem 2.5.3. □

Remark 2.5.6. *From Theorem 2.5.5, the convergence rate estimate* (2.5.5) *contains* $\left(\frac{C_0 H}{h} - 1\right)^{m_0}$ *which depends on the condition number* $\kappa(BA) = \frac{C_0 H}{h}$*. However, since* m_0 *is a fixed number, the asymptotic convergence rate is bounded by* $\rho < 1$ *which is uniform with respect to the coefficients and the underlying mesh* $\mathcal{T}_h$*.*

Without the assumption on the subdomains Ω_m $(m = 1, \cdots, M)$, *Theorem 2.5.5 becomes,*

$$\frac{\left\|u - u_k\right\|_A}{\left\|u - u_0\right\|_A} \leq 2\left(\frac{C_0 H}{h} - 1\right)^{m_0}\left(1 - \frac{2}{C_1\sqrt{|\log H|} + 1}\right)^{k-m_0} \quad \textit{for } k \geq m_0.$$

In this case, the number of iterations needed for $\frac{\left\|u-u_k\right\|_A}{\left\|u-u_0\right\|_A} < \epsilon$ *with the given tolerance* $0 < \epsilon < 1$ *satisfies,*

$$k \geq m_0 + \left(\log\left(\frac{2}{\epsilon}\right) + m_0 \log\left(\frac{C_0 H}{h} - 1\right)\right)/c_0(H),$$

where $c_0(H) = \log\left(\frac{C_l\sqrt{|\log H|}+1}{C_l\sqrt{|\log H|}-1}\right)$.

Remark 2.5.7. *By similar arguments, the results above can be generalized to the* inexact solver additive Schwarz preconditioners *(e.g. [38]) and also to the* multilevel additive Schwarz preconditioners *(e.g. [129]).*

2.6 Matrix Representations

In this section, we discuss the algebraic representations of these preconditioners and the relationship between the operator forms defined in (2.3.2) (or (2.5.1)) and their matrix forms. We intend to show that introducing the weighted L^2-projections Q_l^ω is for theoretical purpose only. In other words, the algebraic representation of the preconditioners introduced in this chapter is independent of the definition of Q_l^ω. Here we

restrict ourself to the additive preconditioners (BPX preconditioner in Section 2.3 or domain decomposition preconditioner in Section 2.5) only.

Let $\mathcal{V}$ be the finite element space, with the nodal basis $\left\{\phi_1, \ldots, \phi_n\right\}$. Then given any function $v \in \mathcal{V}$, there exists a unique $\nu \in \mathbb{R}^n$ such that

$$v = \sum_{i=1}^{n} \nu_i \phi_i.$$

Let $\tilde{v} = \nu$ be the vector representation of v. Given two linear vector spaces $\mathcal{V}$ and $\mathcal{W}$ and a linear operator $A \in \mathcal{L}(\mathcal{V}, \mathcal{W})$, the matrix representation of A with respect to a basis $\left\{\phi_1, \ldots, \phi_n\right\}$ of $\mathcal{V}$ and a basis $\left\{\psi_1, \ldots, \psi_k\right\}$ of $\mathcal{W}$ is the matrix $\tilde{A} = \left(\tilde{a}_{ij}\right) \in \mathbb{R}^{k \times n}$ satisfying

$$A\phi_j = \sum_{i=1}^{k} \tilde{a}_{ij} \psi_i, \text{ for } 1 \leq j \leq n.$$

From this definition, it is not difficult to show that for any two operators $A, B \in \mathcal{L}(\mathcal{V})$ and $v \in \mathcal{V}$, we have

$$\widetilde{AB} = \widetilde{A}\widetilde{B} \text{ and } \widetilde{Av} = \tilde{A}\tilde{v}. \tag{2.6.1}$$

Given any subspace $\mathcal{V}_0 \subset \mathcal{V}$ equipped with a basis $\left\{\phi_1^0, \ldots, \phi_{n_0}^0\right\}$, there exists a unique matrix $\mathcal{I}_0 = (e_{ij}) \in \mathbb{R}^{n \times n_0}$ such that

$$\phi_j^0 = \sum_{i=1}^{n} e_{ij} \phi_i, \text{ for } j = 1, \ldots, n_0.$$

The matrix $\mathcal{I}_0$ is the matrix representation of the natural inclusion operator $I_0 : \mathcal{V}_0 \to \mathcal{V}$. $\mathcal{I}_0$ is known a *prolongation* matrix, while its transpose $\mathcal{I}_0^t$ is known as a *restriction* matrix.

Define the mass matrix $\mathbb{M}$ and the stiffness matrix $\mathcal{A}$ by

$$\mathbb{M} = \left(\left(\phi_i, \phi_j \right)_{0,\omega} \right)_{n\times n} \text{ and } \mathcal{A} = \left(\left(A\phi_i, \phi_j \right)_{0,\omega} \right)_{n\times n}.$$

By definition, we have $(u,v)_{0,\omega} = (\tilde{u}, \mathbb{M}\tilde{v})_{\ell^2}$, where $(\cdot,\cdot)_{\ell^2}$ is the standard Euclidian inner product. It is straightforward to show that $\mathcal{A} = \mathbb{M}\tilde{A}$. Obviously, the prolongation and restriction matrices satisfy the following important relation:

$$\left(u, v_0 \right)_{0,\omega} = \left(\mathbb{M}\tilde{u}, \mathcal{I}_0 \tilde{v}_0 \right)_{\ell^2} = \left(\mathcal{I}_0^t \mathbb{M}\tilde{u}, \tilde{v}_0 \right)_{\ell^2}.$$

For the weighted L^2-projection $Q_l^\omega : \mathcal{V} \to \mathcal{V}_l$, we have by definition

$$\left(u, v_l \right)_{0,\omega} = \left(Q_l^\omega u, v_l \right)_{0,\omega} = \left(\widetilde{Q_l^\omega u}, \mathbb{M}_l \tilde{v}_l \right)_{\ell^2} = \left(\widetilde{Q_l^\omega} \tilde{u}, \mathbb{M}_l \tilde{v}_l \right)_{\ell^2},$$

where $\mathbb{M}_l$ is the mass matrix on $\mathcal{V}_l$. On the other hand, noticing that

$$\left(u, v_l \right)_{0,\omega} = (u, I_l v_l)_{0,\omega} = \left(\tilde{u}, \mathbb{M}\widetilde{I_l v_l} \right)_{\ell^2} = \left(\tilde{u}, \mathbb{M}\mathcal{I}_l \tilde{v}_l \right)_{\ell^2},$$

we deduce that the matrix representation of the weighted L^2-projection Q_l^ω, denoted by $\mathcal{Q}_l^\omega$ is

$$\mathcal{Q}_l^\omega = {\mathbb{M}_l}^{-1} \mathcal{I}_l^t \mathbb{M}. \tag{2.6.2}$$

For the given smoother R_l, let $\mathcal{R}_l$ be its matrix representation. To derive the algebraic representation of the preconditioner

$$B = \sum_{l=0}^{L} R_l Q_l^{\omega} = \sum_{l=0}^{L} I_l R_l Q_l^{\omega},$$

we apply (2.6.1) and (2.6.2) to obtain

$$\begin{aligned} \widetilde{B} &= \sum_{l=0}^{L} \widetilde{I}_l \widetilde{R}_l \widetilde{Q}_l^{\omega} = \sum_{l=0}^{L} \mathcal{I}_l \left(\mathcal{R}_l \mathbb{M}_l \right) \left(\mathbb{M}_l^{-1} \mathcal{I}_l^t \mathbb{M} \right) \\ &= \left(\sum_{l=0}^{L} \mathcal{I}_l \mathcal{R}_l \mathcal{I}_l^t \right) \mathbb{M}. \end{aligned}$$

Therefore,

$$\mathcal{B} := \sum_{l=0}^{L} \mathcal{I}_l \mathcal{R}_l \mathcal{I}_l^t$$

is the standard matrix representation of the additive Schwarz preconditioner B.

We summarize this section by the following relationship between the iterative methods for the operator equation (2.1.1) and for the algebraic equation (2.1.2). The linear iterations of (2.1.1) and (2.1.2) can be written as

$$u^{k+1} = u^k + B\left(F - Au^k\right) \quad \text{and} \quad \mu^{k+1} = \mu^k + \mathcal{B}\left(b - \mathcal{A}\mu^k\right), \quad k = 0, 1, \cdots,$$

respectively.

Proposition 2.6.1 ([120])**.** *u is a solution of* (2.1.1) *if and only if $\mu = \widetilde{u}$ is the solution of* (2.1.2) *with $b = \mathbb{M}\widetilde{F}$. The linear iterations are equivalent if and only if $\widetilde{B} = \mathcal{B}\mathbb{M}$. In this case, $\sigma(\mathcal{B}\mathcal{A}) = \sigma(BA)$.*

Chapter 3

Auxiliary Space Preconditioners for H(curl) and H(div) Systems

The Hilbert spaces $\mathbf{H}(\mathbf{curl})$ and $\mathbf{H}(\mathrm{div})$ consist of square-integrable vector fields on a domain $\Omega \subset \mathbb{R}^3$ with square-integrable curl and divergence respectively. These spaces arise naturally in the variational problems,

$$\text{find } \mathbf{u} \in \mathbf{H}(\mathbf{curl}): \quad (\mu \mathbf{curl}\, \mathbf{u}, \mathbf{curl}\, \mathbf{v}) + (\sigma \mathbf{u}, \mathbf{v}) = (\mathbf{f}, \mathbf{v}) \quad \forall \mathbf{v} \in \mathbf{H}(\mathbf{curl}), \tag{3.0.1}$$

$$\text{find } \mathbf{u} \in \mathbf{H}(\mathrm{div}): \quad (\lambda\, \mathrm{div}\ \mathbf{u}, \mathrm{div}\ \mathbf{v}) + (\mu \mathbf{u}, \mathbf{v}) = (\mathbf{f}, \mathbf{v}) \quad \forall \mathbf{v} \in \mathbf{H}(\mathrm{div}), \tag{3.0.2}$$

where $\mathbf{f} \in \mathbf{L}^2(\Omega)$ is a vector field and the coefficients $\mu(x)$, $\sigma(x)$, and $\lambda(x)$ are assumed to be uniformly positive but may have large variations in whole domain Ω. In some applications essential boundary conditions are imposed. In this case, the variational problems (3.0.1)-(3.0.2) are restricted to $\mathbf{H}_0(\mathbf{curl})$ and $\mathbf{H}_0(\mathrm{div})$ respectively, where $\mathbf{H}_0(\mathbf{curl})$ is the subspace of $\mathbf{H}(\mathbf{curl})$, consisting of vector fields whose tangential component vanishes on $\partial\Omega$, and $\mathbf{H}_0(\mathrm{div})$ is the subspace of $\mathbf{H}(\mathrm{div})$, consisting of vector fields, whose normal component vanishes on $\partial\Omega$.

The presentation of this chapter is mainly following from Hiptmair and Xu [68], where nodal auxiliary space preconditioning techniques were first introduced. In [68], the preconditioners were designed for constant coefficients cases, that is, the coefficients μ, σ and λ are constants in the whole domain. In this chapter, we generalize these

techniques to deal with $\mathbf{H}(\mathbf{curl})$ problem,

$$\text{find } \mathbf{u} \in \mathbf{H}_0(\mathbf{curl}) \ : \ (\omega \mathbf{curl}\, \mathbf{u}, \mathbf{curl}\, \mathbf{v}) + \tau(\omega \mathbf{u}, \mathbf{v}) = (\mathbf{f}, \mathbf{v}), \ \ \forall \mathbf{v} \in \mathbf{H}_0(\mathbf{curl}), \quad (3.0.3)$$

where $\tau > 0$ is a constant, and $\omega > 0$ is piecewise constant but may possible have large variation across the interfaces. This is a simplified model of (3.0.1). In some applications (see [85, 71] for example), the coefficients in (3.0.1) satisfy that $\mu(x)/\sigma(x)$ is a constant. In this case, the equation (3.0.1) can be reduced to (3.0.3).

The remainder of this chapter is organized as follows. In Section 3.1, we present an abstract theory of the auxiliary space preconditioning technique. Based on this framework, the preconditioners for systems (3.0.1)-(3.0.2) are essentially stable regular decompositions of the Hilbert spaces $\mathbf{H}(\mathbf{curl})$ and $\mathbf{H}(\mathrm{div})$. Thus, in Section 3.2, we discuss the regular decompositions in detail. In Section 3.3, we adapt these regular decompositions to the discrete setting with the corresponding conforming finite element spaces. Furthermore, for the $\mathbf{H}(\mathbf{curl})$ systems, we also establish some weighted stable regular decompositions in order to deal with the interface problems in Section 3.4. Then, we assemble these theoretical foundations into preconditioners in Section 3.5. Finally, in Section 3.6, we make some remarks on the implementation of these preconditioners.

3.1 Auxiliary Space Preconditioners

The method of subspace correction discussed in Chapter 2 is an algorithm for the solution of equations in a vector space by solving problems on appropriately chosen *subspaces*. Such subspaces are, however, not always available, or the subspace problems

might be difficult to solve. This happens for the finite element discretizations of $\mathbf{H}(\mathbf{curl})$ and $\mathbf{H}(\mathrm{div})$ systems, since the resulting linear systems have kernels of large dimension. The auxiliary space method (cf. [121]) is for designing preconditioners using auxiliary spaces which are not necessarily subspaces of the original subspace. In this section, we give the general framework of the auxiliary space preconditioners introduced in [121].

Given a Hilbert space V, we aim to solve the systems in the variational form: find $u \in V$ such that

$$a(u, v) = (f, v), \forall v \in V,$$

or in operator form

$$Au = f \in V' \tag{3.1.1}$$

where $A : V \to V'$ is the operator induced by the bilinear form $a(\cdot, \cdot)$. In general, to find a solution directly is not optimal with respect to the number of arithmetic operations. Therefore, we introduce the so called "fictitious space" (cf. [88]) and "auxiliary space" (cf. [121]) preconditioning techniques.

Fictitious Space Lemma

There are two main ingredients to construct a fictitious space preconditioner.

(1) A fictitious spaces $\bar{V}$ with the inner product $\bar{a}(\cdot, \cdot) = \|\cdot\|^2_{\bar{A}}$ and the induced operator $\bar{A}$.

(2) A continuous linear mapping $\Pi : \overline{V} \to V$.

Let $A : V \to V'$ and $\bar{A} : \bar{V} \to \bar{V}'$ be the isomorphisms associated with $a(\cdot,\cdot)$ and $\bar{a}(\cdot,\cdot)$ respectively. The fictitious space preconditioner B is given by

$$B = \Pi \circ \bar{A}^{-1} \circ \Pi^* : V' \to V. \tag{3.1.2}$$

The idea can be summarized in the following diagram:

$$\begin{array}{ccc} V & \xrightarrow{A} & V' \\ \Pi\uparrow & & \downarrow\Pi^* \\ \bar{V} & \xrightarrow{\bar{A}} & \bar{V}' \end{array}$$

Obviously, the efficiency of this approximation depends on the choice of the fictitious spaces $\bar{V}$, and $\bar{A}$. A naive choice of the fictitious space is to choose $\bar{V} = V$ with $\bar{a}(\cdot,\cdot) = a(\cdot,\cdot)$ (that is, $\bar{A} \equiv A$) and the linear mapping $\Pi := Id$.

Lemma 3.1.1 (Fictitious space lemma [88, 121])**.** *Assume that* Π *is surjective, and there exist positive constants* c_0 *and* c_1*, such that*

$$\forall v \in V,\ \exists \bar{v} \in \bar{V},\ s.t.\ v = \Pi\bar{v},\ \text{and } \|\bar{v}\|_{\bar{A}} \le c_0 \|v\|_A. \tag{3.1.3}$$

and

$$\|\Pi\bar{v}\|_A \le c_1 \|\bar{v}\|_{\bar{A}}, \quad \forall \bar{v} \in \bar{V}. \tag{3.1.4}$$

Then

$$c_0^{-2} \|v\|_A^2 \le a(BAv, v) \le c_1 \|v\|_A^2, \ \ \forall v \in V. \tag{3.1.5}$$

Proof. To prove the upper bound, we use the Cauchy-Schwarz inequality and the definition of B (3.1.2),

$$\begin{aligned} a(BAv,v) &\leq a(BAv,BAv)^{\frac{1}{2}}a(v,v)^{\frac{1}{2}} \\ &= \left\|\Pi\bar{A}^{-1}\Pi^*Av\right\|_A \|v\|_A \\ &\leq c_1\left\|\bar{A}^{-1}\Pi^*Av\right\|_{\bar{A}} \|v\|_A \quad \text{by assumption (3.1.4)} \\ &= c_1\left\langle\Pi^*Av,\bar{A}^{-1}\Pi^*Av\right\rangle_{\bar{V}'\times\bar{V}}^{\frac{1}{2}} \|v\|_A \\ &= c_1 a(BAv,v)^{\frac{1}{2}}\|v\|_A \end{aligned}$$

Thus we get the upper bound

$$a(BAv,v) \leq c_1^2\|v\|_A.$$

To prove the lower bound, for any $v \in V$, by assumption (3.1.3),

$$\exists\bar{v}\in\bar{V},\ s.t.\ v=\Pi\bar{v},\ \text{and}\ \|\bar{v}\|_{\bar{A}} \leq c_0\|v\|_A.$$

Thus

$$\begin{aligned} a(v,v) &= \langle Av,\Pi\bar{v}\rangle_{V'\times V} = \left\langle\Pi^*Av,\bar{v}\right\rangle_{\bar{V}'\times\bar{V}} \\ &= \bar{a}\left(\bar{A}^{-1}\Pi^*Av,\bar{v}\right) \\ &\leq \bar{a}\left(\bar{A}^{-1}\Pi^*Av,\bar{A}^{-1}\Pi^*Av\right)^{\frac{1}{2}}\|\bar{v}\|_{\bar{A}} \\ &\leq c_0 a(BAv,v)^{\frac{1}{2}}\|v\|_A \quad \text{by assumption (1).} \end{aligned}$$

Hence

$$a(BAv, v) \geq c_0^{-2} \|v\|_A.$$

□

From (3.1.5), we immediately get an estimate for the spectral condition number of the preconditioned system.

Corollary 3.1.2. *With the assumptions in Lemma 3.1.1, we have*

$$\kappa(BA) = \frac{\lambda_{\max}(BA)}{\lambda_{\min}(BA)} \leq (c_0 c_1)^2.$$

The auxiliary space method introduced in [121] can be viewed as a fictitious space method for a special choice of the space $\bar{V}$ and the operator Π. Specifically, we consider

$$\bar{V} = V \times W_1 \times \cdots \times W_J \,, \tag{3.1.6}$$

where $W_1, \ldots, W_J$, $J \in \mathbb{N}$ are auxiliary (Hilbert) spaces equipped with inner products $\overline{a}_j(\cdot,\cdot)$, $j = 1, \ldots, J$. The inner product in $\bar{V}$ is defined as follows:

$$\bar{a}\left(\bar{v}, \bar{v}\right) := s(v_0, v_0) + \sum_{i=1}^{J} \bar{a}_j \left(w_j, w_j\right) \tag{3.1.7}$$

for any $\bar{v} = \left(v_0, w_1, \cdots, w_J\right)^T \in \bar{V}$ with $v_0 \in V$ and $w_i \in W_i$. A distinctive feature of the auxiliary space method is the presence of V in (3.1.6) as a component of $\bar{V}$. In this definition, the inner product in V is $s(\cdot,\cdot)$, and in general is different from $a(\cdot,\cdot)$. The

operator $S : V \mapsto V$ induced by $s(\cdot,\cdot)$ on V is called a smoother. For each W_j we need $\Pi_j : W_j \mapsto V$ which gives

$$\Pi := \left(Id, \Pi_1, \cdots, \Pi_J\right) : \bar{V} \mapsto V \ . \tag{3.1.8}$$

The auxiliary space preconditioner is given by

$$B = S^{-1} + \sum_{j=1}^{J} \Pi_j \bar{A}_j^{-1} \Pi_j^* . \tag{3.1.9}$$

The verification of the assumptions of Lemma 3.1.1 for the preconditioner B in (3.1.9) boils down to 3 components:

(1) there exist constants $c_j > 0$ such that

$$\|\Pi_j w_j\|_A \leq c_j \overline{a}_j \left(w_j, w_j\right)^{\frac{1}{2}} \ , \quad w_j \in W_j \ , \tag{3.1.10}$$

(2) there exists a constant $c_s > 0$ such that

$$\|v\|_A \leq c_s s(v,v)^{\frac{1}{2}} \quad \forall v \in V \ , \tag{3.1.11}$$

(3) for every $v \in V$ there are $v_0 \in V$ and $w_j \in W_j$ such that $v = v_0 + \sum_{j=1}^{J} \Pi_j w_j$ and

$$s\left(v_0, v_0\right) + \sum_{j=1}^{J} \overline{a}_j \left(w_j, w_j\right) \leq c_0^2 \|v\|_A^2 \ . \tag{3.1.12}$$

From Lemma 3.1.1, B admits the following estimate:

$$\kappa(BA) \leq c_0^2 \left(c_s^2 + c_1^2 + \cdots + c_J^2 \right) . \tag{3.1.13}$$

3.2 Regular Decomposition

From the abstract theory in the previous section, a key prerequisite of successful auxiliary space preconditioners is the uniform stability of decompositions (cf. (3.1.12)). The aim of this section is to provide this stable decomposition, the so-called *regular decomposition*, which turns out to be essential in designing the robust preconditioners for the $\mathbf{H}(\mathbf{curl})$ and $\mathbf{H}(\mathrm{div})$ systems (see [94, 68]). The theories origin from [12, 44] for Maxwell's equations. These decompositions state that roughly speaking, the gap between $\mathbf{H}^1(\Omega)$ and $\mathbf{H}(D, \Omega)$ can be bridged by contributions from the kernel of D for $D = \mathbf{curl}$ or div .

Let $\Omega \subset \mathbb{R}^3$ be a contractible Lipschitz domain. Then we have the following exact sequence property, (see [64, 85, 7]).

Lemma 3.2.1 (Exact Sequence Property)**.** *Let* $D = \mathbf{curl}$ *or* div, *and* D^- *be* $\mathbf{grad}$ *or* $\mathbf{curl}$ *respectively. Suppose that* $\Omega \subset \mathbb{R}^3$ *is contractible, then we have the following exact sequence properties*

$$\mathbf{H}(D0, \Omega) := \{\mathbf{v} \in \mathbf{H}(D, \Omega) : \ D\,\mathbf{v} = 0\} = D^- H(D^-, \Omega),$$

$$\mathbf{H}_0(D0, \Omega) := \left\{\mathbf{v} \in \mathbf{H}_0(D, \Omega) : \ D\,\mathbf{v} = 0\right\} = D^- H_0(D^-, \Omega).$$

3.2.1 Regular Decomposition for $\mathbf{H}(\mathbf{curl})$

In this subsection, we present the regular decomposition for the vector fields in the Hilbert spaces $\mathbf{H}(\mathbf{curl})$ and $\mathbf{H}_0(\mathbf{curl})$. The main results are based on the following Lemma:

Lemma 3.2.2 (Existence of Regular vector potential)**.** *Let*

$$\mathbf{H}(\operatorname{div} 0, \mathbb{R}^3) = \left\{ \mathbf{v} \in \mathbf{H}(\operatorname{div}, \mathbb{R}^3) \ : \ \operatorname{div} \ \mathbf{v} = 0 \right\}.$$

Then for any $\mathbf{v} \in \mathbf{H}(\operatorname{div} 0, \mathbb{R}^3)$ *there exists a* $\mathbf{\Phi} \in \mathbf{H}^1_{\text{loc}}\left(\mathbb{R}^3\right)$ *such that*

$$\mathbf{curl}\ \mathbf{\Phi} = \mathbf{v} \ \textit{and} \ \operatorname{div} \ \mathbf{\Phi} = 0.$$

Moreover,

$$\|\mathbf{\Phi}\|_{1,\text{loc},\mathbb{R}^3} \lesssim \|\mathbf{v}\|_{0,\mathbb{R}^3}.$$

Proof. See [53, 3, 64]. □

Based on this Lemma, we prove the following regular decomposition for $\mathbf{H}(\mathbf{curl})$.

Theorem 3.2.3 (Regular decomposition of $\mathbf{H}(\mathbf{curl})$)**.** *For any* $\mathbf{u} \in \mathbf{H}(\mathbf{curl})$ *there exist a* $\mathbf{\Phi} \in \mathbf{H}^1(\Omega)$ *and* $p \in H^1(\Omega)$ *such that*

$$\mathbf{u} = \mathbf{\Phi} + \mathbf{grad}\ p.$$

This decomposition satisfies

$$\|\mathbf{\Phi}\|_{1,\Omega} \lesssim \|\mathbf{curl}\ \mathbf{u}\|_{0,\Omega},\ \textit{and}\ \|\mathbf{grad}\ p\|_{0,\Omega} \lesssim \|\mathbf{u}\|_{\mathbf{H}(\mathbf{curl})}.$$

Proof. Let $\mathbf{v} = \mathbf{curl}\ \mathbf{u}$ then it is easy to see $\mathbf{v} \in \mathbf{H}(\operatorname{div} 0, \Omega)$. Let $O \subset \mathbb{R}^3$ be an open ball such that $\Omega \subset\subset O$. We solve the following auxiliary Neumann problem

$$\begin{cases} -\Delta\, \chi &= 0 & \text{in } O \setminus \Omega \\ \dfrac{\partial \chi}{\partial \mathbf{n}} &= 0 & \text{on } \partial O \\ \dfrac{\partial \chi}{\partial \mathbf{n}} &= \mathbf{v} \cdot \mathbf{n} & \text{on } \partial\Omega. \end{cases}$$

This problem has a well defined solution since $\int_{\partial\Omega} \mathbf{v} \cdot \mathbf{n} = \int_{\Omega} \operatorname{div}\ \mathbf{v} = 0$. Let

$$\widetilde{\mathbf{v}} = \begin{cases} \mathbf{v} & \text{in } \Omega \\ -\mathbf{grad}\ \chi & \text{in } O \setminus \Omega \\ 0 & \text{in } \mathbb{R}^3 \setminus O. \end{cases}$$

Then it is easy to check that $\widetilde{\mathbf{v}} \in \mathbf{H}(\operatorname{div} 0, \mathbb{R}^3)$. By Lemma 3.2.2, there exists a $\mathbf{\Phi} \in \mathbf{H}^1_{\text{loc}}\left(\mathbb{R}^3\right)$ such that

$$\begin{cases} \mathbf{curl}\ \mathbf{\Phi} &= \widetilde{\mathbf{v}} \\ \operatorname{div}\ \mathbf{\Phi} &= 0. \end{cases}$$

And $\mathbf{\Phi}$ satisfies that

$$\|\mathbf{\Phi}\|_{1,\Omega} \lesssim \|\widetilde{\mathbf{v}}\|_{0,\mathbb{R}^3} \leq \|\mathbf{v}\|_{0,\Omega} + |\chi|_{1,O\setminus\Omega}.$$

By the regularity of elliptic equation, we know that $|\chi|_{1,O\setminus\Omega} \lesssim \|\mathbf{v}\cdot\mathbf{n}\|_{H^{-1/2}(\partial\Omega)}$. Since $\mathbf{v}\in\mathbf{H}(\mathrm{div};\Omega)$, by the trace theorem of $\mathbf{H}(\mathrm{div},\Omega)$ (cf. [85, Theorem 3.24]) we get

$$\|\mathbf{v}\cdot n\|_{H^{-1/2}(\partial\Omega)} \lesssim \|\mathbf{v}\|_{\mathbf{H}(\mathrm{div},\Omega)} = \|\mathbf{v}\|_{\mathbf{L}^2(\Omega)},$$

since div $\mathbf{v}=0$ in Ω. Therefore, we have

$$\|\mathbf{\Phi}\|_{1,\Omega} \lesssim \|\mathbf{v}\|_{0,\Omega}.$$

This proves the theorem. □

For $\mathbf{H}_0(\mathbf{curl})$ we have a similar decomposition. Note that the only difference between Theorem 3.2.3 and Theorem 3.2.4 is the boundary condition.

Theorem 3.2.4 (Regular decomposition of $\mathbf{H}_0(\mathbf{curl})$)**.** *For any* $\mathbf{u}\in\mathbf{H}_0(\mathbf{curl})$ *there exist a* $\mathbf{\Phi}\in\mathbf{H}_0^1(\Omega)$ *and* $p\in H_0^1(\Omega)$ *such that*

$$\mathbf{u} = \mathbf{\Phi} + \mathbf{grad}\, p.$$

This decomposition satisfies

$$\|\mathbf{\Phi}\|_{1,\Omega} \lesssim \|\mathbf{curl}\,\mathbf{u}\|_{0,\Omega},\ \textit{and}\ \|\mathbf{grad}\, p\|_{0,\Omega} \lesssim \|\mathbf{u}\|_{\mathbf{H}_0(\mathbf{curl})}.$$

Proof. The proof is similar to that of Theorem 3.2.3. Since $\mathbf{u} \in \mathbf{H}_0(\mathbf{curl})$, we can extend $\mathbf{u}$ to

$$\widetilde{\mathbf{u}} = \begin{cases} \mathbf{u} & \text{in } \Omega \\ 0 & \text{in } \mathbb{R}^3 \setminus \Omega. \end{cases}$$

Obviously, $\widetilde{\mathbf{u}} \in \mathbf{H}(\mathbf{curl}, \mathbb{R}^3)$ with compact support. Set $\mathbf{v} = \mathbf{curl}\ \widetilde{\mathbf{u}} \in \mathbf{H}(\operatorname{div} 0, \mathbb{R}^3)$, and by Lemma 3.2.2, there exists a $\mathbf{\Psi} \in \mathbf{H}^1_{\text{loc}}\left(\mathbb{R}^3\right)$ such that

$$\begin{cases} \mathbf{curl}\ \mathbf{\Psi} &= \mathbf{v} \\ \operatorname{div}\ \mathbf{\Psi} &= 0 \end{cases}$$

Since $\widetilde{\mathbf{u}} - \mathbf{\Psi}$ is **curl** free, then by the exact sequence Lemma 3.2.1, there exists a $\widetilde{\phi} \in H^1_{\text{loc}}\left(\mathbb{R}^3\right)$ with

$$\widetilde{\mathbf{u}} - \mathbf{\Psi} = \mathbf{grad}\ \widetilde{\phi}.$$

Since $\widetilde{\mathbf{u}} = 0$ on $\mathbb{R}^3 \setminus \bar{\Omega}$, we have

$$\mathbf{grad}\ \widetilde{\phi} = -\mathbf{\Psi} \in \mathbf{H}^1_{\text{loc}}\left(\mathbb{R}^3\right) \text{ on } \mathbb{R}^3 \setminus \bar{\Omega}.$$

Therefore $\widetilde{\phi} \in H^2_{\text{loc}}(\mathbb{R}^3 \setminus \bar{\Omega})$. Now let $\phi \in H^2(\Omega)$ be the extension of $\widetilde{\phi}$ to Ω. Then we have the following decomposition:

$$\mathbf{u} = \mathbf{\Psi} + \mathbf{grad}\ \phi + \mathbf{grad}\ (\widetilde{\phi} - \phi).$$

Let $\boldsymbol{\Phi} = \boldsymbol{\Psi} + \mathbf{grad}\ \phi$ and $p = \widetilde{\phi} - \phi$. It is easy to check that this decomposition satisfies the boundary condition.

By Lemma 3.2.2 and the H^2 extension of ϕ, this decomposition satisfies

$$\|\boldsymbol{\Phi}\|_{1,\Omega} \lesssim \|\mathbf{curl}\ \mathbf{u}\|_{0,\Omega}.$$

Then by a triangle inequality

$$\|\mathbf{grad}\ p\|_{0,\Omega} \leq \|\mathbf{u}\|_{0,\Omega} + \|\boldsymbol{\Phi}\|_{0,\Omega} \lesssim \|\mathbf{u}\|_{\mathbf{H}_0(\mathbf{curl})}.$$

This completes the proof. □

In some circumstances, the $\mathbf{H}(\mathbf{curl})$ systems are imposed by mixed boundary conditions. To deal with this situation, in the remainder of this subsection we consider the regular decomposition for the vector fields in the Hilbert space

$$\mathbf{H}_{\Gamma}(\mathbf{curl}) := \left\{ \mathbf{u} \in \mathbf{H}(\mathbf{curl}) : \mathbf{u} \times \mathbf{n}|_{\Gamma} = 0, \ \text{ for } \Gamma \subset \partial\Omega \right\}.$$

Similarly, we have the following regular decomposition for $\mathbf{u} \in \mathbf{H}_{\Gamma}(\mathbf{curl})$.

Theorem 3.2.5 (Regular decomposition of $\mathbf{H}_{\Gamma}(\mathbf{curl})$)**.** *For any* $\mathbf{u} \in \mathbf{H}_{\Gamma}(\mathbf{curl})$ *there exist a* $\boldsymbol{\Phi} \in \mathbf{H}^1_{\Gamma}(\Omega)$ *and* $p \in H^1_{\Gamma}(\Omega)$ *such that*

$$\mathbf{u} = \boldsymbol{\Phi} + \mathbf{grad}\ p.$$

This decomposition satisfies

$$\|\mathbf{\Phi}\|_{1,\Omega} \lesssim \|\mathbf{curl}\ \mathbf{u}\|_{0,\Omega},\ \textit{and}\ \|\mathbf{grad}\ p\|_{0,\Omega} \lesssim \|\mathbf{u}\|_{\mathbf{H}_{\Gamma}(\mathbf{curl})}.$$

Proof. The idea of the proof is similar to Theorem 3.2.4. We need to take special care of the boundary conditions. Without loss of generality, we assume that Γ is simply connected (otherwise, we just treat different connected components similarly). Let $\widetilde{\Omega}$ be a ball such that $\Omega \subset\subset \widetilde{\Omega}$, and $\widetilde{\Omega} = \Omega \cup O_{\Gamma} \cup O$ where O_{Γ} is the subdomain with $\partial O_{\Gamma} \cap \partial\Omega = \Gamma$ (see Figure 3.1). We extend $\mathbf{u}$ to $\bar{\mathbf{u}} \in \mathbf{H}_0(\mathbf{curl}, \widetilde{\Omega})$ defined by $\bar{\mathbf{u}}|_{\Omega} := \mathbf{u}$, $\bar{\mathbf{u}}|_{O_{\Gamma}} := 0$. On the subdomain O, we define $\bar{\mathbf{u}}$ as the $\mathbf{H}(\mathbf{curl})$ extension of $\mathbf{u}$ such that $\bar{\mathbf{u}}|_{\partial\Omega\setminus\Gamma} = \mathbf{u}|_{\partial\Omega\setminus\Gamma}$ and 0 on the remaining boundary of O. We refer to [2] for the existence of such an extension.

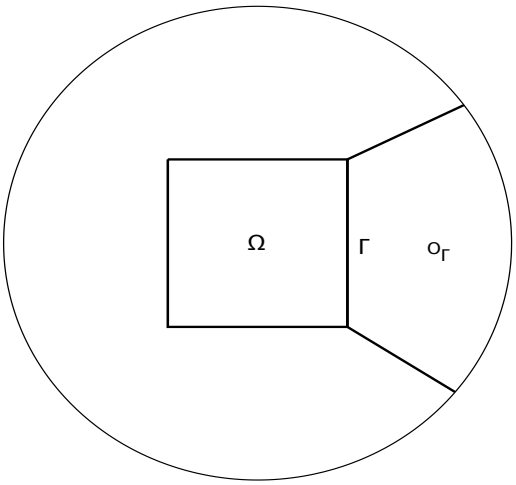

Fig. 3.1. Extension of $\mathbf{u} \in \mathbf{H}_{\Gamma}(\mathbf{curl}, \Omega)$ to $\bar{\mathbf{u}} \in \mathbf{H}_0(\mathbf{curl}, \widetilde{\Omega})$

The remaining proof is similar to that of Theorem 3.2.4. Since $\bar{\mathbf{u}} \in \mathbf{H}_0(\mathbf{curl}, \widetilde{\Omega})$, we can extend $\bar{\mathbf{u}}$ to

$$\widetilde{\mathbf{u}} = \begin{cases} \bar{\mathbf{u}} & \text{in } \widetilde{\Omega} \\ 0 & \text{in } \mathbb{R}^3 \setminus \widetilde{\Omega}. \end{cases}$$

Obviously, $\widetilde{\mathbf{u}} \in \mathbf{H}(\mathbf{curl}, \mathbb{R}^3)$ with compact support. Set $\mathbf{v} = \mathbf{curl}\ \widetilde{\mathbf{u}} \in \mathbf{H}(\operatorname{div} 0, \mathbb{R}^3)$, and by Lemma 3.2.2, there exists a $\boldsymbol{\Psi} \in \mathbf{H}^1_{\text{loc}}(\mathbb{R}^3)$ such that

$$\begin{cases} \mathbf{curl}\ \boldsymbol{\Psi} &= \mathbf{v} \\ \operatorname{div}\ \boldsymbol{\Psi} &= 0 \end{cases}$$

Notice that $\widetilde{\mathbf{u}} - \boldsymbol{\Psi}$ is **curl** free, then there exists a $\widetilde{\phi} \in \mathbf{H}^1_{loc}(\mathbb{R}^3)$ with

$$\widetilde{\mathbf{u}} - \boldsymbol{\Psi} = \mathbf{grad}\ \widetilde{\phi}.$$

Since $\widetilde{\mathbf{u}} = 0$ on $\mathbb{R}^3 \setminus (\bar{\Omega} \cup O_\Gamma)$, we have

$$\mathbf{grad}\ \widetilde{\phi} = -\boldsymbol{\Psi} \in \mathbf{H}^1_{loc}(\mathbb{R}^3) \text{ on } \mathbb{R}^3 \setminus \left(\bar{\Omega} \cup O_\Gamma\right).$$

Therefore $\widetilde{\phi} \in \mathbf{H}^2_{loc}\left(\mathbb{R}^3 \setminus \left(\bar{\Omega} \cup O_\Gamma\right)\right)$. Now let $\phi \in H^2(\Omega)$ be the extension of $\widetilde{\phi}$ to Ω. Then we have the following decomposition:

$$\mathbf{u} = \boldsymbol{\Psi} + \mathbf{grad}\ \phi + \mathbf{grad}\ (\widetilde{\phi} - \phi).$$

Let $\mathbf{\Phi} = \mathbf{\Psi} + \mathbf{grad}\ \phi$ and $p = \widetilde{\phi} - \phi$. Obviously this decomposition satisfies the boundary conditions. The estimates follow in the same way as in Theorem 3.2.4. □

Remark 3.2.6. *For some other geometric structure of* Γ, *Theorem 3.2.5 still holds, for example,* Γ *is a closed surface, or* Γ *is a "screen" (see [85, 39]). In these cases, the proof is almost the same as that in Theorem 3.2.4.*

3.2.2 Regular Decomposition for $\mathbf{H}(\mathrm{div})$

Now we consider the regular decomposition for vector fields in the Hilbert spaces $\mathbf{H}(\mathrm{div})$ and $\mathbf{H}_0(\mathrm{div})$. We have the following regular decomposition for $\mathbf{H}(\mathrm{div})$.

Theorem 3.2.7 (Regular decomposition of $\mathbf{H}(\mathrm{div}, \Omega)$)**.** *For any* $\mathbf{u} \in \mathbf{H}(\mathrm{div})$ *there exist a* $\mathbf{\Phi} \in \mathbf{H}^1(\Omega)$ *and* $\mathbf{\Psi} \in \mathbf{H}^1(\Omega)$ *such that*

$$\mathbf{u} = \mathbf{\Phi} + \mathbf{curl}\ \mathbf{\Psi}.$$

Moreover, $\mathbf{\Phi} = 0$ *if and only if* $\mathrm{div}\ \mathbf{u} = 0$.

Proof. This theorem can be proved by Fourier transformation (e.g. [53, 64]). Here we present a simpler proof. Let O be an open ball such that $\Omega \subset\subset O$, and let $f = \mathrm{div}\ \mathbf{u}$ in Ω and 0 in $O \setminus \Omega$. Since $\mathbf{u} \in \mathbf{H}(\mathrm{div})$, then $f \in L^2(\Omega)$. Therefore, solving the following Dirichlet problem

$$\begin{cases} \Delta\, p &= f \quad \text{in } O \\ p &= 0 \quad \text{on } \partial O. \end{cases}$$

yields a solution $p \in H^2(\Omega)$. Let $\mathbf{\Phi} = \mathbf{grad}\ p \in \mathbf{H}^1(\Omega)$, then $\mathrm{div}\ \mathbf{u} = \mathrm{div}\ \mathbf{\Phi}$ in Ω.

Now let $\mathbf{w} = \mathbf{u} - \mathbf{\Phi} \in \mathbf{H}(\operatorname{div} 0, \Omega)$, by exact sequence property (cf. Lemma 3.2.1), there exists a $\mathbf{v} \in \mathbf{H}(\mathbf{curl})$ such that $\mathbf{w} = \mathbf{curl}\ \mathbf{v}$. Moreover by Theorem 3.2.3, the vector field $\mathbf{v}$ in $\mathbf{H}(\mathbf{curl})$ has a regular decomposition $\mathbf{v} = \mathbf{\Psi} + \mathbf{grad}\ \phi$ for some $\mathbf{\Psi} \in \mathbf{H}^1(\Omega)$. Therefore, we have

$$\mathbf{w} = \mathbf{curl}\ \mathbf{\Psi}.$$

Thus we have the regular decomposition

$$\mathbf{u} = \mathbf{\Phi} + \mathbf{curl}\ \mathbf{\Psi}.$$

This completes the proof. □

For the space $\mathbf{H}_0(\operatorname{div})$, we have a similar decomposition. The main results are based on the following Lemma:

Lemma 3.2.8 (Existence of regular velocity field)**.** *For any*

$$v \in L^2_0(\Omega) = \left\{ v \in L^2(\Omega) \ : \ \int_\Omega v dx = 0 \right\},$$

there exists a $\mathbf{\Phi} \in \mathbf{H}^1_0(\Omega)$ *such that*

$$\operatorname{div}\ \mathbf{\Phi} = v \ \textit{in}\ \Omega.$$

Proof. See Girault and Raviart [53, Corollary 2.4]. For 2D case, constructive proofs can be found in [8, 28]. □

Theorem 3.2.9 (Regular decomposition of $H_0(\mathrm{div})$)**.** *For any* $\mathbf{u} \in \mathbf{H}_0(\mathrm{div})$ *there exist a* $\mathbf{\Phi} \in \mathbf{H}_0^1(\Omega)$ *and* $\mathbf{\Psi} \in \mathbf{H}_0^1(\Omega)$ *such that*

$$\mathbf{u} = \mathbf{\Phi} + \mathbf{curl}\ \mathbf{\Psi}.$$

Moreover, $\mathbf{\Phi} = 0$ *if and only if* $\mathrm{div}\ \mathbf{u} = 0$.

Proof. Since $\mathbf{u} \in \mathbf{H}_0(\mathrm{div})$, we have $\int_\Omega \mathrm{div}\ \mathbf{u} = \int_{\partial\Omega} \mathbf{u}\cdot\mathbf{n} = 0$, i.e., $\mathrm{div}\ \mathbf{u} \in L_0^2(\Omega)$. By Lemma 3.2.8, there exists a $\mathbf{\Phi} \in \mathbf{H}_0^1(\Omega)$ such that

$$\mathrm{div}\ \mathbf{\Phi} = \mathrm{div}\ \mathbf{u} \text{ in } \Omega.$$

Then $\mathbf{w} = \mathbf{u} - \mathbf{\Phi} \in \mathbf{H}(\mathrm{div}\,0, \mathbb{R}^3)$, by exact sequence property (cf. Lemma 3.2.1) and Theorem 3.2.4, there exists a $\mathbf{\Psi} \in \mathbf{H}_0^1(\Omega)$ such that $\mathbf{w} = \mathbf{curl}\ \mathbf{\Psi}$. □

Remark 3.2.10. *For the mixed boundary* $\mathbf{H}(\mathrm{div})$ *problems, it was proved that the regular decomposition for* $\mathbf{H}_\Gamma(\mathrm{div})$ *is still true for two dimensional case in [36]. But for 3D* $\mathbf{H}(\mathrm{div})$ *problems, the regular decomposition is still an open question.*

The main results of this section can be summarized in the following lemma.

Lemma 3.2.11 (Regular decomposition)**.** *Let* $D = \mathbf{curl}$ *(or* div*) and* $D^- = \mathbf{grad}$ *(or* **curl** *respectively). Then for any* $\mathbf{v} \in \mathbf{H}(D)$*, there exist* $\mathbf{\Phi} \in \mathbf{H}^1(\Omega)$ *and* $p \in H(D^-)$ *such that*

$$\mathbf{v} = \mathbf{\Phi} + D^-\ p \quad \textit{and} \quad \|\mathbf{\Phi}\|_1 + \|p\|_{H(D^-)} \lesssim \|\mathbf{v}\|_{\mathbf{H}(D)}.$$

For details of these spaces and relevant operators, we refer to [53, 3, 62, 64, 85, 7].

3.3 Discrete Regular Decomposition

To realize the preconditioners for the finite element discretization of the model equations (3.0.1)-(3.0.2), the decomposition discussed in the previous section should be adapted to the discrete setting. First we discuss briefly the related finite element spaces and the corresponding interpolation operators.

Given the quasi-uniform triangulation $\mathcal{T}_h$ of Ω, the finite element subspaces discussed in this chapter are the standard nodal (for $H(\mathbf{grad})$), edge (for $\mathbf{H}(\mathbf{curl})$) and face (for $\mathbf{H}(\mathrm{div})$) elements that can be viewed as discrete differential forms. This includes the so-called first and second families of Nédélec elements (cf. [86, 87]) for $\mathbf{H}(\mathbf{curl})$ systems and Raviart-Thomas elements (cf. [95]) and the BDM elements (cf. [30, 32, 31]) for $\mathbf{H}(\mathrm{div})$ systems. Here we focus on the lowest order cases, and denote these spaces by $V_h(\mathbf{grad})$, $V_h(\mathbf{curl})$ and $V_h(\mathrm{div})$. For a thorough discussion, we refer to [64, 7]. A fundamental property of these families of finite element spaces is that they permit a discrete counterpart of Lemma 3.2.1:

$$V_h(D0) := \left\{ v_h \in V_h(D) \ : \ D\, v_h = 0 \right\} = D^{-} V_h\left(D^{-}\right). \tag{3.3.1}$$

The degrees of freedom specified for $V_h(D)$ determine the *nodal interpolation operator* Π_h^D. When $D = \mathbf{grad}$, the operator $\Pi_h^{\mathbf{grad}}$ is the standard linear interpolation. For $D = \mathbf{curl}$, the interpolation is based on the path integrals along the edges

$$\Pi_h^{\mathbf{curl}} \mathbf{v} = \sum_{e \in \mathcal{E}_h} \left(\int_e \mathbf{v} \cdot dl \right) \mathbf{b}_e,$$

where $\mathcal{E}_h$ is the set of (interior) edges of $\mathcal{T}_h$ and $\mathbf{b}_e$ is the edge element basis function associated with the edge e. For $D = \mathrm{div}$, the operator Π_h^{div} is defined by

$$\Pi_h^{\mathrm{div}}\mathbf{v} = \sum_{f\in\mathcal{F}_h}\left(\int_f \mathbf{v}\cdot ds\right)\mathbf{b}_f,$$

where $\mathcal{F}_h$ denotes the set of (interior) faces on $\mathcal{T}_h$ and $\mathbf{b}_f$ is the face element basis function associated with the face f. The interpolation Π_h^0 is the L^2-projection onto $V_h(0)$.

These interpolation operators except for Π_h^0, however, are not well defined in the related Hilbert spaces because of lack of the smoothness of the functions in these spaces. Specifically, $\Pi_h^{\mathbf{grad}}$ is well-defined on the continuous functions, and Π_h^0 is well-defined on all the L^2 functions. For the domain of Π_h^{div}, one can choose $\mathbf{H}^1$. The operator $\Pi_h^{\mathbf{curl}}$ is bounded on the space of $\mathbf{H}^1$ vector fields whose **curl** belong to L^p $(p > 2)$, (see [85]). In particular, it is well defined for $\mathbf{H}^1$ vector fields whose **curl** belong to $V_h(\mathrm{div})$. In general, we have the following approximation property.

Lemma 3.3.1. *Interpolation operators Π_h^D are bounded on*

$$\left\{v \in H^1(\Omega) \,:\, Dv \in V_h\left(D^+\right)\right\} \subset H^1(\Omega).$$

Moreover, we have the following estimate

$$\left\|h^{-1}\left(I - \Pi_h^D\right)\mathbf{\Psi}\right\|_{0,\Omega} \lesssim \|\mathbf{\Psi}\|_{1,\Omega},$$

for any $\mathbf{\Psi} \in H^1(\Omega)$ such that $D\mathbf{\Psi} \in V_h(D^+)$.

Proof. The conclusions for $\Pi_h^{\mathbf{grad}}$ and Π_h^0 are standard (see [41, 28]). For Π_h^{div}, a standard scaling argument and Bramble-Hilbert lemma give the error estimate (cf. [31])

$$\left\| h^{-1} \left(\mathbf{\Psi} - \Pi_h^{\mathrm{div}} \mathbf{\Psi} \right) \right\|_{0,\Omega} \lesssim \|\mathbf{\Psi}\|_{1,\Omega}.$$

Because of the dependence on the edge moments, the situation is more complicated for the operator $\Pi_h^{\mathbf{curl}}$. To prove the estimate for $\Pi_h^{\mathbf{curl}}$, we follow [66]. First consider the case when the mesh consists of only the unit simplex $\hat{T}$. Let $\hat{\Pi}^{\mathbf{curl}}$ be the interpolant on the reference element. Using the equivalence of norms in the finite element space, we get

$$\left\| \hat{\Pi}^{\mathbf{curl}} \hat{\mathbf{\Psi}} \right\| \leq C \left(\left\| \hat{\mathbf{\Psi}} \right\|_1 + \left\| \mathbf{curl} \hat{\mathbf{\Psi}} \right\|_\infty \right) \leq C \left\| \hat{\mathbf{\Psi}} \right\|_1$$

for all $\hat{\mathbf{\Psi}} \in \mathbf{H}^1\left(\hat{T}\right)$ such that $\mathbf{curl}\hat{\mathbf{\Psi}} \in V_h(\mathrm{div})$. A Bramble-Hilbert argument then gives $\left\| \hat{\mathbf{\Psi}} - \hat{\Pi}^{\mathbf{curl}} \hat{\mathbf{\Psi}} \right\| \leq C \left| \hat{\mathbf{\Psi}} \right|_1$ for $\hat{\mathbf{\Psi}} \in \mathbf{H}^1\left(\hat{T}\right)$ such that $\mathbf{curl}\hat{\mathbf{\Psi}} \in V_h(\mathrm{div})$ where now only the $\mathbf{H}^1$ seminorm appears on the right hand side. If we scale this estimate to a general simplex $T = F^{-1}\hat{T}$ with affine mapping F, using the appropriate contravariant transform $\hat{\mathbf{\Psi}} \mapsto (DF)^*(\hat{\mathbf{\Psi}} \circ F)$, and add up over all the simplices in the mesh, we get the L^2 error estimate. □

In the weighted norm, we have the following estimate.

Corollary 3.3.2. *Interpolation operator* Π_h^D *is bounded on*

$$\left\{ \mathbf{v} \in \mathbf{H}^1(\Omega) | D\,\mathbf{v} \in V_h\left(D^+\right) \right\} \subset \mathbf{H}^1(\Omega).$$

Moreover, we have the following estimate

$$\left\| h^{-1} \left(I - \Pi_h^D \right) \mathbf{\Phi} \right\|_{0,\omega} \lesssim \|\mathbf{\Phi}\|_{1,\omega},$$

for any $\mathbf{\Phi} \in \mathbf{H}^1(\Omega)$ *such that* $D\,\mathbf{\Phi} \in V_h(\mathrm{div})$.

Proof. Note that in the above proof, the arguments are carried through element by element. That is, we have

$$\left\| h^{-1} \left(I - \Pi_h^D \right) \mathbf{\Phi} \right\|_{0,T}^2 \lesssim \|\mathbf{\Phi}\|_{1,T}^2.$$

The conclusion follows by multiplying this inequality by $\omega|_T$ on both sides and summing up all elements $T \in \mathcal{T}_h$. □

By an application of Stokes theorem, these interpolation operators also satisfy the commutativity properties

$$\mathbf{grad}\, \Pi_h^{\mathbf{curl}} = \Pi_h^{\mathbf{grad}} \mathbf{grad}, \;\; \mathbf{curl}\, \Pi_h^{\mathrm{div}} = \Pi_h^{\mathbf{curl}} \mathbf{curl}, \;\; \mathrm{div}\; \Pi_h^0 = \Pi_h^{\mathrm{div}}\, \mathrm{div}\,.$$

Moreover, by a straightforward scaling arguments, we have, with constants depending only on the shape regularity of $\mathcal{T}_h$,

$$\left\| D\Pi_h^D \mathbf{\Phi}_h \right\|_{0,\Omega} \lesssim \left| \mathbf{\Phi}_h \right|_{1,\Omega}, \;\; \left\| \Pi_h^D \mathbf{\Phi}_h \right\|_{0,\Omega} \lesssim \left\| \mathbf{\Phi}_h \right\|_{0,\Omega}, \; \forall \mathbf{\Phi}_h \in \mathbf{V}_h(\mathbf{grad}). \tag{3.3.2}$$

These estimates are closely related to the constants c_j in (3.1.10).

The exact sequences Lemma 3.2.1 and the commutativity properties can be summarized in the following diagram:

$$\begin{array}{ccccccccccc}
\mathbb{R} & \longrightarrow & C^\infty & \xrightarrow{\mathbf{grad}} & C^\infty & \xrightarrow{\mathbf{curl}} & C^\infty & \xrightarrow{\mathrm{div}} & C^\infty & \longrightarrow & 0 \\
 & & \downarrow \Pi_h^{\mathbf{grad}} & & \downarrow \Pi_h^{\mathbf{curl}} & & \downarrow \Pi_h^{\mathrm{div}} & & \downarrow \Pi_h^{0} & & \\
\mathbb{R} & \longrightarrow & V_h(\mathbf{grad}) & \xrightarrow{\mathbf{grad}} & V_h(\mathbf{curl}) & \xrightarrow{\mathbf{curl}} & V_h(\mathrm{div}) & \xrightarrow{\mathrm{div}} & L^2_h & \longrightarrow & 0
\end{array}$$

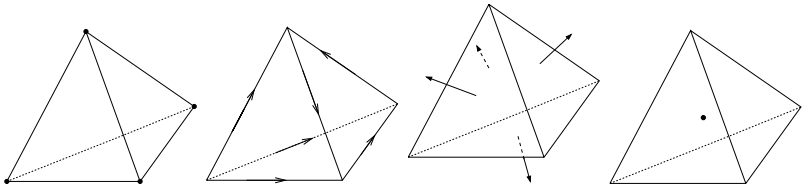

Fig. 3.2. Relationship between $H(\mathbf{grad})$, $\mathbf{H}(\mathbf{curl})$, $\mathbf{H}(\mathrm{div})$ and their discretizations

The main result of this section is the following discrete version of the regular decompositions in Section 3.2:

Theorem 3.3.3 (Discrete Regular Decomposition [68, Lemma 5.1])**.** *For any* $\mathbf{v}_h \in V_h(D)$, *we have*

$$\mathbf{v}_h = \widetilde{\mathbf{v}}_h + \Pi_h^D \mathbf{\Phi}_h + D^- p_h$$

where $\widetilde{\mathbf{v}}_h \in V_h(D)$, $\mathbf{\Phi}_h \in S_h$ *and* $p_h \in V_h(D^-)$, *such that*

(1) $\|h^{-1}\widetilde{\mathbf{v}}_h\|_{0,\Omega}^2 + \|\mathbf{\Phi}_h\|_{1,\Omega}^2 \lesssim \|D\mathbf{v}_h\|_{0,\Omega}^2$.

(2) $\|p_h\|_{V(D^-)} \lesssim \|\mathbf{v}_h\|_{V(D)}$.

Proof. By continuous regular decomposition Lemma 3.2.11, there exist $\mathbf{\Psi} \in \mathbf{H}^1(\Omega)$ and $p \in V(D^-)$ such that

$$\mathbf{v}_h = \mathbf{\Psi} + D^- p.$$

Since $D\mathbf{\Psi} = D\mathbf{v}_h \in V_h(D^+)$, by Lemma 3.3.1 $\underset{h}{\Pi}^D \mathbf{\Psi}$ is well-defined, and by commuting diagram property (cf. Lemma 3.2.1)

$$D\underset{h}{\Pi}^D \mathbf{\Psi} = \underset{h}{\Pi}^{D^+} D\mathbf{\Psi} = D\mathbf{\Psi},$$

i.e., $D(I - \underset{h}{\Pi}^D)\mathbf{\Psi} = 0$.

Now decompose $\mathbf{\Psi}$ by

$$\mathbf{\Psi} = \underset{h}{\Pi}^D \left(I - Q_h\right) \mathbf{\Psi} + \underset{h}{\Pi}^D Q_h \mathbf{\Psi} + \left(I - \underset{h}{\Pi}^D\right) \mathbf{\Psi}$$

where $Q_h : H^1(\Omega) \to V_h(\mathbf{grad})$ is the L^2-projection (cf. (2.2.1) in Chapter 2), or the quasi-interpolator (Scott-Zhang operator cf. [98]), which satisfies

$$\left\| Q_h \mathbf{\Psi} \right\|_{1,\Omega} \lesssim \|\mathbf{\Psi}\|_{1,\Omega}$$

and

$$\left\| h^{-1} \left(I - Q_h\right) \mathbf{\Psi} \right\|_{0,\Omega} \lesssim \|\mathbf{\Psi}\|_{1,\Omega}.$$

From the above discussion, the last term of the decomposition $\left(I - \Pi_h^D\right)\mathbf{\Psi} \in N(D)$. Thus there exists a $q \in V(D^-)$ such that

$$\left(I - \Pi_h^D\right)\mathbf{\Psi} = D^- q$$

with

$$\left\|h^{-1}D^- q\right\|_{0,\Omega} = \left\|h^{-1}D^-\left(I - \Pi_h^D\right)\mathbf{\Psi}\right\|_{0,\Omega} \lesssim \|\mathbf{\Psi}\|_{1,\Omega} \lesssim \left\|D\,\mathbf{v}_h\right\|_{0,\Omega},$$

where we used Lemma 3.3.1 for the first inequality and the second inequality follows by the regular decomposition.

Therefore, we can define

$$\begin{aligned}
\widetilde{\mathbf{v}}_h &= \Pi_h^D\left(I - Q_h\right)\mathbf{\Psi} && \in V_h(D),\\
\mathbf{\Psi}_h &= Q_h\mathbf{\Psi} && \in V_h(\mathbf{grad}),\\
D^- p_h &= D^-(p+q) && s.t.\ p_h \in V_h(D^-).
\end{aligned}$$

Indeed, $D^-(p+q) \in V_h(D)$ such that we can add a contribution from $V(D^-)$ to $p+q$ and obtain a discrete function. □

3.4 Weighted Regular Decomposition for H(curl)

In order to deal with the interface problem (3.0.3), we consider the regular decomposition for $\mathbf{H}(\mathbf{curl})$ in the setting of the weighted norms. For simplicity, let $\Omega = \Omega_1 \cup \Omega_2$ where on Ω_1 and Ω_2 the equation has different constant coefficients $\omega_1 > 0$ and $\omega_2 > 0$

respectively (see Figure 3.3). Without loss of generality, we may assume

$$\omega_1 \geq \omega_2 > 0.$$

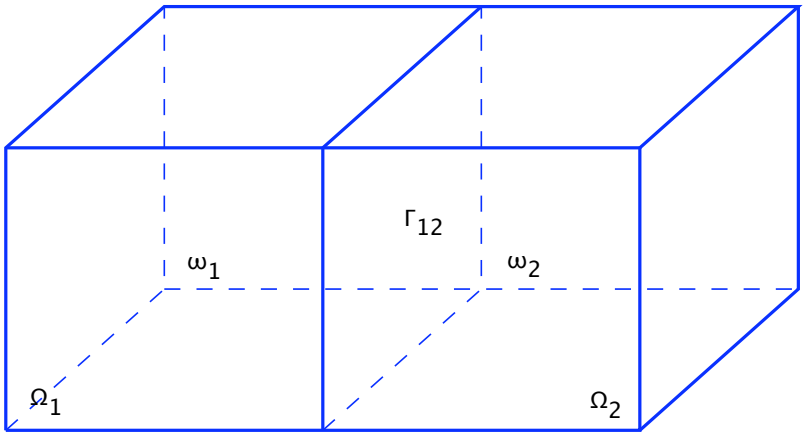

Fig. 3.3. Two domains with $\omega_1 \geq \omega_2 > 0$

Follows from the regular decomposition for the mixed boundary conditions case, we obtain the following regular decomposition result for the weighted norms.

Theorem 3.4.1. *For any* $\mathbf{u} \in \mathbf{H}_0(\mathbf{curl})$, *we have*

$$\mathbf{u} = \mathbf{\Phi} + \mathbf{grad}\, p,$$

where $\mathbf{\Phi} \in \mathbf{H}_0^1(\Omega)$ *and* $p \in H_0^1(\Omega)$ *such that*

(1) $\|\mathbf{\Phi}\|_{1,\omega}^2 \lesssim \|\mathbf{curl}\ \mathbf{u}\|_{0,\omega,\Omega}^2$

(2) $\|\mathbf{grad}\ p\|_{0,\omega}^2 \lesssim \|\mathbf{u}\|_{0,\omega}^2 + \|\mathbf{curl}\ \mathbf{u}\|_{0,\omega}^2$.

Proof. We consider the decomposition on the Ω_1 first. Let $\Gamma_1 = \partial\Omega \cap \partial\Omega_1$ be the Dirichlet boundary of Ω_1. Then by the regular decomposition Theorem 3.2.5, we have $\mathbf{u}|_{\Omega_1} = \mathbf{\Phi}_1 + \mathbf{grad}\ p_1$ with $\mathbf{\Phi}_1 \in \mathbf{H}_\Gamma^1(\Omega_1)$ and $p_1 \in \mathbf{H}_\Gamma^1(\Omega_1)$ such that

$$\left\|\mathbf{\Phi}_1\right\|_{1,\Omega_1} \lesssim \|\mathbf{curl}\ \mathbf{u}\|_{0,\Omega_1} \quad \text{and} \quad \left\|\mathbf{grad}\ p_1\right\|_{0,\Omega_1} \lesssim \|\mathbf{u}\|_{\mathbf{H}\left(\mathbf{curl},\Omega_1\right)}.$$

Let $\Gamma_{12} = \partial\Omega_1 \cap \partial\Omega_2$ be the interface. We extend $\mathbf{\Phi}_1$ and p_1 to harmonic functions on Ω_2, and denote these extensions by $\widetilde{\mathbf{\Phi}}_1$ and $\widetilde{p}_1$. By the properties of harmonic extension (cf. [104]), we obtain

$$\left\|\widetilde{\mathbf{\Phi}}_1\right\|_{1,\Omega_2} \lesssim \|\mathbf{\Phi}\|_{\frac{1}{2},\Gamma_{12}} \lesssim \|\mathbf{\Phi}\|_{1,\Omega_1} \lesssim \|\mathbf{curl}\ \mathbf{u}\|_{0,\Omega_1},$$

and

$$\left\|\widetilde{p}_1\right\|_{1,\Omega_2} \lesssim \|p\|_{\frac{1}{2},\Gamma_{12}} \lesssim \|\mathbf{\Phi}\|_{1,\Omega_1} \lesssim \|\mathbf{u}\|_{\mathbf{H}\left(\mathbf{curl},\Omega_1\right)}.$$

Let $\widetilde{\mathbf{u}} := \widetilde{\mathbf{\Phi}}_1 + \mathbf{grad}\widetilde{p}_1$ and define $\mathbf{u}_2^0 = \mathbf{u}|_{\Omega_2} - \widetilde{\mathbf{u}}|_{\Omega_2}$ in Ω_2. Now applying Theorem 3.2.4 to $\mathbf{u}_2^0 \in \mathbf{H}_0\left(\mathbf{curl},\Omega_2\right)$, we get the decomposition $\mathbf{u}_2^0 = \mathbf{\Phi}_2^0 + \mathbf{grad}\ p_2^0$ with

$\mathbf{\Phi}_2^0 \in \mathbf{H}_0^1\left(\Omega_2\right)$ and $p_2^0 \in H_0^1\left(\Omega_2\right)$. This decomposition of $\mathbf{u}_2^0$ satisfies that

$$\begin{aligned}
\left\|\mathbf{\Phi}_2^0\right\|_{1,\Omega_2} &\lesssim \left\|\mathbf{curl}\ \mathbf{u}_2^0\right\|_{0,\Omega_2} \\
&\leq \|\mathbf{curl}\ \mathbf{u}\|_{0,\Omega_2} + \left\|\mathbf{curl}\widetilde{\mathbf{\Phi}}_1\right\|_{0,\Omega_2} \\
&\leq \|\mathbf{curl}\ \mathbf{u}\|_{0,\Omega_2} + \left\|\widetilde{\mathbf{\Phi}}_1\right\|_{1,\Omega_2} \\
&\lesssim \|\mathbf{curl}\ \mathbf{u}\|_{0,\Omega_2} + \|\mathbf{curl}\ \mathbf{u}\|_{0,\Omega_1},
\end{aligned}$$

and similarly,

$$\begin{aligned}
\left\|\mathbf{grad}\ p_2^0\right\|_{0,\Omega_2} &\lesssim \left\|\mathbf{u}_2^0\right\|_{\mathbf{H}\left(\mathbf{curl},\Omega_2\right)} \\
&\leq \|\mathbf{u}\|_{\mathbf{H}\left(\mathbf{curl},\Omega_2\right)} + \left\|\widetilde{\mathbf{\Phi}}_1\right\|_{\mathbf{H}\left(\mathbf{curl},\Omega_2\right)} \\
&\leq \|\mathbf{u}\|_{\mathbf{H}\left(\mathbf{curl},\Omega_2\right)} + \left\|\widetilde{\mathbf{\Phi}}_1\right\|_{1,\Omega_2} \\
&\lesssim \|\mathbf{u}\|_{\mathbf{H}\left(\mathbf{curl},\Omega_2\right)} + \|\mathbf{curl}\ \mathbf{u}\|_{0,\Omega_1}.
\end{aligned}$$

Now we define the decomposition of $\mathbf{u}$ in the whole domain by $\mathbf{u} = \mathbf{\Phi} + \mathbf{grad}\ p$ where

$$\mathbf{\Phi} = \begin{cases} \mathbf{\Phi}_1 & \text{in } \Omega_1 \\ \mathbf{\Phi}_2^0 + \widetilde{\mathbf{\Phi}}_1 & \text{in } \Omega_2 \end{cases} \quad \text{and} \quad p = \begin{cases} p_1 & \text{in } \Omega_1 \\ p_2^0 + \widetilde{p}_1 & \text{in } \Omega_2 \end{cases}.$$

Recall that $\omega_1 \geq \omega_2 > 0$, this decomposition satisfies

$$\begin{aligned}
\|\mathbf{\Phi}\|_{1,\omega} &\leq \omega_1^{\frac{1}{2}} \left\|\mathbf{\Phi}_1\right\|_{1,\Omega_1} + \omega_2^{\frac{1}{2}} \left\|\mathbf{\Phi}_2^0\right\|_{1,\Omega_2} + \omega_2^{\frac{1}{2}} \left\|\widetilde{\mathbf{\Phi}}_1\right\|_{1,\Omega_2} \\
&\lesssim \omega_1^{\frac{1}{2}} \|\mathbf{curl}\ \mathbf{u}\|_{0,\Omega_1} + \omega_2^{\frac{1}{2}} \left(\|\mathbf{curl}\ \mathbf{u}\|_{0,\Omega_2} + \|\mathbf{curl}\ \mathbf{u}\|_{0,\Omega_1}\right) + \omega_2^{\frac{1}{2}} \|\mathbf{curl}\ \mathbf{u}\|_{0,\Omega_1} \\
&= \left(1 + \frac{2\omega_2^{\frac{1}{2}}}{\omega_1^{\frac{1}{2}}}\right) \omega_1^{\frac{1}{2}} \|\mathbf{curl}\ \mathbf{u}\|_{0,\Omega_1} + \omega_2^{\frac{1}{2}} \|\mathbf{curl}\ \mathbf{u}\|_{0,\Omega_2} \\
&\lesssim \|\mathbf{curl}\ \mathbf{u}\|_{0,\omega},
\end{aligned}$$

and similarly,

$$\begin{aligned}
\|\mathbf{grad}\ p\|_{0,\omega} &\leq \omega_1^{\frac{1}{2}} \left\|\mathbf{grad}\ p_1\right\|_{0,\Omega_1} + \omega_2^{\frac{1}{2}} \left\|\mathbf{grad}\ p_2^0\right\|_{0,\Omega_2} + \omega_2^{\frac{1}{2}} \left\|\mathbf{grad}\widetilde{p}_1\right\|_{0,\Omega_2} \\
&\lesssim \omega_1^{\frac{1}{2}} \|\mathbf{u}\|_{\mathbf{H}(\mathbf{curl},\Omega_1)} + \omega_2^{\frac{1}{2}} \left(\|\mathbf{u}\|_{\mathbf{H}(\mathbf{curl},\Omega_2)} + \|\mathbf{u}\|_{\mathbf{H}(\mathbf{curl},\Omega_1)}\right) + \omega_2^{\frac{1}{2}} \|\mathbf{u}\|_{\mathbf{H}(\mathbf{curl},\Omega_1)} \\
&= \left(1 + \frac{2\omega_2^{\frac{1}{2}}}{\omega_1^{\frac{1}{2}}}\right) \omega_1^{\frac{1}{2}} \|\mathbf{u}\|_{\mathbf{H}(\mathbf{curl},\Omega_1)} + \omega_2^{\frac{1}{2}} \|\mathbf{u}\|_{H(\mathbf{curl},\Omega_2)} \\
&\lesssim \|\mathbf{curl}\ \mathbf{u}\|_{0,\omega} + \|\mathbf{u}\|_{0,\omega}.
\end{aligned}$$

This completes the proof. □

Remark 3.4.2. *Obviously, the above result can be generalized to more general interface problems. For example, the subdomains have no "cross edge", that is, there is no edge which belongs to more than two subdomains. In this case, the same conclusion holds.*

The reason is that the coefficients satisfy certain monotonicity, so one can do the decomposition on the subdomain with large coefficients first, then follows the same idea for the neighboring subdomains as we did in the proof of Theorem 3.4.1.

For more general interface problem, whether this result holds or not is still an open problem. For general case, the existence of the regular decomposition Theorem 3.2.5 is still unclear. Furthermore, the weighted decomposition Theorem 3.4.1 is not necessarily true.

Weighted Discrete Regular Decomposition Based on the weighted regular decomposition Theorem 3.4.1, we obtain the following discrete version.

Theorem 3.4.3. *For any* $\mathbf{v}_h \in V_h(\mathbf{curl})$ *there exist* $\mathbf{\Phi}_h \in \mathbf{V}_h(\mathbf{grad})$, $p_h \in V_h(\mathbf{grad})$ *and* $\widetilde{\mathbf{v}}_h \in V_h(\mathbf{curl})$ *such that*

$$v_h = \widetilde{\mathbf{v}}_h + \Pi_h^{\mathbf{curl}} \mathbf{\Phi}_h + \mathbf{grad}\, p_h,$$

and

$$\left\| h^{-1} \widetilde{\mathbf{v}}_h \right\|_{0,\omega}^2 + \left\| \mathbf{\Phi}_h \right\|_{1,\omega}^2 \lesssim \left\| \mathbf{curl}\, \mathbf{v}_h \right\|_{0,\omega}^2, \quad \left| p_h \right|_{1,\omega}^2 \lesssim \left\| v_h \right\|_{0,\omega}^2 + \left\| \mathbf{curl}\, \mathbf{v}_h \right\|_{0,\omega}. \quad (3.4.1)$$

Proof. The idea of the proof mainly follows Theorem 3.3.3 which is due to [68].

Notice that if $\mathbf{v}_h \in V_h(\mathbf{curl})$, by Theorem 3.4.1 we can decompose $\mathbf{v}_h$ as

$$\mathbf{v}_h = \mathbf{\Phi} + \mathbf{grad}\, p,$$

such that

$$\|\mathbf{\Phi}\|_{1,\omega} \lesssim \left\|\mathbf{curl}\ \mathbf{v}_h\right\|_{0,\omega} \quad \text{and} \quad \|\mathbf{grad}\ p\|_{0,\omega} \lesssim \left\|\mathbf{curl}\ \mathbf{v}_h\right\|_{0,\omega} + \left\|\mathbf{v}_h\right\|_{0,\omega}$$

with constants only depending on Ω.

First, by Lemma 3.3.2, $\Pi_h^{\mathbf{curl}}\mathbf{\Phi}$ is well defined. Furthermore, the commuting diagram property implies that

$$\mathbf{curl}\ \Pi_h^{\mathbf{curl}}\mathbf{\Phi} = \Pi_h^{\mathrm{div}}\mathbf{curl}\ \mathbf{\Phi} = \mathbf{curl}\ \mathbf{\Phi}.$$

This identity implies that $\mathbf{curl}\ \left(Id - \Pi_h^{\mathbf{curl}}\right)\mathbf{\Phi} = 0$. Therefore we can rewrite $\mathbf{\Phi}$ as

$$\mathbf{\Phi} = \Pi_h^{\mathbf{curl}}\left(\mathbf{\Phi} - Q_h^{\omega}\mathbf{\Phi}\right) + \Pi_h^{\mathbf{curl}}Q_h^{\omega}\mathbf{\Phi} + \left(Id - \Pi_h^{\mathbf{curl}}\right)\mathbf{\Phi}$$

where the third term belongs to the kernel of **curl**. By the exact sequence property (cf. Lemma 3.2.1),

$$\exists q \in H(\mathbf{grad}): \quad \left(Id - \Pi_h^{\mathbf{curl}}\right)\mathbf{\Phi} = \mathbf{grad}\ q,$$

which satisfies

$$\left\|h^{-1}\mathbf{grad}\ q\right\|_{0,\omega} = \left\|h^{-1}\left(Id - \Pi_h^{\mathbf{curl}}\right)\mathbf{\Phi}\right\|_{0,\omega} \lesssim \|\mathbf{\Phi}\|_{1,\omega} \lesssim \left\|\mathbf{curl}\ \mathbf{v}_h\right\|_{0,\omega}. \qquad (3.4.2)$$

Therefore one can define the terms in the decomposition in the theorem as

$$\widetilde{\mathbf{v}}_h := \Pi_h^{\mathbf{curl}} \left(\mathbf{\Phi} - Q_h^{\Omega} \mathbf{\Phi} \right) \in V_h(\mathbf{curl}) \tag{3.4.3}$$

$$\mathbf{\Phi}_h := Q_h^{\omega} \mathbf{\Phi} \in \mathbf{V}_h(\mathbf{grad}), \tag{3.4.4}$$

$$\mathbf{grad}\, p_h := \mathbf{grad}\,(p+q), \;\; p_h \in V_h(\mathbf{grad}). \tag{3.4.5}$$

Note that $\mathbf{grad}\,(p+q) \in V_h(\mathbf{curl})$, thus we can add a contribution from $H_0^1(\Omega)$ to $p+q$ and obtain a discrete function.

Then the stability of the decomposition can be established as follows: first, making use of Lemma 3.3.2 and the approximation property of the weighted L^2-projection, we obtain

$$\begin{aligned}
\left\| h^{-1} \widetilde{\mathbf{v}}_h \right\|_{0,\omega} &\leq \left\| h^{-1} \left(Id - \Pi_h^{\mathbf{curl}} \right) \left(\mathbf{\Phi} - Q_h^{\omega} \mathbf{\Phi} \right) \right\|_{0,\omega} + \left\| h^{-1} \left(Id - Q_h^{\omega} \right) \mathbf{\Phi} \right\|_{0,\omega} \\
&\lesssim \left\| \left(Id - Q_h^{\omega} \right) \mathbf{\Phi} \right\|_{1,\omega} + \left\| \mathbf{\Phi} \right\|_{1,\omega} \\
&\lesssim \left\| \mathbf{\Phi} \right\|_{1,\omega} \lesssim \left\| \mathbf{curl}\, \mathbf{v}_h \right\|_{0,\omega}.
\end{aligned}$$

Due to the definition, the next estimate is a simple consequence of the stability of Q_h^{ω}.

$$\left\| \mathbf{\Phi}_h \right\|_{1,\omega} \lesssim \left\| \mathbf{\Phi} \right\|_{1,\omega} \lesssim \left\| \mathbf{curl}\, \mathbf{v}_h \right\|_{0,\omega}.$$

Finally, the estimates established so far plus a triangle inequality yield

$$\left\| \mathbf{grad}\, p_h \right\|_{0,\omega} \lesssim \left\| \mathbf{v}_h \right\|_{0,\omega} + \left\| \mathbf{curl}\, \mathbf{v}_h \right\|_{0,\omega}.$$

This completes the proof. □

3.5 Auxiliary Space Preconditioners for H(curl) and H(div) Systems

We rely on the splitting in Section 3.2-3.4 to define the preconditioners. First of all, we consider solving the finite element discretization of (3.0.1)-(3.0.2) with the constant coefficients case: find $\mathbf{u}_h \in V_h(D)$ such that

$$a(\mathbf{u}_h, \mathbf{v}_h) = \left(D\mathbf{u}_h, D\mathbf{v}_h\right) + \tau \left(\mathbf{u}_h, \mathbf{v}_h\right) = \left(\mathbf{f}, \mathbf{v}_h\right), \ \ \forall \mathbf{v} \in V_h(D), \tag{3.5.1}$$

with the induced operator A defined as $(\cdot,\cdot)_A := a(\cdot,\cdot)$. Based on the discrete regular decomposition, we have the following result.

Theorem 3.5.1 ([68, Theorem 6.1])**.** *Assume $0 < \tau \leq 1$. For any $\mathbf{v}_h \in V_h(D)$, there are $\mathbf{\Phi}_h \in \mathbf{V}_h(\mathbf{grad})$ and $p_h \in V_h(D^-)$ such that*

$$\sum_{\mathbf{b}\in\mathcal{B}(D)} \mathbf{v}_{\mathbf{b}} + \Pi_h^D \mathbf{\Phi}_h + D^- p_h = \mathbf{v}_h, \tag{3.5.2}$$

$$\sum_{\mathbf{b}\in\mathcal{B}(D)} \left\|\mathbf{v}_{\mathbf{b}}\right\|_A^2 + \left\|\mathbf{\Phi}_h\right\|_{1,\Omega}^2 + \tau \left\|D^- p_h\right\|_{0,\Omega}^2 \lesssim \left\|\mathbf{v}_h\right\|_A^2, \tag{3.5.3}$$

where $\mathbf{v}_{\mathbf{b}} \in span\{\mathbf{b}\}$ with $\mathbf{b} \in \mathcal{B}(D)$ locally supported basis functions. The constant here only depends on Ω, D and the shape regularity of $\mathcal{T}_h$.

Therefore, the above theorem provides a stable decomposition of $\mathbf{v}_h \in V_h(D)$ into three different components. The first component $\sum_{\mathbf{b}\in\mathcal{B}(D)} \mathbf{v}_{\mathbf{b}}$ is in $V_h(D)$. So in terms of the concepts developed in Section 3.1, we introduce the smoothing operator

characterized by the inner product:

$$s\left(\mathbf{v}_h, \mathbf{v}_h\right) := \sum_{\mathbf{b}\in\in\mathcal{B}(D)} a\left(\mathbf{v}_{\mathbf{b}}, \mathbf{v}_{\mathbf{b}}\right). \tag{3.5.4}$$

The matrix representation of this smoother coincides with the diagonal $\mathbf{D}_A$ of $\mathbf{A}_D$. Since all the basis functions are local supported, one can easily show that

$$\left\|\widetilde{\mathbf{v}}_h\right\|_A^2 = \left\|\sum_{\mathbf{b}\in\in\mathcal{B}(D)} \alpha_{\mathbf{b}}\mathbf{b}\right\|_A^2 \leq C \sum_{\mathbf{b}\in\mathcal{B}(D)} \left|\alpha_{\mathbf{b}}\right|^2 \|\mathbf{b}\|_A^2 = Cs(\mathbf{v},\mathbf{v}), \tag{3.5.5}$$

where C is a constant only depending on the shape-regularity of $\mathcal{T}_h$. This implies that c_s in (3.1.11) can be chosen independent of jumps in coefficients and mesh size.

3.5.1 Preconditioners for Constant Coefficients Case

For the case $D = \mathbf{curl}$, we introduce two auxiliary spaces:

(1) the space $W_1 := \mathbf{V}_h(\mathbf{grad})$ with inner product $\bar{a}_1\left(\mathbf{\Psi}_h, \mathbf{\Psi}_h\right) := \left\|\mathbf{\Psi}_h\right\|_{1,\Omega}^2$. The corresponding transfer operator is $\Pi_1 := \Pi_h^{\mathbf{curl}}$ and, thanks to (3.3.2), (3.1.10) holds with constant c_1 depending only on the shape-regularity of the mesh.

(2) the discrete potential space $W_2 := V_h(\mathbf{grad})$ equipped with inner product $\bar{a}_2\left(p_h, p_h\right) := \left|p_h\right|_{1,\Omega}^2$, and transfer operator $\Pi_2 := \mathbf{grad} : V_h(\mathbf{grad}) \mapsto V_h(\mathbf{curl})$, whose norm is bounded uniformly by 1.

We write $\mathbf{G}$ for the matrix related to $\mathbf{grad}$ and L for the discrete Laplacian (matrix) on linear Lagrangian finite element space $V_h(\mathbf{grad})$. Then the matrix of the resulting

auxiliary space preconditioner for the $\mathbf{H}(\mathbf{curl};\Omega)$ problem reads

$$\mathbf{B}_{\mathbf{curl}} := \mathbf{D}_{A}^{-1} + \mathbf{P}_{h}^{\mathbf{curl}}(\mathbf{L}+\tau\mathbf{M})^{-1}\mathbf{P}_{h}^{\mathbf{curl}T} + \tau^{-1}\mathbf{G}L^{-1}\mathbf{G}^{T}, \tag{3.5.6}$$

where $\mathbf{L}$ is the matrix related to the bilinear form $(\mathbf{grad}\mathbf{\Phi}, \mathbf{grad}\mathbf{\Psi})$ on $\mathbf{V}_{h}(\mathbf{grad})$, and $\mathbf{M}$ is the matrix related to the $\mathbf{L}^{2}$-inner product on $\mathbf{V}_{h}(\mathbf{grad})$.

Theorem 3.5.2. *For $0 < \tau \leq 1$ the condition number $\kappa\left(B_{\mathbf{curl}}A_{\mathbf{curl}}\right) \leq C$, where the constant C only depends on Ω and the shape regularity of the mesh.*

Proof. Theorem 3.5.1 provides the bound for c_{0} from (3.1.12). the constant c_{s} follows from (3.5.12) and c_{1} and c_{2} were discussed above. Therefore (3.1.13) leads to the conclusion. □

When $D = \mathrm{div}$, we have the discrete potential $p_{h} \in V_{h}(\mathbf{curl})$ which is not entirely desirable. In order to avoid solving a $\mathbf{H}(\mathbf{curl})$-elliptic equations for p_{h}, we apply the decomposition Theorem 3.3.3 recursively and replace p_{h} by a $\mathbf{\Phi}_{h} \in \mathbf{V}(\mathbf{grad})$ and some "high frequency" edge element function. Therefore,

$$\begin{aligned}
\mathbf{v}_{h} &= \sum_{\mathbf{b}\in\mathcal{B}(\mathrm{div})} \mathbf{v}_{\mathbf{b}} + \Pi_{h}^{\mathrm{div}}\mathbf{\Psi}_{h} + \mathbf{curl}\, p_{h} \\
&= \sum_{\mathbf{b}\in\mathcal{B}(\mathrm{div})} \mathbf{v}_{\mathbf{b}} + \Pi_{h}^{\mathrm{div}}\mathbf{\Psi}_{h} + \sum_{\mathbf{q}\in\mathcal{B}(\mathbf{curl})} \mathbf{curl}\, p_{\mathbf{q}} + \mathbf{curl}\, \Pi_{h}^{\mathbf{curl}}\mathbf{\Phi}_{h},
\end{aligned}$$

where $\mathbf{\Phi}_h,\ \mathbf{\Psi} \in \mathbf{V}(\mathbf{grad})$. In this decomposition, we have used the fact that $\mathbf{curl\ grad} = 0$. From Theorem 3.5.1, we have

$$\sum_{\mathbf{b}\in\mathcal{B}(\mathrm{div})} \left\|\mathbf{v}_{\mathbf{b}}\right\|_A^2 + \left\|\mathbf{\Psi}_h\right\|_{1,\Omega}^2 + \sum_{\mathbf{q}\in\mathcal{B}(\mathbf{curl})} \left\|\mathbf{curl}\, p_{\mathbf{q}}\right\|_{0,\Omega}^2 + \left\|\mathbf{\Phi}_h\right\|_{1,\Omega}^2 \lesssim \left\|\mathbf{v}_h\right\|_A^2, \quad (3.5.7)$$

The decomposition suggests that we choose the following auxiliary spaces:

(1) the space $W_1 := \mathbf{V}_h(\mathbf{grad})$ with inner product $\bar{a}_1\left(\mathbf{\Psi}_h, \mathbf{\Psi}_h\right) := \left\|\mathbf{\Psi}_h\right\|_{1,\Omega}^2$. The corresponding transfer operator is $\Pi_1 := \Pi_h^{\mathrm{div}}$ and, thanks to (3.3.2), (3.1.10) holds with constant c_1 depending only on the shape-regularity of the mesh. The related interpolation matrix $\mathbf{P}_h^{\mathrm{div}}$ assigns to each face of the mesh with unit normal $\mathbf{n}$ and area $|F|$ the number $\frac{1}{3}|F|\left(w_1 + w_2 + w_3\right)\cdot\mathbf{n}$, where w_i is the vectorial nodal value at vertex i of the face.

(2) $W_2 := V_h(\mathbf{curl})$ equipped with inner product $\bar{a}_2\left(\mathbf{w}_h, \mathbf{w}_h\right) := \tau\left\|\mathbf{curlw}_h\right\|_{0,\Omega}^2$. Evidently, the Galerkin discretization of $\bar{a}_2$ leads to a diagonal matrix denoted by $\mathbf{D}_{\mathbf{curl}}$. The transfer operator associated with W_2 is **curl** and $c_2 = 1$ is obvious. Its matrix representation $\mathbf{C}$ coincides with the incidence matrix of (interior) edges and faces of the mesh.

(3) $W_3 := V_h(\mathbf{grad})$ with norm $\sqrt{\tau}\|\cdot\|_{1,\Omega}$, and transfer operator **curl**. Again, we immediately get $c_3 = 1$ for the constant. Owing to the commuting diagram property, the matrix associated with this transfer is given by $\mathbf{CP}_h^{\mathbf{curl}}$.

Summing up, the matrix representation of the auxiliary space preconditioner for the variational problem discretized on $V_h(\mathrm{div})$ is given by

$$\mathbf{B}_{\mathrm{div}} := \mathbf{D}_A^{-1} + \mathbf{P}_h^{\mathrm{div}} \left(\mathbf{L} + \tau \mathbf{M}\right)^{-1} \mathbf{P}_h^{\mathrm{div}T} + \tau^{-1} \mathbf{C}\mathbf{P}_{\mathbf{curl}} \left(\mathbf{L} + \tau \mathbf{M}\right)^{-1} \mathbf{P}_h^{\mathbf{curl}T} \mathbf{C}^T. \quad (3.5.8)$$

Similar to Theorem 3.5.2, we obtain the following condition number estimate by the same arguments.

Theorem 3.5.3. *For $0 < \tau \leq 1$ the condition number $\kappa\left(B_{\mathrm{div}} A_{\mathrm{div}}\right) \leq C$, where the constant C only depends on Ω and the shape regularity of the mesh.*

3.5.2 A Preconditioner for $\mathbf{H}_0(\mathbf{curl})$ with Jump Coefficients

Now we turn to (3.0.3): find $\mathbf{u}_h \in V_h(\mathbf{curl})$ such that

$$\left(\omega \mathbf{curl}\, \mathbf{u}_h, \mathbf{curl}\, \mathbf{v}_h\right) + \tau \left(\omega \mathbf{u}_h, \mathbf{v}_h\right) = \left(\mathbf{f}, \mathbf{v}_h\right), \ \ \forall \mathbf{v}_h \in V_h(\mathbf{curl}).$$

The design of robust preconditioner for this case relies on the splitting in Theorem 3.4.3. Similar to Theorem 3.5.1, we have the following stable decomposition theorem.

Theorem 3.5.4. *For any $\mathbf{v}_h \in V_h(\mathbf{curl})$, there are $\mathbf{\Phi}_h \in \mathbf{V}_h(\mathbf{grad})$ and $p_h \in V_h(\mathbf{grad})$ such that*

$$\sum_{\mathbf{b} \in \mathcal{B}(D)} \mathbf{v}_{\mathbf{b}} + \Pi_h^D \mathbf{\Phi}_h + D^- p_h = \mathbf{v}_h, \quad (3.5.9)$$

$$\sum_{\mathbf{b} \in \mathcal{B}(D)} \left\|\mathbf{v}_{\mathbf{b}}\right\|_A^2 + \left\|\mathbf{\Phi}_h\right\|_{1,\omega}^2 + \tau \left\|D^- p_h\right\|_{0,\omega}^2 \lesssim \left\|\mathbf{v}_h\right\|_A^2, \quad (3.5.10)$$

where $\mathbf{v_b} \in span\{\mathbf{b}\}$ *with* $\mathbf{b} \in \mathcal{B}(D)$ *locally supported basis functions. The constant here only depends on* Ω, D *and the shape regularity of* $\mathcal{T}_h$, *but is independent of the coefficients* ω *and the mesh size.*

Proof. The proof is similar to the proof of Theorem 3.5.1. By Theorem 3.4.3, we have

$$\mathbf{v}_h = \widetilde{\mathbf{v}}_h + \Pi_h^{\mathbf{curl}} \mathbf{\Phi}_h + \mathbf{grad}\, p_h.$$

Now, we expand $\widetilde{\mathbf{v}}_h$ by the basis functions $\mathbf{b} \in \mathcal{B}(\mathbf{curl})$ as

$$\widetilde{\mathbf{v}}_h = \sum_{\mathbf{b} \in \mathcal{B}(\mathbf{curl})} \mathbf{v_b}.$$

By the inverse inequality, we obtain

$$\begin{aligned}
\sum_{\mathbf{b} \in \mathcal{B}(\mathbf{curl})} \left\| \mathbf{v_b} \right\|_A^2 &= \sum_{\mathbf{b} \in \mathcal{B}(\mathbf{curl})} \left(\left\| \mathbf{curl}\, \mathbf{v_b} \right\|_{0,\omega}^2 + \left\| \mathbf{v_b} \right\|_{0,\omega}^2 \right) \\
&\lesssim \sum_{\mathbf{b} \in \mathcal{B}(\mathbf{curl})} \left\| h^{-1} \mathbf{v_b} \right\|_{0,\omega}^2 + \sum_{\mathbf{b} \in \mathcal{B}(\mathbf{curl})} \left\| \mathbf{v_b} \right\|_{0,\omega}^2 \\
&\lesssim \left\| h^{-1} \widetilde{\mathbf{v}}_h \right\|_{0,\omega}^2 + \left\| \widetilde{\mathbf{v}}_h \right\|_{0,\omega}^2 \\
&\lesssim \left\| \mathbf{v}_h \right\|_A^2.
\end{aligned}$$

In the last step, we used the estimate in Theorem 3.4.3. The remaining bounds follow immediately from Theorem 3.4.3. □

Similarly, we introduce the smoother by

$$s\left(\mathbf{v}_h,\mathbf{v}_h\right):=\sum_{\mathbf{b}\in\mathcal{B}(D)}\left(\omega\mathbf{curl}\ \mathbf{v}_{\mathbf{b}},\mathbf{curl}\ \mathbf{v}_{\mathbf{b}}\right)+\tau\left(\omega\mathbf{v}_{\mathbf{b}},\mathbf{v}_{\mathbf{b}}\right), \tag{3.5.11}$$

and its matrix representation coincides with the diagonal $\mathbf{D}_A$ of $\mathbf{A}_{\mathbf{curl}}$. Since all the basis functions are local supported, the following estimate

$$\left\|\widetilde{\mathbf{v}}_h\right\|_A^2=\left\|\sum_{\mathbf{b}\in\mathcal{B}(\mathbf{curl})}\alpha_{\mathbf{b}}\mathbf{b}\right\|_A^2\leq C\sum_{\mathbf{b}\in\mathcal{B}(\mathbf{curl})}\left|\alpha_{\mathbf{b}}\right|^2\left\|\mathbf{b}\right\|_A^2=Cs(\mathbf{v},\mathbf{v}), \tag{3.5.12}$$

also holds for the weighted norm, where C is a constant only depends on the shape-regularity of $\mathcal{T}_h$. This implies that c_s in (3.1.11) can be chosen independent of jumps in coefficients and mesh size.

Because all the arguments in proving (3.3.2) are local, we can multiply by appropriate weights on both sides. Therefore, a weighted version of (3.3.2) also holds:

$$\left\|\mathbf{curl}\Pi_h^{\mathbf{curl}}\mathbf{\Phi}_h\right\|_{0,\omega}\lesssim\left|\mathbf{\Phi}_h\right|_{1,\omega},\ \ \left\|\Pi_h^{\mathbf{curl}}\mathbf{\Phi}_h\right\|_{0,\omega}\lesssim\left\|\mathbf{\Phi}_h\right\|_{0,\omega},\ \forall\mathbf{\Phi}_h\in\mathbf{V}_h(\mathbf{grad}). \tag{3.5.13}$$

In this case, we introduce two (weighted) auxiliary spaces:

(1) the space $W_1:=\mathbf{V}_h(\mathbf{grad})$ with inner product

$$\bar{a}_1\left(\mathbf{\Psi}_h,\mathbf{\Psi}_h\right):=\left\|\mathbf{grad}\mathbf{\Psi}_h\right\|_{0,\omega}^2+\left\|\mathbf{\Psi}_h\right\|_{0,\omega}^2.$$

The corresponding transfer operator is $\Pi_1 := \Pi_h^{\mathbf{curl}}$ and, thanks to (3.5.13), (3.1.10) holds with constant c_1 depending only on the shape-regularity of the mesh.

(2) the discrete potential space $W_2 := V_h(\mathbf{grad})$ equipped with inner product

$$\bar{a}_2\left(p_h, p_h\right) := \left|p_h\right|_{1,\omega}^2,$$

and transfer operator $\Pi_2 := \mathbf{grad} : V_h(\mathbf{grad}) \mapsto V_h(\mathbf{curl})$, whose norm is bounded uniformly by 1.

Then the matrix of the resulting auxiliary space preconditioner for equation (3.0.3) reads

$$\mathbf{B}_{\mathbf{curl}}^{\omega} := \mathbf{D}_A^{-1} + \mathbf{P}_h^{\mathbf{curl}}(\mathbf{L}(\omega) + \tau\mathbf{M}(\omega))^{-1}\mathbf{P}_h^{\mathbf{curl}^T} + \tau^{-1}\mathbf{G}L(\omega)^{-1}\mathbf{G}^T, \qquad (3.5.14)$$

where $\mathbf{L}(\omega)$ is the matrix related to the bilinear form $(\omega\ \mathbf{grad}\ \mathbf{\Phi}, \mathbf{grad}\ \mathbf{\Psi})$ on $\mathbf{V}_h(\mathbf{grad})$, $\mathbf{M}(\omega)$ is the matrix related to the weighted $\mathbf{L}^2$-inner product on $\mathbf{V}_h(\mathbf{grad})$, and $L(\omega)$ is the matrix related to the bilinear form $(\omega\mathbf{grad}\ \phi, \mathbf{grad}\ \psi)$ on $\mathcal{V}_h(\mathbf{grad})$.

Similarly, we can easily verify the following theorem.

Theorem 3.5.5. *The condition number* $\kappa\left(B_{\mathbf{curl}}^{\omega} A_{\mathbf{curl}}^{\omega}\right) \leq C$, *where the constant* C *is independent of the coefficients and the mesh size.*

3.6 Remarks on the Implementation

As we can see from (3.5.6), (3.5.8) and (3.5.14), these preconditioners make use of efficient solvers for discrete H^1 linear systems (cf. Chapter 2). In this section, we discuss some implementation details about the related operators in the preconditioners.

First of all, the matrix $\mathbf{G}$ of the discrete **grad** operator is actually the signed incidence matrix of the edge-to-node connectivity. Similarly, the matrix $\mathbf{C}$ of the discrete **curl** operator is actually the signed incidence matrix of the face-to-edge connectivity. The smoother operator $\mathbf{D}_A$ can be chosen as simple relaxation methods such as point Jacobi or symmetric Gauss-Seidel methods. In Chapter 4, the matrices $\mathbf{G}$ and $\mathbf{C}$ are denoted by $\mathbb{D}_0$ and $\mathbb{D}_1$ respectively.

Given the triangulation $\mathcal{T}_h$, let n_n, n_e and n_f be the number of (interior) nodes, edges, and faces respectively. The matrix representation of the grid transfer operators $\Pi_h^{\mathbf{curl}}$ and Π_h^{div} can be evaluated easily. Take $\mathbf{P}_h^{\mathbf{curl}}$ for example. Given a vector field $\mathbf{E}$, it can be written as $\mathbf{E} := \sum_{i=1}^{3} E_i \mathbf{e}_i$ where $\mathbf{e}_i$ denotes an axis of the global Cartesian coordinate frame. Each component E_i can be expanded with linear Lagrange-type basis functions associated with the vertices of the mesh. On each axis component, we want to express the nodal basis $\lambda_j(x)\mathbf{e}_i$ as the linear combination of the basis functions of the edge element. Therefore, the elements in the matrix are based on computing line integrals from the tangential components $\mathbf{t}_k$:

$$\int_{e_k} \lambda_j(x)\mathbf{e}_i \cdot \mathbf{t}_k = \frac{1}{2} \left| e_k \right| \mathbf{e}_i \cdot \mathbf{t}_k.$$

Therefore, $\mathbf{P}_h^{\mathbf{curl}}$ actually contains three matrices of dimension $n_e \times n_n$, one matrix for each coordinate direction. Similarly, $\mathbf{P}_h(\text{div})$ contains three matrices of dimension $n_f \times n_n$, one matrix corresponding to each coordinate direction. The elements in the matrix are based on computing the face integrals from the normal components.

To invert the matrices $\mathbf{L}+\tau\mathbf{M}$ (or $\mathbf{L}(\omega)+\tau\mathbf{M}(\omega)$) and L, we can form these matrices by using the grid transform matrices $\mathbf{P}_h^{\mathbf{curl}}$ or $\mathbf{P}_h^{\mathrm{div}}$. Specifically, for $\mathbf{B}_h^{\mathbf{curl}}$ in (3.5.6), we may form the matrix $\mathbf{L}+\tau\mathbf{M}$ by using the stiffness matrix $\mathbf{A}_{\mathbf{curl}}$ and grid transform matrix $\mathbf{P}_h^{\mathbf{curl}}$:

$$\mathbf{P}_h^{\mathbf{curl}T}\mathbf{A}_{\mathbf{curl}}\mathbf{P}_h^{\mathbf{curl}}.$$

By doing this, we avoid to assemble the stiffness matrix $\mathbf{L}+\tau\mathbf{M}$ by using the triangulation information $\mathcal{T}_h$. Similarly, the matrix τL can be obtained by $\mathbf{G}^T\mathbf{A}_{\mathbf{curl}}\mathbf{G}$. Then the "auxiliary space $\mathbf{H}(\mathbf{curl})$ solver" consists of the following three components:

(1) The smoother $\mathbf{D}_A^{\mathbf{curl}}$ of $\mathbf{A}_{\mathbf{curl}}$ (it could be the standard Jacobi or symmetric Gauss-Seidel methods).

(2) An AMG solver $B_h^{\mathbf{grad}}$ for $\mathbf{G}^T\mathbf{A}_{\mathbf{curl}}\mathbf{G}$ (note here $\mathbf{G}^T\mathbf{A}_{\mathbf{curl}}\mathbf{G}$ corresponding to a finite element discretization of second order elliptic equations).

(3) An (vector) AMG solver $\mathbf{B}_h^{\mathbf{grad}}$ for $\left(\mathbf{P}_h^{\mathbf{curl}}\right)^T\mathbf{A}_{\mathbf{curl}}\mathbf{P}_h^{\mathbf{curl}}$.

For $\mathbf{H}(\mathbf{curl})$ systems, this implementation makes use of the stiffness matrix $\mathbf{A}_{\mathbf{curl}}$, the coordinates of the grid points, along with the discrete gradient operator $\mathbf{G}$. For $\mathbf{H}(\mathrm{div})$ systems, it makes use of stiffness matrix $\mathbf{A}_{\mathrm{div}}$, the coordinates of the grid points, as well as the discrete curl operator $\mathbf{C}$. This implementation is almost "black-box" because it only uses the information of the discrete gradient matrix plus vertex coordinates. For $\mathbf{H}(\mathbf{curl})$ systems, the preconditioners have been included and tested in LLNL's *hypre* package (cf. [50]) based on its parallel algebraic multigrid solver "BoomerAMG" (cf.

[59]). Extensive numerical experiments demonstrate that this preconditioner is also efficient and robust for more general equations (see Hiptmair and Xu [68], and Kolev and Vassilevski [77, 79]) such as

$$\mathbf{curl}(\mu(x)\mathbf{curl}\ \mathbf{u}) + \sigma(x)u = f \tag{3.6.1}$$

where μ and σ may be discontinuous, degenerating, and have large variations. For the implementation and numerical experiments for $\mathbf{H}(\mathrm{div})$ systems, we refer to Chapter 4 (see Algorithm 4).

Chapter 4

Compatible AMG Preconditioners for H(curl) and H(div) Systems

Compatible discretization is a general framework that transforms partial differential equations into discrete algebraic problems. The resulting discrete problems mimic fundamental properties of the continuum equations. This framework covers compatible finite element, finite volume, and finite difference methods. All of these different discretization methods adopt similar procedures to construct discrete exterior derivatives (incidence matrices), which unify the various operators of vector calculus. The main differences between the various discretization methods can be viewed as differences in the approaches used to construct discrete Hodge operators (which include all metric information).

Recently, Bochev, Hu, Siefert and Tuminaro [16] proposed an AMG approach based on the *compatible gauge reformulation* for Maxwell's equations. This approach is based on *compatible* (or *mimetic*) discretization [17, 18]. It makes use of a discrete Hodge decomposition on co-chains to reformulate the discrete **H**(**curl**) system into an equivalent 2×2 block linear system whose diagonal blocks are discrete Hodge Laplace operators acting on 1-cochains and 0-cochains respectively.

Let Ω denote a bounded, simply connected, contractible domain in $\mathbb{R}^3$ with Lipschitz continuous boundary $\partial\Omega$. We assume that $\partial\Omega$ consists of two disjointed parts, Γ and Γ^*, i.e., $\partial\Omega = \Gamma \cup \Gamma^*$ and $\Gamma \cap \Gamma^* = \emptyset$. In this chapter, we are looking at the

compatible discretization of the following two model equations.

$$\begin{cases} \mathbf{curl}(\mu\ \mathbf{curl}\ \mathbf{E}) + \sigma\mathbf{E} &= f \quad \text{in } \Omega, \\ \mathbf{E}\times\mathbf{n} &= 0 \quad \text{on } \Gamma, \\ (\mu\ \mathbf{curl}\ \mathbf{E})\times\mathbf{n} &= 0 \quad \text{on } \Gamma^*, \end{cases} \tag{4.0.1}$$

The first equation, (4.0.1), arises naturally in the eddy current equations in the electric field (after discretization on time) $\mathbf{E}$, where σ is related to the electrical conductivity and μ is the magnetic permeability.

$$\begin{cases} -\mathbf{grad}\ (\lambda\ \mathrm{div}\ \mathbf{B}) + \mu\mathbf{B} &= f \quad \text{in } \Omega, \\ \mu\mathbf{B}\cdot\mathbf{n} &= 0 \quad \text{on } \Gamma, \\ \lambda\ \mathrm{div}\ \mathbf{B} &= 0 \quad \text{on } \Gamma^*, \end{cases} \tag{4.0.2}$$

The second equation, (4.0.2), is ubiquitous in problems arising in fluid and solid mechanics [31, 53]. It occurs, in particular, in the solution of second order elliptic PDEs by first order least-square methods or by mixed methods with augmented Lagrangians (see [109, 4, 61, 116] and the references cited therein). Here, we assume that all coefficients σ, λ and μ are positive throughout the domain, but may possibly vary widely.

The variational formulations of problems (4.0.1)-(4.0.2) naturally lead to the Hilbert spaces $\mathbf{H}(\mathbf{curl})$ and $\mathbf{H}(\mathrm{div})$. The detailed discussion on the properties of these two spaces can be found in Chapter 3.

The rest of this chapter is organized as follows. Section 4.1 reviews basic facts about the discretization framework used in this dissertation. In Section 4.2, we apply

this framework to obtain a compatible discretization for the $\mathbf{H}(\mathrm{div})$ system and its equivalent reformulation. AMG solvers for the reformulated system are developed in Section 4.2.2. In Section 4.4, we present numerical experiments in 3D that illustrate the new technique in the context of smoothed aggregation of AMG. In all experiments we use finite element discretizations based on the lowest order Raviart-Thomas element and lowest order Nédélec element on structured tetrahedral elements.

4.1 Compatible Discretization Framework

We first translate scalar and vector functions to their differential form equivalents and consider the computational grid to be an algebraic topological complex. The grid consists of 0-cells (nodes), 1-cells (edges), 2-cells (faces), and 3-cells (volumes) which form k-chains ($k = 0, 1, 2, 3$). For simplicity, we focus on simplicial grids. However, most of the developments easily carry over to general polyhedral domain partitions. We refer to the survey papers [64, 7] and the monograph [20] for a review of the basic concepts of differential forms necessary for the numerical framework.

In this section, we give a short introduction of a general framework for compatible discretizations developed in [14]. This framework is based on algebraic topology and includes certain finite element (e.g. [15, 105]), finite volume (e.g. [90]), and finite difference (e.g. [99]) schemes as particular cases. As a result, the AMG algorithm developed in this paper is readily applicable to discrete problems generated by any of these schemes.

4.1.1 Computational Grid

We consider computational grid $\mathcal{T}_h$ consisting of 0-cells (nodes), 1-cells (edges), 2-cells (faces), and 3-cells (volumes). A *k-cell* s_k is an ordered collection $\left[p_0, \ldots, p_k\right]$ of distinct points $p_0, \ldots, p_k \in \mathbb{R}^d$. A *k-chain* is a formal linear combinations of k-cells

$$c_k = \sum_i a_i s_k^i,$$

where a_i are real constants and s_k^i are the k-cells (see [43]). For example, in 3-dimensional space, a 0-simplex is a simply point (vertex) $[p_0]$; a 1-simplex is an oriented edge denoted by an ordered pair of vertices $[p_0, p_1]$; a 2-simplex is an oriented triangle denoted by an ordered triple of vertices $[p_0, p_1, p_2]$; a 3-simplex is an oriented closed tetrahedron denoted by an ordered quadruple of vertices $[p_0, p_1, p_2, p_3]$. Fig. 4.1 illustrates k-simplices in 3-dimensional space.

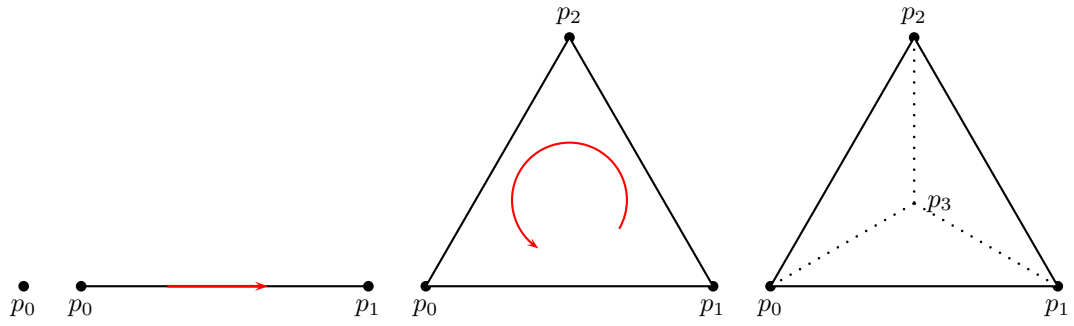

Fig. 4.1. 0-, 1-, 2- and 3-simplex in $\mathbb{R}^3$

The sets of k-chains forming $\mathcal{T}_h$ are denoted by $\mathcal{C}_k$ $(k = 0, 1, 2, 3)$. We will assume that $\mathcal{T}_h$ is such that the collection $\{\mathcal{C}_0, \mathcal{C}_1, \mathcal{C}_2, \mathcal{C}_3\}$ is a complex, i.e., for any $c \in \mathcal{C}_k$, $\partial_k c \in \mathcal{C}_{k-1}$, where $\partial_k : \mathcal{C}_k \mapsto \mathcal{C}_{k-1}$ is the boundary operator on k-chains (cf. [35]) defined as follows. The *boundary* ∂ of a k-simplex is a $(k-1)$-chain defined by the formula

$$\partial \left[p_0, \ldots, p_k\right] = \sum_{i=1}^{k} (-1)^i \left[p_0, \ldots, p_{i-1}, p_i, \ldots, p_k\right] \tag{4.1.1}$$

(see Figure 4.2 for example). By definition, it is not difficult to check that we have the

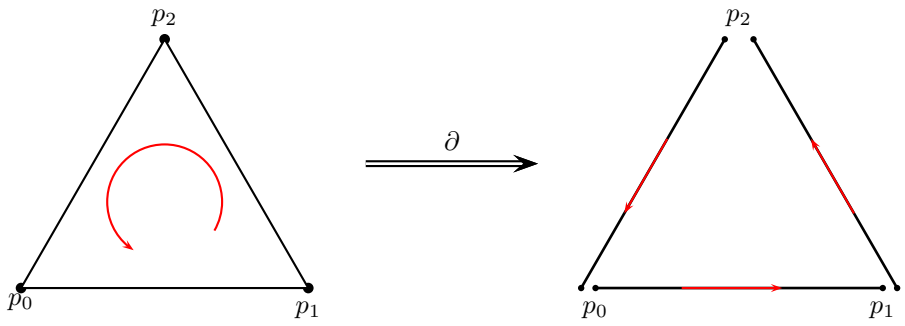

Fig. 4.2. The boundary operator ∂

identity $\partial_k \partial_{k+1} = 0$. This identity gives rise to the exact sequence since Range $\left(\partial_k\right) \subset$ Ker $\left(\partial_{k-1}\right)$:

$$0 \longleftarrow \mathcal{C}_0 \xleftarrow{\partial_1} \mathcal{C}_1 \xleftarrow{\partial_2} \mathcal{C}_2 \xleftarrow{\partial_3} \mathcal{C}_3 \longleftarrow 0\,. \tag{4.1.2}$$

The dual of $\mathcal{C}_k$ is denoted by $\mathcal{C}^k$ and its members are called *k-cochains* (cf. [43]). While $\mathcal{C}_k$ and $\mathcal{C}^k$ are isomorphic, they have different meanings in our discretization framework. The set $\mathcal{C}_k$ represents the physical objects that form the grid, while $\mathcal{C}^k$ is a collection of real numbers associated with the grid objects. For example, $c_1 \in \mathcal{C}_1$ is a formal sum of (oriented) grid edges, while its isomorphic image $c^1 \in \mathcal{C}^1$ is a set of real numbers[1] assigned to the edges of c_1. Therefore, the elements of $\mathcal{C}^0$ provide values associated with the 0-cells (grid nodes); the elements of $\mathcal{C}^1$ are values associated with the 1-cells (grid edges); $\mathcal{C}^2$ contains values assigned to the 2-cells (grid faces) of the grid, and $\mathcal{C}^3$ is contains values assigned to the 3-cells (grid volumes). We will use $\mathcal{C}^0$ and $\mathcal{C}^3$ to approximate scalar functions and $\mathcal{C}^1$ and $\mathcal{C}^2$ to approximate vector functions. The symbols $\mathcal{C}^k_\Gamma$ will denote the subspaces of $\mathcal{C}^k$ constrained by zero on the Dirichlet boundary Γ for $k = 0, 1, 2$. Such spaces are needed to approximate scalar and vector functions subject to appropriate boundary conditions[2].

Chains and cochains, which correspond to domains of integration and integrands respectively, are not only the fundamental geometric concepts to define integration on general manifolds in a mathematical rigorous sense, but they also provide a powerful tool to discretize a continuum theory in a generalized sense.

---

[1] Clearly, $\mathcal{C}^k$ is isomorphic to $\mathbb{R}^{\tilde{k}}$, where $\tilde{k} = \dim \mathcal{C}^k$. For simplicity, the isomorphic image of the cochain $c^k \in \mathcal{C}^k$ in $\mathbb{R}^{\tilde{k}}$ will be denoted by the same symbol.

[2] For example, $\mathcal{C}^0_\Gamma$ approximates scalar functions such that $\phi = 0$ on Γ; $\mathcal{C}^1_\Gamma$ can be used to approximate vector field $\mathbf{E}$ such that $\mathbf{n} \times \mathbf{E} = 0$ on Γ. The space $\mathcal{C}^2_\Gamma$ is appropriate for vector field $\mathbf{B}$ that has a vanishing normal component on Γ.

4.1.2 Natural Operators

Let $\langle \cdot, \cdot \rangle$ denote the duality pairing of $\mathcal{C}_k$ and $\mathcal{C}^k$. The adjoint of ∂_k, defined by $\langle a, \partial_k c \rangle = \langle \delta_k a, c \rangle$, induces an operator $\delta_k : \underset{\Gamma}{\mathcal{C}^k} \mapsto \underset{\Gamma}{\mathcal{C}^{k+1}}$ called coboundary. This operator satisfies $\delta_{k+1}\delta_k = 0$ and gives rise to the exact sequence

$$\mathbb{R} \longrightarrow \underset{\Gamma}{\mathcal{C}^0} \xrightarrow{\delta_0} \underset{\Gamma}{\mathcal{C}^1} \xrightarrow{\delta_1} \underset{\Gamma}{\mathcal{C}^2} \xrightarrow{\delta_2} \mathcal{C}^3 \longrightarrow 0\,. \tag{4.1.3}$$

It is not hard to see that the matrix representation $\mathbb{D}_k$ of δ_k is the signed incidence matrix between $\mathcal{C}^k$ and $\mathcal{C}^{k+1}$. Following [72] we call $\mathbb{D}_0$, $\mathbb{D}_1$, and $\mathbb{D}_2$ *natural* approximations of the gradient, curl and divergence operators. Note that from $\delta_{k+1}\delta_k = 0$ it follows that

$$\mathbb{D}_{k+1}\mathbb{D}_k = 0;\ k = 0, 1, 2\,, \tag{4.1.4}$$

and so our natural operators mimic the well-known vector calculus identities $\nabla \times \nabla = 0$, and $\nabla \cdot \nabla \times = 0$. We shall point out that natural operations are not enough to provide compatible discretizations of the basic second order operators because their ranges and domains do not match. For example, we cannot approximate $\nabla \times \nabla \times$ by $\mathbb{D}_1\mathbb{D}_1$ because $\mathbb{D}_1$ is, in general, a rectangular matrix. The number of its columns and rows equals the number of 1-cells and 2-cells in the grid, which are not the same.

4.1.3 Metric Structures and Derived Operators

Let $\mathbb{M}_k : \overset{k}{\mathcal{C}}_\Gamma \mapsto \overset{k}{\mathcal{C}}_\Gamma$; $k = 0, 1, 2, 3$ denote symmetric positive definite mass matrices. The matrix $\mathbb{M}_k$ endows $\overset{k}{\mathcal{C}}_\Gamma$ with an inner product structure,

$$\left(a^k, b^k\right)_{\mathcal{C}^k} = \left(a^k\right)^T \mathbb{M}_k \left(b^k\right) \quad \forall a^k, b^k \in \mathcal{C}^k \,. \tag{4.1.5}$$

The matrices $\mathbb{M}_0$ and $\mathbb{M}_3$ approximate weighted L^2-inner products of scalar functions:

$$\mathbb{M}_0 \longrightarrow \int_\Omega \gamma p \hat{p}\, d\Omega \,; \quad \mathbb{M}_3 \longrightarrow \int_\Omega \lambda \phi \hat{\phi}\, d\Omega \,,$$

while $\mathbb{M}_1$ and $\mathbb{M}_2$ approximate the weighted L^2-inner products of vector functions

$$\mathbb{M}_1 \longrightarrow \int_\Omega \sigma \mathbf{E}\hat{\mathbf{E}}\, d\Omega \,; \quad \mathbb{M}_2 \longrightarrow \int_\Omega \mu \mathbf{B}\hat{\mathbf{B}}\, d\Omega \,.$$

Whenever it is necessary, we will also use the notation $\mathbb{M}_0(\gamma)$, $\mathbb{M}_1(\sigma)$, $\mathbb{M}_2(\mu)$ and $\mathbb{M}_3(\lambda)$ to show the dependency of the coefficients of these mass matrices explicitly.

We define the derived operator $\overset{*}{\mathbb{D}}_k : \overset{k+1}{\mathcal{C}}_\Gamma \mapsto \overset{k}{\mathcal{C}}_\Gamma$ as the adjoint of $\mathbb{D}_k$ with respect to the inner product (4.1.5):

$$(\overset{*}{\mathbb{D}}_k a^{k+1}, b^k)_{\mathcal{C}^k} = (a^{k+1}, \mathbb{D}_k b^k)_{\mathcal{C}^{k+1}} \,. \tag{4.1.6}$$

From (4.1.6) it is easy to see that for $k = 0, 1, 2$

$$\overset{*}{\mathbb{D}}_k = \mathbb{M}_k^{-1} \mathbb{D}_k^T \mathbb{M}_{k+1} \,. \tag{4.1.7}$$

The matrices $\mathbb{D}^*_2$, $\mathbb{D}^*_1$ and $\mathbb{D}^*_0$ provide a second set of discrete differential operators. Specifically, they are approximations of scaled gradient, curl and divergence operators

$$\mathbb{D}^*_2 \;\rightarrow\; -\mu^{-1}\nabla\lambda\,; \quad \mathbb{D}^*_1 \;\rightarrow\; \sigma^{-1}\nabla\times\mu\,; \quad \mathbb{D}^*_0 \;\rightarrow\; -\gamma^{-1}\nabla\cdot\sigma\,,$$

augmented with the natural boundary conditions. Using (4.1.7) and (2.5.2)

$$\mathbb{D}^*_k\mathbb{D}^*_{k+1} = \mathbb{M}^{-1}_k\mathbb{D}^T_k\mathbb{M}_{k+1}\mathbb{M}^{-1}_{k+1}\mathbb{D}^T_{k+1}\mathbb{M}_{k+2} = \mathbb{M}^{-1}_k\mathbb{D}^T_k\mathbb{D}^T_{k+1}\mathbb{M}_{k+2} = 0\,,$$

and so, the basic vector calculus identities hold for the derived operators as well. The commuting diagram, and the relationships among the operators defined above can be summarized in Figure 4.3. Here, the operators $\Pi^{\mathbf{grad}}_h$, $\Pi^{\mathbf{curl}}_h$, Π^{div}_h, and Π^0_h are the canonical interpolations on $H^1(\Omega)$, $\mathbf{H}(\mathbf{curl})$, $\mathbf{H}(\mathrm{div})$, and $L^2(\Omega)$ to the corresponding finite element spaces $V_h(\mathbf{grad})$, $V_h(\mathbf{curl})$, $V_h(\mathrm{div})$, and $V_h(0)$ respectively (see Chapter 3 for more details). The lower half of the commuting diagram presents the relationships among the discrete differential operators. For example, from this diagram we can easily find out that

$$\mathbb{D}^*_2 = \mathbb{M}^{-1}_2\mathbb{D}^T_2\mathbb{M}_3.$$

Remark 4.1.1. *Given the the triangulation $\mathcal{T}_h$, the discrete differential operators $\mathbb{D}_k$ depend only on the connectivity of the grid structure. If we define $\mathbb{M}_k$ to be the usual mass matrices obtained from the nodal ($k=0$), edge ($k=1$) or face ($k=2$) elements,*

$$
\begin{array}{ccccccccccc}
\mathbb{R} & \xrightarrow{I} & C^\infty(\Omega) & \xrightarrow{\mathbf{grad}} & \mathbf{C}^\infty(\Omega) & \xrightarrow{\mathbf{curl}} & \mathbf{C}^\infty(\Omega) & \xrightarrow{\mathrm{div}} & L^2(\Omega) & \longrightarrow & 0 \\
 & & \downarrow \Pi_h^{\mathbf{grad}} & & \downarrow \Pi_h^{\mathbf{curl}} & & \downarrow \Pi_h^{\mathrm{div}} & & \downarrow \Pi_h^0 & & \\
\mathbb{R} & \xrightarrow{I} & V_h(\mathbf{grad}) & \underset{\mathbb{D}_0^T}{\xrightarrow{\mathbb{D}_0}} & V_h(\mathbf{curl}) & \underset{\mathbb{D}_1^T}{\xrightarrow{\mathbb{D}_1}} & V_h(\mathrm{div}) & \underset{\mathbb{D}_2^T}{\xrightarrow{\mathbb{D}_2}} & V_h(0) & \longrightarrow & 0 \\
 & & \downarrow \mathbb{M}_0(\gamma) & & \downarrow \mathbb{M}_1(\sigma) & & \downarrow \mathbb{M}_2(\mu) & & \downarrow \mathbb{M}_3(\lambda) & & \\
\mathbb{R} & \xleftarrow{I} & V_h(\mathbf{grad}) & \xleftarrow{\mathbb{D}_0^*} & V_h(\mathbf{curl}) & \xleftarrow{\mathbb{D}_1^*} & V_h(\mathrm{div}) & \xleftarrow{\mathbb{D}_2^*} & V_h(0) & \longleftarrow & 0
\end{array}
$$

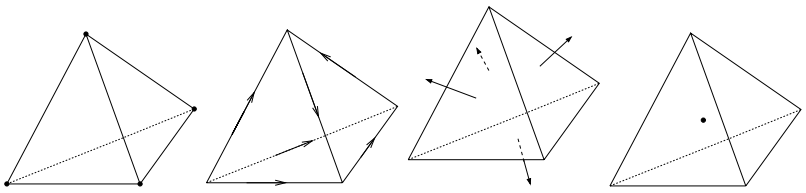

Fig. 4.3. De Rham complex and the lowest order finite element spaces

then the compatible discretization of the $H(\mathbf{grad})$, $\mathbf{H}(\mathbf{curl})$ *and* $\mathbf{H}(\mathrm{div})$ *systems are*

$$\left(\mathbb{D}_k^T \mathbb{M}_{k+1} \mathbb{D}_k + \mathbb{M}_k\right) u^k = f^k, \quad k = 0, 1, 2. \tag{4.1.8}$$

In particular, $A^k = \mathbb{D}_k^T \mathbb{M}_{k+1} \mathbb{D}_k + \mathbb{M}_k$ *are standard stiffness matrices for the finite element discretizations of* $H(\mathbf{grad})$, $\mathbf{H}(\mathbf{curl})$ *and* $\mathbf{H}(\mathrm{div})$ *systems respectively.*

Compared to the other two systems, $H(\mathbf{grad})$ *equation is the most thoroughly studied. There is a vast literature in the studying of efficient solvers for the linear system* $A^0 u^0 = f^0$ *(see Chapter 2). So the main focus of this and the next chapter will be on the design of the efficient solvers for the* $\mathbf{H}(\mathbf{curl})$ *and* $\mathbf{H}(\mathrm{div})$ *systems.*

Remark 4.1.2. *From the implementation point of view, the benefits of this compatible discretization framework are obvious. The discrete differential operators* $\mathbb{D}_k$ $(k = 0, 1, 2)$ *depend only on the mesh topology. These operators can be easily obtained for the given mesh. In fact,* $\mathbb{D}_0$, $\mathbb{D}_1$ *and* $\mathbb{D}_2$ *are the signed edge-to-node, face-to-edge, element-to-face adjacent matrices respectively. Moreover, because* $\mathbb{D}_k$ $(k = 0, 1, 2)$ *are independent of the coefficients of PDEs, if the mesh remains the same, the only thing we need to recalculate is the mass matrices* $\mathbb{M}_k$ $(k = 0, 1, 2, 3)$ *when the coefficients of the equations are changed.*

Because the range of $\mathbb{D}_k$ is contained in the domain of $\mathbb{D}_k^*$ and vice versa, we can use the natural and the derived operators to define discrete versions of the second order differential operators, including a discrete Hodge Laplace operator. Specifically,

for $k = 0, 1, 2$ we have the second order operators

$$\mathbb{D}^*_k \mathbb{D}_k = \mathbb{M}^{-1}_k \mathbb{D}^T_k \mathbb{M}_{k+1} \mathbb{D}_k : \mathcal{C}^k_\Gamma \mapsto \mathcal{C}^k_\Gamma \tag{4.1.9}$$

$$\mathbb{D}_k \mathbb{D}^*_k = \mathbb{D}_k \mathbb{M}^{-1}_k \mathbb{D}^T_k \mathbb{M}_{k+1} : \mathcal{C}^{k+1}_\Gamma \mapsto \mathcal{C}^{k+1}_\Gamma \tag{4.1.10}$$

and the discrete Hodge Laplacian

$$\mathbb{L}_k : \mathcal{C}^k_\Gamma \mapsto \mathcal{C}^k_\Gamma; \quad \mathbb{L}_k = \mathbb{D}^*_k \mathbb{D}_k + \mathbb{D}_{k-1} \mathbb{D}^*_{k-1}; \quad k = 0, 1, 2, 3 \tag{4.1.11}$$

with the understanding that $\mathbb{D}_3 = 0$ and $\mathbb{D}^*_{-1} = 0$.

The discrete operators in (4.1.9)-(4.1.11) approximate the second order elliptic differential operators. In Section 4.2.1 we will use these operators to motivate and explain our reformulation strategy.

Remark 4.1.3. *The mass matrices $\mathbb{M}_k$ is essential in the definition of the inner product* (4.1.5) *and the resulting adjoint operators $\mathbb{D}^*_k$. If we define the inner product by some other way, we will come up with different $\mathbb{D}^*_k$s and different discrete equations. From the preconditioning point of view, we should introduce the new inner product such that*

(1) First of all, we hope that the newly defined inner products are good approximations of standard ones, so that the new equation should be 'equivalent' to the original problem in some sense. Ultimately, we can use this new equation as a good preconditioner of the original one.

(2) Secondly, the new equation induced by this new inner product should be easy to solve.

For this purpose, we can introduce a second set of inner products defined by the lumped mass matrices $\widetilde{\mathbb{M}}_k$ $(k = 0, 1, 2, 3)$, which induce the following inner products

$$\begin{aligned}
(u, v)_{\mathcal{C}^0} &= \sum_{i=1}^{n_0} u_i v_i \int_\Omega \gamma \left|\phi_{i}\right|^2, \ \ \forall u, v \in \mathcal{C}^0_\Gamma \\
(u, v)_{\mathcal{C}^1} &= \sum_{i=1}^{n_1} u_i v_i \int_\Omega \sigma \left|\phi_{E_i}\right|^2, \ \ \forall u, v \in \mathcal{C}^1_\Gamma \\
(u, v)_{\mathcal{C}^2} &= \sum_{i=1}^{n_2} u_i v_i \int_\Omega \mu \left|\phi_{F_i}\right|^2, \ \ \forall u, v \in \mathcal{C}^2_\Gamma \\
(u, v)_{\mathcal{C}^3} &= \sum_{i=1}^{n_3} u_i v_i \int_\Omega \lambda \left|\phi_{V_i}\right|^2, \ \ \forall u, v \in \mathcal{C}^3_\Gamma,
\end{aligned}$$

where n_i $(i = 0, 1, 2, 3)$ is the number of degrees of freedom in $\mathcal{C}^i$. By define these new inner products, we have the following result.

Proposition 4.1.4. *Suppose the mesh is quasi-uniform, then for $k = 0, 1, 2, 3$, the new mass matrix $\widetilde{\mathbb{M}}_k$ is spectral equivalent to $\mathbb{M}_k$.*

Proof. The proof idea is the same as Lemma 2.1.1 in Chapter 2. □

These inner products can be used to define a second set of derived operators $\widetilde{\mathbb{D}}^*_k : \mathcal{C}^{k+1}_\Gamma \mapsto \mathcal{C}^k_\Gamma$ given

$$\widetilde{\mathbb{D}}^*_k = \mathbb{M}_k^{-1} \mathbb{D}_k^T \widetilde{\mathbb{M}}_{k+1}, k = 0, 1, 2$$

respectively, and such that $\widetilde{\mathbb{D}}^*_k \widetilde{\mathbb{D}}^*_{k+1} = 0$. These operators give rise to the discrete Hodge Laplace operators

$$\widetilde{\mathbb{L}}_k : \mathcal{C}^k_\Gamma \mapsto \mathcal{C}^k_\Gamma ; \qquad \widetilde{\mathbb{L}}_k = \widetilde{\mathbb{D}}^*_k \mathbb{D}_k ;$$

that are different versions of $\mathbb{L}_k$ respectively.

The following general result from [14] is needed for the reformulation of the discrete $\mathbf{H}(\mathrm{div})$ equation.

Theorem 4.1.5 ([14, Corollary 4.1])**.** *The dimensions of the kernels of the analytic and discrete Hodge Laplacians are the same.*

Theorem 4.1.5 reveals that the null-space of the discrete Hodge Laplacian and, by extension the structure of the discrete Hodge decomposition of discrete functions in $\mathcal{C}^k_\Gamma$, are topological invariants that are independent of the particular choice of metric, i.e., the matrices $\mathbb{M}_k$. As a result, the assertion of this theorem is valid for both $\mathbb{L}_0$, $\mathbb{L}_1$, $\mathbb{L}_2$, and $\widetilde{\mathbb{L}}_0$, $\widetilde{\mathbb{L}}_1$, $\widetilde{\mathbb{L}}_2$. The properties of these operators, relevant to the reformulation process, are summarized in the following corollary, which is a generalization of [16, Corollary 3.2].

Corollary 4.1.6. *Assume that Ω is contractible. Then, every $u^k \in \mathcal{C}^k_\Gamma$ $(k = 1, 2)$ has the discrete Hodge decomposition*

$$u^k = \mathbb{D}_{k-1} p^{k-1} + \widetilde{\mathbb{D}}^*_k b^{k+1} \tag{4.1.12}$$

where $p^{k-1} \in \mathcal{C}^{k-1}_\Gamma$ and $b^{k+1} \in \mathcal{C}^{k+1}_\Gamma$ solve the equations

$$\widetilde{\mathbb{D}}^*_{k-1} \mathbb{D}_{k-1} p^{k-1} = \widetilde{\mathbb{D}}^*_{k-1} u^k \quad \text{and} \quad \mathbb{D}_k \widetilde{\mathbb{D}}^*_k b^{k+1} = \mathbb{D}_k u^k , \tag{4.1.13}$$

respectively.

4.2 Compatible Gauge AMG Preconditioners for H(curl) and H(div) Systems

Using the discrete operators defined in the last section, the compatible discretizations of **H**(**curl**) and **H**(div) systems (4.0.1)-(4.0.2) are straightforward. Specifically, we approximate u by a k-cochain $u^k \in \underset{\Gamma}{\mathcal{C}^k}$ $(k = 1, 2)$ that is associated with the k-cells (the edges when $k = 1$, and faces when $k = 2$) of the mesh that are not in Γ. Then the compatible discrete versions of the second order differential operators are provided by the second order discrete operators $\underset{k}{\mathbb{D}^*}\underset{k}{\mathbb{D}}$ for $k = 1$, or 2 respectively. As a result, the compatible, fully discrete systems of (4.0.1)-(4.0.2) are given by

$$(\underset{k}{\mathbb{D}^T}\underset{k+1}{\mathbb{M}}\underset{k}{\mathbb{D}} + \underset{k}{\mathbb{M}})u^k = f^k, \quad k = 1, 2 \tag{4.2.1}$$

with the mass matrices containing the corresponding material parameters. Here $f^k \in \underset{\Gamma}{\mathcal{C}^k}$ is a discrete version of the corresponding right hand sides in (4.0.1)-(4.0.2). An equivalent "weak" form of (4.2.1) is given by the variational equation: seek $u^k \in \underset{\Gamma}{\mathcal{C}^k}$ such that

$$\left(u^k, \hat{u}^k\right)_{\underset{\Gamma}{\mathcal{C}^k}} + \left(\underset{k}{\mathbb{D}}u^k, \underset{k}{\mathbb{D}}\hat{u}^k\right)_{\underset{\Gamma}{\mathcal{C}^{k+1}}} = \left(f^k, \hat{u}^k\right)_{\underset{\Gamma}{\mathcal{C}^k}} \quad \forall \hat{u}^k \in \underset{\Gamma}{\mathcal{C}^k}. \tag{4.2.2}$$

The design of the compatible gauge AMG preconditioner when $k = 1$ was discussed in details in [16] for the fully discrete system of (4.0.1). So in the remaining of

this chapter, we mainly focus on the design of preconditioners for $\mathbf{H}(\mathrm{div})$ system

$$(\mathbb{D}_2^T \mathbb{M}_3 \mathbb{D}_2 + \mathbb{M}_2) u^2 = f^2. \tag{4.2.3}$$

Most of the techniques can parallel applied to $\mathbf{H}(\mathbf{curl})$ systems.

4.2.1 Reformulation of the $\mathbf{H}(\mathrm{div})$ System

For the discretized $\mathbf{H}(\mathrm{div})$ system, we form the Hodge Laplacian, which corresponds to adding a **curl curl** term to the **grad** div operator, namely

$$\mathbb{L}_2 = \mathbb{D}_2^* \mathbb{D}_2 + \mathbb{D}_1 \mathbb{D}_1^*. \tag{4.2.4}$$

The following main theorem states an analog of Theorem 4.2 in [16].

Theorem 4.2.1. *Assume that* u^2 *is a solution of* (4.2.3) *and let*

$$u^2 = \mathbb{D}_1 e^1 + \widetilde{\mathbb{D}}_2^* b^3 \tag{4.2.5}$$

denote its discrete Hodge decomposition with respect to the inner product induced by $\widetilde{\mathbb{M}}_2$. *The pair* (a^2, e^1), *where* $a^2 = \widetilde{\mathbb{D}}_2^* b^3$, *solves the linear system*

$$\begin{bmatrix} \mathbb{M}_2 + \mathbb{D}_2^T \mathbb{M}_3 \mathbb{D}_2 + \widetilde{\mathbb{M}}_2 \mathbb{D}_1 \mathbb{M}_1^{-1} \mathbb{D}_1^T \widetilde{\mathbb{M}}_2 & \mathbb{M}_2 \mathbb{D}_1 \\ \mathbb{D}_1^T \mathbb{M}_2 & \mathbb{D}_1^T \mathbb{M}_2 \mathbb{D}_1 \end{bmatrix} \begin{bmatrix} a^2 \\ e^1 \end{bmatrix} = \begin{bmatrix} \mathbb{M}_2 f^2 \\ \mathbb{D}_1^T \mathbb{M}_2 f^2 \end{bmatrix}. \tag{4.2.6}$$

Proof. We denote $a^2 := \widetilde{\mathbb{D}}^*_2 b^3$. Applying the decomposition (4.2.5) to the weak form (4.2.2) yields

$$\left(\mathbb{D}_1 e^1 + a^2, \hat{u}^2\right)_{\mathcal{C}^2_\Gamma} + \left(\mathbb{D}_2 a^2, \mathbb{D}_2 \hat{u}^2\right)_{\mathcal{C}^3} = \left(f^2, \hat{u}^2\right)_{\mathcal{C}^2_\Gamma}, \ \forall \hat{u}^2 \in \mathcal{C}^2_\Gamma.$$

In the above equality, we used the fact that $\mathbb{D}_2 \mathbb{D}_1 \equiv 0$. We note that the assumed Hodge decomposition implies that $\widetilde{\mathbb{D}}^*_1 a^2 = 0$ (since $\widetilde{\mathbb{D}}^*_1 \widetilde{\mathbb{D}}^*_2 = 0$), thus

$$\left(\widetilde{\mathbb{D}}^*_1 a^2, \widetilde{\mathbb{D}}^*_1 \hat{u}^2\right)_{\mathcal{C}^1_\Gamma} \equiv 0, \ \ \forall \hat{u}^2 \in \mathcal{C}^2_\Gamma.$$

As a result, this term can be added to the last equation to obtain:

$$\left(\mathbb{D}_1 e^1 + a^2, \hat{u}^2\right)_{\mathcal{C}^2_\Gamma} + \left(\mathbb{D}_2 a^2, \mathbb{D}_2 \hat{u}^2\right)_{\mathcal{C}^3} + \left(\widetilde{\mathbb{D}}^*_1 a^2, \widetilde{\mathbb{D}}^*_1 \hat{u}^2\right)_{\mathcal{C}^1_\Gamma} = \left(f^2, \hat{u}^2\right)_{\mathcal{C}^2_\Gamma}, \ \forall \hat{u}^2 \in \mathcal{C}^2_\Gamma.$$

It is easy to see that the above weak form is equivalent to the following linear system:

$$\mathbb{M}_2 a^2 + \left(\mathbb{D}^T_2 \mathbb{M}_3 \mathbb{D}_2 + \widetilde{\mathbb{M}}_2 \mathbb{D}_1 \mathbb{M}^{-1}_1 \mathbb{D}^T_1 \widetilde{\mathbb{M}}_2\right) a^2 + \mathbb{M}_2 \mathbb{D}_1 e^1 = \mathbb{M}_2 f^2$$

which is the first equation in (4.2.6).

Applying the decomposition (4.2.5) to (4.2.3), and then multiplying by $\mathbb{D}^T_1$ on both sides give

$$\mathbb{D}^*_1 a^2 + \mathbb{D}^*_1 \mathbb{D}_1 e^1 = \mathbb{D}^*_1 f^2.$$

By definition $\mathbb{D}^*_1 = \mathbb{M}^{-1}_1 \mathbb{D}^T_1 \mathbb{M}_2$, the second set of equations in the block system follows by multiplying $\mathbb{M}_1$ on both sides. This completes the proof. □

Here, we notice that the (2,2) block $\mathbb{D}^*_1 \mathbb{D}_1$ is singular. A further decomposition [16, Corollary 3.2] of

$$e^1 = \mathbb{D}_0 e^0 + \widetilde{\mathbb{D}}^*_1 b^2 := \mathbb{D}_0 e^0 + a^1$$

yields the following block system

$$\begin{bmatrix} A_{11} & \mathbb{M}_2 \mathbb{D}_1 \\ \mathbb{D}^T_1 \mathbb{M}_2 & A_{22} \end{bmatrix} \begin{bmatrix} a^2 \\ a^1 \end{bmatrix} = \begin{bmatrix} \mathbb{M}_2 f^2 \\ \mathbb{D}^T_1 \mathbb{M}_2 f^2 \end{bmatrix} \tag{4.2.7}$$

where $A_{11} = \mathbb{M}_2 + \mathbb{D}^T_2 \mathbb{M}_3 \mathbb{D}_2 + \widetilde{\mathbb{M}}_2 \mathbb{D}_1 \mathbb{M}^{-1}_1 \mathbb{D}^T_1 \widetilde{\mathbb{M}}_2$ and $A_{22} = \mathbb{D}^T_1 \mathbb{M}_2 \mathbb{D}_1 + \widetilde{\mathbb{M}}_1 \mathbb{D}_0 \mathbb{M}^{-1}_0 \mathbb{D}_0 \widetilde{\mathbb{M}}_1$. In the above formulation, we used the fact that $\mathbb{D}_1 \mathbb{D}_0 = 0$ and $\widetilde{\mathbb{D}}^*_0 \widetilde{\mathbb{D}}^*_1 = 0$.

Remark 4.2.2. *The reformulation* (4.2.7) *seems more complicate than the original equation* (4.2.3) *that we are actually solving. The idea here is to use the diagonal blocks* A_{11} *and* A_{22} *as preconditioners of* (4.2.3)*, which is the main focus of the next section.*

As was point out in [16], the gauge terms in A_{11} *and* A_{22} *play an important role in avoiding the large null-space caused by* **grad** div *operator and* **curl curl** *operator respectively. For the* $\mathbf{H}(\mathbf{curl})$ *problems, numerical experiments in [16] show that adding a gauge term to the* **curl curl** *operator results in a better conditioning than the original system, especially when the original system is indefinite. However, the formulation of the gauge terms (*$\widetilde{\mathbb{M}}_2 \mathbb{D}_1 \mathbb{M}^{-1}_1 \mathbb{D}^T_1 \widetilde{\mathbb{M}}_2$ *and* $\widetilde{\mathbb{M}}_1 \mathbb{D}_0 \mathbb{M}^{-1}_0 \mathbb{D}_0 \widetilde{\mathbb{M}}_1$*) requires the inversion of* $\mathbb{M}_1$

and $\mathbb{M}_0$. *Even if we can use mass lumping to simplify the computation, it makes the system more complicate and ruins the sparse patten of the original system.*

The interesting fact is that according to the numerical tests (see Section 4.4 for more details), it is not so clear now whether these gauge terms are necessary or not. We need a more rigorous investigation of the roles of these gauge terms for more complex problems in future work.

4.2.2 The AMG Algorithm

Now we are in position to combine the reformulation and preconditioning to develop a linear solver for the compatible discretization (4.2.3) of the $\mathbf{H}(\mathrm{div})$ system (4.0.2). The approach considered in this chapter focuses on developing AMG methods for the (1,1) and (2,2) blocks in (4.2.7) separately. Note that these diagonal blocks are Laplace-like. Once constructed, these AMG solvers are combined as a block Jacobi preconditioner in preconditioning (4.2.3).

We propose an AMG technique for the whole 2×2 system which employs a Hiptmair smoother (see for example [61]) at the finest level, but allows subsequent levels and the (1,1) and (2,2) blocks to be handled with standard AMG method. To do this, the face element of the (1,1) block and the edge element version of the (2,2) block must be converted to a more standard nodal form on the coarse mesh. This is accomplished by two special prolongators that transfer solutions from a nodal to a face and edge representation respectively. The net effect of these special prolongators is that the corresponding Galerkin projection of the (1,1) and (2,2) block will, in fact, yield an operator resembling

a vector nodal Laplacian which is amenable to some standard AMG method for further coarsening.

4.2.2.1 The Specialized Prolongators

As discussed earlier, in order to use standard AMG solvers for (1,1) and (2,2) blocks, we must convert the face element (for the (1,1)-block) and the edge element (for the (2,2)-block) into standard nodal element. To do this, we define specialized prolongators P_{11} and P_{22} to transfer solutions from a nodal to a face and edge representation respectively. Instead of introducing the near null-space to define the prolongators as was done in [16], here we make use of the interpolation Π_h^{div} and $\Pi_h^{\mathbf{curl}}$ (see Figure 4.3) as in Chapter 3 (also see [11, 68]). For the implementation of Π_h^{div} and $\Pi_h^{\mathbf{curl}}$, we refer to Section 3.6 in Chapter 3. We use Π_h^{div} and $\Pi_h^{\mathbf{curl}}$ as the grid transfer operators for the (1,1) and (2,2) block respectively.

Algorithm 1: $\left[P_{11}, P_{22}\right]$=Node_Prolongators()

1 $P_{11} = \Pi_h^{\text{div}}$;
2 $P_{22} = \Pi_h^{\mathbf{curl}}$;

The resulting (nodal) operators are given by

$$A_{11}^H = P_{11}^T A_{11} P_{11}, \quad A_{22}^H = P_{22}^T A_{22} P_{22}$$

where A_{11} and A_{22} are the (1,1) and (2,2) blocks of (4.2.7), A_{11}^H and A_{22}^H refer to their projections on a the nodal spaces respectively. Note that A_{11}^H and A_{22}^H are discretized vector Laplacian like operators which are amenable to standard AMG algorithms.

Remark 4.2.3. *In practical computation, we may skip the fine level relaxation because it has already been contained in the special relaxation in the following subsection. So in the definition of the prolongations P_{11} and P_{22}, one may also consider to transfer the solution from a coarse grid to a fine grid. This can be achieved by standard aggregation techniques (see [107, 106, 29] for example).*

There are many ways to obtain aggregates corresponding to nodes (see [16] for more details). For simplicity, here we use perfect aggregation. By "perfect", we mean that the aggregates are formed manually. Note that we only need to form these aggregates on the finest level.

$$\{\mathcal{A}_i\} \leftarrow \textit{Aggregate manually.}$$

Then for each fine node n_i and each aggregate $\mathcal{A}_j$ define

$$\left(P_{nf}\right)_{i,j} = \begin{cases} 1, & \text{if } n_i \in \mathcal{A}_j \\ 0, & \text{otherwise} \end{cases}.$$

Finally, we define the grid transfer operators P_{11} and P_{22} as

$$P_{11} = \Pi_h^{\mathrm{div}} P_{nf}, P_{22} = \Pi_h^{\mathbf{curl}} P_{nf}.$$

Notice that the effect of P_{11} *is to interpolate coarse nodal quantities to fine face-oriented quantities, and the effect of* P_{22} *is to interpolate coarse nodal quantities to fine edge-oriented quantities.*

4.2.2.2 Relaxation

As before, we consider the following hybrid scheme. Suppose that the conjugate gradient iteration is actually applied to solve (4.2.3) and that (4.2.7) is *only used within the preconditioner*. To do this, it is necessary to convert residual of (4.2.3) to right hand sides of (4.2.7) within the preconditioner. This is done by applying $[\mathbb{I} \quad \mathbb{D}_1]^T$ to the residual. Approximate solutions to the $(1,1)$ and $(2,2)$ blocks of (4.2.7) are then converted back to a form suitable for (4.2.3) via $e^2 = \mathbb{D}_1 a^1 + a^2$ as a correction to the solution.

Algorithm 2 illustrates such a smoother proposed by Hiptmair that combines standard smoothing of the original equations with standard smoothing of the equations projected to the null-space (e.g. [61]). It is important to realize that this special

---

Algorithm 2: $\tilde{u} = \mathsf{FineRelaxation}\left(A, \mathbb{D}_1, \tilde{u}, b\right)$

---

1 $\tilde{u} \leftarrow \mathsf{StandardRelaxation}\left(A, \tilde{u}, b\right)$;

2 $c \leftarrow \mathsf{StandardRelaxation}\left(\mathbb{D}_1^T A \mathbb{D}_1, 0, \mathbb{D}_1^T (b - A\tilde{u})\right)$;

3 $\tilde{u} \leftarrow \tilde{u} + \mathbb{D}_1 c$;

4 $\tilde{u} \leftarrow \mathsf{StandardRelaxation}\left(A, \tilde{u}, b\right)$;

---

smoother is only needed on the finest level. A standard smoother can be used on A_{11}^{H} and A_{22}^{H} within the AMG procedures for the (1,1) and (2,2) blocks. Finally, an additive version of the Hiptmair smoother may also be considered for FineRelaxation().

4.2.2.3 AMG Preconditioner

We now give the entire AMG-based preconditioner for the block Jacobi version in Algorithm 3. PreFineRelaxation() is identical to Algorithm 2 except step one is omitted. PostFineRelaxation() is identical to Algorithm 2 except step four is omitted to keep the preconditioner symmetric when StandardRelaxation() employs a symmetric algorithm. Of course, residual calculations can also be avoided using additive forms of this smoother.

The algorithm essentially involves two AMG solves for nodal vector Laplacians: A_{11}^{H} corresponding to the (1,1) block and A_{22}^{H} corresponding to the (2,2) block. In addition, some relaxation steps must be performed on the original fine mesh system. The detailed algorithm is listed in Algorithm 3.

From Algorithm 3, we observe that there are three major components in the preconditioner:

(1) Hiptmair smoother for $\mathbf{H}$(div) (see also Hiptmair [61]).

(2) AMG for $P_{11}^{T} A_{11} P_{11}$ within the (1,1)-block.

(3) AMG for $P_{22}^{T} A_{22} P_{22}$ within the (2,2)-block.

Algorithm 4 is the additive version of Algorithm 3.

Remark 4.2.4. *As we can see from Algorithm 4, the additive version consists of 4-components. Actually, the* StandardRelaxations *for* u_1 *and* u_2 *constitute the additive*

Algorithm 3: $\tilde{u}$ =Block Preconditioner(r)

% Setup Phase

Form $A^H_{11} \leftarrow P^T_{11} A_{11} P_{11}$ efficiently;

Standard_AMG_Setup(A^H_{11});

Form $A^H_{22} \leftarrow P^T_{22} A_{22} P_{22}$ efficiently;

Standard_AMG_Setup(A^H_{22});

% Solve Phase

$\tilde{u} \leftarrow$ PreFineRelaxation $\left(\mathbb{D}_2^T \mathbb{M}_3 \mathbb{D}_2 + \mathbb{M}_2, \mathbb{D}_1, 0, r \right)$;

$\tilde{r} \leftarrow r - \left(\mathbb{D}_2^T \mathbb{M}_3 \mathbb{D}_2 + \mathbb{M}_2 \right) \tilde{u}$;

% Perform V-cycles on A^H_{11} and A^H_{22}

$a \leftarrow$ Standard_AMG_Vcycle $\left(A^H_{11}, 0, P^T_{11} \tilde{r} \right)$;

$p \leftarrow$ Standard_AMG_Vcycle $\left(A^H_{22}, 0, P^T_{22} \mathbb{D}^T_1 \tilde{r} \right)$;

$\tilde{u} \leftarrow \tilde{u} + P_{11} a + \mathbb{D}_1 P_{22} p$;

$\tilde{u} \leftarrow$ PostFineRelaxation $\left(\mathbb{D}_2^T \mathbb{M}_3 \mathbb{D}_2 + \mathbb{M}_2, \mathbb{D}_1, \tilde{u}, r \right)$;

Algorithm 4: $u =$Block Preconditioner(b)

% Setup Phase

Form $A^H_{11} \leftarrow P^T_{11} A_{11} P_{11}$ efficiently;

Standard_AMG_Setup(A^H_{11});

Form $A^H_{22} \leftarrow P^T_{22} A_{22} P_{22}$ efficiently;

Standard_AMG_Setup(A^H_{22});

% Solve Phase

$u_1 \leftarrow$ StandardRelaxation $\left(\mathbb{D}^T_2 \mathbb{M}_3 \mathbb{D}_2 + \mathbb{M}_2, 0, b\right)$;

$x \leftarrow$ StandardRelaxation $\left(\mathbb{D}^T_1 \mathbb{M}_2 \mathbb{D}_1, 0, \mathbb{D}^T_1 b\right)$;

$u_2 \leftarrow \mathbb{D}_1 x$;

$a \leftarrow$ Standard_AMG_Vcycle $\left(A^H_{11}, 0, P^T_{11} b\right)$;

$u_3 \leftarrow P_{11} a$;

$p \leftarrow$ Standard_AMG_Vcycle $\left(A^H_{22}, 0, P^T_{22} \mathbb{D}^T_1 b\right)$;

$u_4 \leftarrow \mathbb{D}_1 P_{22} p$;

$u \leftarrow u_1 + u_2 + u_3 + u_4$;

version of the Hiptmair smoother for the $\mathbf{H}(\mathrm{div})$ *system (see Algorithm 2). For* u_3 *and* u_4*, we used the* Standard_AMG_Vcycle *to solve the vector elliptic equations respectively. Therefore, in total, one needs to solve six elliptic equations (two vector Laplacians).*

In operator form, the above algorithm can be written as a preconditioner operator $\mathbf{B}_h^{\mathrm{div}}$

$$\mathbf{B}_h^{\mathrm{div}} = \mathbf{S}_h^{\mathrm{div}} + \mathbf{C}\mathbf{S}_h^{\mathbf{curl}}\mathbf{C}^T + \mathbf{P}_{\mathrm{div}}\mathbf{B}_h^{\mathbf{grad}}\mathbf{P}_{\mathrm{div}}^T + \mathbf{C}\mathbf{P}_{\mathbf{curl}}\mathbf{B}_h^{\mathbf{grad}}\mathbf{P}_{\mathbf{curl}}^T\mathbf{C}^T, \tag{4.2.8}$$

where $\mathbf{C} = \mathbb{D}_1$ *is the discrete* **curl** *operator, and* $\mathbf{S}_h^{\mathbf{curl}}$ *and* $\mathbf{S}_h^{\mathrm{div}}$ *are the standard smoothers for the edge- and face-element respectively. This operator is exactly the same as HX preconditioner for the* $\mathbf{H}(\mathrm{div})$ *system in equation* (3.5.8) *in Chapter 3 (cf. [68, (7.7)]). It was proved that the condition number* $\kappa(\mathbf{B}_h^{\mathrm{div}}A) \leq C$ *for the* $\mathbf{H}(\mathrm{div})$ *system with constant coefficients (cf. Theorem 3.5.3 in Chapter 3). For the detailed analysis of this preconditioner, we refer to Chapter 3.*

4.3 Application to Mixed Formulations

As an application, in this section, we present the augmented Lagrangian method for solving mixed finite element discretization of elliptic boundary value problem (see e.g., [31]):

$$\Delta p = f \text{ in } \Omega, \quad p|_{\partial\Omega} = 0. \tag{4.3.1}$$

The aim is to show that implementing an efficient iterative method for the resulting indefinite linear system reduces to designing an efficient method for the solution of an auxiliary nearly singular $\mathbf{H}(\mathrm{div})$ problem.

The model problem (4.3.1) can be cast into the following variational form by introducing the variable $u := \nabla p$: Find $(u, p) \in \mathbf{H}(\mathrm{div}) \times L^2(\Omega)$ such that

$$\begin{cases} (u, v) + (p, \mathrm{div}\, v) = 0, & \forall v \in \mathbf{H}(\mathrm{div}) \\ (\mathrm{div}\, u, q) = (f, q), & \forall q \in L^2(\Omega). \end{cases} \tag{4.3.2}$$

The existence and uniqueness of the solution to (4.3.2) follow by standard inf-sup condition which can be established easily for this model problem (cf. [31]). Given a quasi-uniform conforming triangulation $\mathcal{T}_h$, the mixed finite element method is to solve the model problem (4.3.2) in the finite element spaces: $V_h(\mathrm{div}) \subset \mathbf{H}(\mathrm{div})$ and $V_h(0) \subset L^2(\Omega)$. That is,to find $(u_h, p_h) \in V_h(\mathrm{div}) \times V_h(0)$ such that

$$\begin{cases} \left(u_h, v_h\right) + \left(p_h, \mathrm{div}\, v_h\right) = 0, & \forall v_h \in V_h(\mathrm{div}) \\ \left(\mathrm{div}\, u_h, q_h\right) = \left(f, q_h\right), & \forall q_h \in V_h(0). \end{cases} \tag{4.3.3}$$

A sufficient condition for the well-posedness of the mixed method (4.3.3) is the discrete inf-sup condition. Several finite element spaces satisfying the inf-sup condition have been introduced, such as those of Raviart-Thomas [95] and Brezzi-Douglas-Marini [30]. Here we restrict ourselves to the Raviart-Thomas spaces.

In the compatible discretization framework discussed in Section 4.1, the mixed finite element method (4.3.3) results in the following linear system:

$$\begin{bmatrix} A & B^* \\ B & 0 \end{bmatrix} \begin{bmatrix} u \\ p \end{bmatrix} = \begin{bmatrix} 0 \\ f \end{bmatrix}, \tag{4.3.4}$$

where $A = \mathbb{M}_2$ and $B = \mathbb{D}_2^T \mathbb{M}_3$.

The augmented Lagrangian method solves the following equivalent problem to (4.3.4) by the Uzawa method:

$$\begin{bmatrix} A + \epsilon^{-1} B^* B & B^* \\ B & 0 \end{bmatrix} \begin{bmatrix} u \\ p \end{bmatrix} = \begin{bmatrix} \epsilon^{-1} B^* f \\ f \end{bmatrix}. \tag{4.3.5}$$

The iteration reads: given $(u^{(k)}, p^{(k)})$, the new iterate $(u^{(k+1)}, p^{(k+1)})$ is obtained by solving the following systems:

$$\begin{cases} \left(A + \epsilon^{-1} B^* B\right) u^{(k+1)} &= \epsilon^{-1} B^* f - B^* p^{(k)}, \\ p^{(k+1)} &= p^{(k)} - \epsilon^{-1} \left(f - B u^{(k+1)}\right). \end{cases} \tag{4.3.6}$$

Convergence of this method has been discussed in many works (see for example [51, 108, 81]).

Theorem 4.3.1 ([81, Lemma 2.1])**.** *Let* $\left(u^{(0)}, p^{(0)}\right)$ *be a given initial guess and for* $k \geq 1$, *let* $\left(u^{(k)}, p^{(k)}\right)$ *be the iterates obtained via the augmented Lagrangian method. Then the following estimates hold:*

$$\begin{aligned} \left\| p - p^{(k)} \right\|_{0,\Omega} &\leq \left(\frac{\epsilon}{\epsilon + \mu_0} \right)^k \left\| p - p^{(0)} \right\|_{0,\Omega}, \\ \left\| u - u^{(k)} \right\|_A &\leq \sqrt{\epsilon} \left\| p - p^{(k)} \right\|_{0,\Omega} \leq \sqrt{\epsilon} \left(\frac{\epsilon}{\epsilon + \mu_0} \right)^k \left\| p - p^{(0)} \right\|_{0,\Omega}, \end{aligned}$$

where μ_0 *is the minimum eigenvalue of* $S = BA^{-1}B^*$.

Proof. Let $\underset{p}{e}^{(k)} := p - p^{(k)}$ and $\underset{u}{e}^{(k)} := u - u^{(k)}$ be the errors after k iterations ($k > 0$). By definition, $\left(\underset{p}{e}^{(k)}, \underset{u}{e}^{(k)}\right)$ satisfies:

$$\begin{cases} \left(A + \epsilon^{-1} B^* B\right) \underset{u}{e}^{(k)} &= -B^* \underset{p}{e}^{(k-1)}, \\ \underset{p}{e}^{(k)} &= \left(I - \epsilon^{-1} B \left(A + \epsilon^{-1} B^* B\right)^{-1} B^*\right) \underset{p}{e}^{(k-1)}. \end{cases}$$

A simple application of Shermann-Morrison-Woodburry formula (e.g. [54, (2.1.4)]) for $\left(\epsilon A + B^* B\right)^{-1}$ gives

$$\epsilon^{-1} B \left(A + \epsilon^{-1} B^* B\right)^{-1} B^* = B \left(\epsilon A + B^* B\right)^{-1} B^* = S_\epsilon - S_\epsilon \left(I + S_\epsilon\right)^{-1} S_\epsilon,$$

where $S_\epsilon = \epsilon^{-1} S = \epsilon^{-1} B A^{-1} B^*$. It is straightforward to verify that

$$I - \epsilon^{-1} B \left(A + \epsilon^{-1} B^* B\right)^{-1} B^* = I - S_\epsilon + S_\epsilon \left(I + S_\epsilon\right)^{-1} S_\epsilon = \left(I + S_\epsilon\right)^{-1}.$$

Therefore

$$\underset{p}{e}^{(k)} = (I + \epsilon S)^{-1} \underset{p}{e}^{(k-1)},$$

and the first estimate follows immediately. The second inequality is obtained by using the following identity:

$$\begin{aligned}
\left\| \begin{matrix} e_u^{(k)} \\ \end{matrix} \right\|_A^2 &= \left(A \begin{matrix} e_u^{(k)}, e_u^{(k)} \end{matrix} \right) = \left(\left(A + \epsilon^{-1} B^* B - \epsilon^{-1} B^* B \right) \begin{matrix} e_u^{(k)}, e_u^{(k)} \end{matrix} \right) \\
&= -\left(B^* \begin{matrix} e_p^{(k-1)}, e_u^{(k)} \end{matrix} \right) - \left(\epsilon^{-1} B \begin{matrix} e_u^{(k)}, B e_u^{(k)} \end{matrix} \right) \\
&= \epsilon \left(\left(Z \begin{matrix} e_p^{(k-1)}, e_p^{(k-1)} \end{matrix} \right) - \left\| Z \begin{matrix} e_p^{(k-1)} \\ \end{matrix} \right\|_{0,\Omega}^2 \right),
\end{aligned}$$

where $Z = B \left(\epsilon A + B^* B \right)^{-1} B^*$. The proof is complete by observing that $\|Z\|_0 \leq 1$. $\square$

According to this theorem, the iteration procedure (4.3.6) converges very fast to the solution of (4.3.3) for small ϵ. However, one needs to solve a nearly singular $\mathbf{H}(\mathrm{div})$ system

$$\left(\epsilon A + B^* B \right) u^{(k+1)} = B^* f - \epsilon B^* p^{(k)}. \tag{4.3.7}$$

Thus, an efficient and robust $\mathbf{H}(\mathrm{div})$ solver will result in an optimal iterative method for the saddle point problem (4.3.3). We refer to Section 4.4.3 for the numerical justification.

4.4 Numerical Results

In this section, we present some numerical experiments to justify the efficiency and robustness of the algorithms discussed in this chapter. All the numerical experiments are conducted in a three-dimensional unit cube domain $\Omega = \{(x, y, z) \in \mathbb{R}^3 : 0 \leq x, y, z \leq 1\}$ with homogeneous Neumann boundary condition. The domain is meshed by uniform cubes, and each cube is divided into six tetrahedra.

The proposed solver was implemented using CG in MATLAB. The first level and the first grid transfer of Algorithm 3 are also implemented in MATLAB. The ML's smoothed aggregation solver is used for A^H_{11} and A^H_{22}, through the mlmex MATLAB interface (cf. [52]). A single V-cycle of AMG is used for both the (1,1) and (2,2) blocks, using the efficient variant of Algorithm 2 (smoother). Unless otherwise stated, we use two steps of symmetric Gauss-Seidel sub-smoothing on both faces and edges. For all experiments the CG tolerance is 1.0×10^{-10}.

4.4.1 Constant coefficients

As the first experiment, we consider the constant coefficients case. We assume that $\lambda = \mu = 1$ in Ω. Table 4.1 reports the number of iterations with different mesh

Grid		9^3	12^3	15^3	18^3	21^3	24^3	27^3
2 SGS Steps	gauge	12	12	13	13	13	13	13
	No gauge	11	13	13	14	14	14	15
3 SGS Steps	gauge	10	11	11	12	12	12	12
	No gauge	9	10	11	12	12	13	13
4 SGS Steps	gauge	9	10	10	11	11	11	11
	No gauge	8	10	10	10	11	11	11

Table 4.1. Number of iterations for CG-accelerated AMG on the 3D tetrahedral mesh problem with constant coefficients, using Algorithm 3. The size of the problem and the number of SGS smoothing steps are varied.

size. We note that there are 3 or 4 iterations variations for different mesh. This is due to the grid transfer operator P_{11} and P_{22}. In this example, we used the operators

defined in Remark 4.2.3, that is, we skip the nodal relaxation for the finest level. From this experiment, we also observed that the gauge terms have no much influence on the iteration numbers of the algorithm. Therefore, in the numerical experiments later on, we will not include the gauge terms in the preconditioners unless specified.

If we use the grid transfer operators as stated in Algorithm 1, that is, define $P_{11} = P_h^{\text{div}}$ and $P_{22} = P_h^{\mathbf{curl}}$ as the grid transfer operators for the (1,1) and (2,2) blocks respectively, then we have the following results. From Table 4.2, we observe that

Grid	9^3	12^3	15^3	18^3	21^3	24^3	27^3
2 SGS Steps	9	10	10	10	10	10	10
3 SGS Steps	8	9	9	9	9	9	9
4 SGS Steps	8	8	8	9	8	8	8

Table 4.2. Number of iterations for CG-accelerated AMG on the 3D tetrahedral mesh problem with constant coefficients, using Algorithm 3 with grid transfer operators P_{11} and P_{22} as defined in Algorithm 1. The size of the problem and the number of SGS smoothing steps are varied.

the numbers of iterations are almost identical for different mesh size. Therefore, the preconditioner in Algorithm 3 is robust with respect to the mesh size. Table 4.3 shows the comparison of the Algorithm 3 with the Algorithm 4. Here, we use 2 SGS smoothing steps.

Grid	9^3	12^3	15^3	18^3	21^3	24^3	27^3
Algorithm 3	9	10	10	10	10	10	10
Algorithm 4	18	18	18	17	17	17	17

Table 4.3. Number of iterations for CG-accelerated AMG on the 3D tetrahedral mesh problem with constant coefficients, using the grid transfer operators P_{11} and P_{22} as defined in Algorithm 1.

4.4.2 Variable Coefficients

In the following numerical experiments, we used the grid transfer operators P_{11} and P_{22} as defined in Remark 4.2.3.

Variable μ We experiment with jumps in μ by considering two regions with constant values of μ. Specifically, define

$$\Omega_0 = \left\{(x,y,z) : \frac{1}{3} \leq x,y,z \leq \frac{2}{3}\right\}, \quad \Omega_1 = \Omega \setminus \Omega_0;$$

let $\mu \equiv 1$ in Ω_1 and choose $\mu = \mu_0$ to be a constant inside Ω_0. λ is fixed to be 1 throughout the whole domain Ω. Table 4.4 reports the number of iterations on different mesh size. Note that the number of iterations is robust with respect to the variation of the coefficient μ.

Variable λ We now consider the jump on λ. Same as before, we choose $\lambda = \lambda_0$ to be a constant which varies from 10^{-4} to 10^4 inside the domain Ω_0, and $\lambda = 1$ elsewhere. This

Grid	μ_0								
	10^{-8}	10^{-7}	10^{-6}	10^{-5}	10^{-4}	10^{3}	10^{-2}	10^{-1}	1
9^3	11	11	11	11	11	11	11	11	11
18^3	15	15	15	15	16	16	15	15	14
27^3	16	16	19	18	18	18	19	17	15

Table 4.4. Number of iterations for CG-accelerated AMG on the 3D tetrahedral mesh problem with jump coefficients, using Algorithm 3. μ_0 varies inside $[1/3, 2/3]^3$, and 1 elsewhere, and $\lambda \equiv 1$.

time, we fix μ to be 1 in the whole domain Ω. Table 4.5 reports the number of iterations on different mesh size. Again, the number of iterations remains fairly constant.

4.4.3 Augmented Lagrangian Iterations

According to the augmented Lagrangian algorithm presented in Section 4.3, we need to solve the nearly singular $\mathbf{H}(\mathrm{div})$ system (4.4.1) at each iteration. So first of all, the $\mathbf{H}(\mathrm{div})$ solver should be robust with respect to the (penalty) parameter ϵ. Table 4.6 shows the CG-accelerated auxiliary AMG solver for $\mathbf{H}(\mathrm{div})$ system:

$$(\mathrm{div}\, u, \mathrm{div}\, v) + \epsilon(u, v) = (f, v), \quad \forall v \in H(\mathrm{div}) \tag{4.4.1}$$

with respect to different ϵ. The relative residual reduction tolerance is 10^{-10}. The grid transfer operators P_{11} and P_{22} are defined in Algorithm 1.

Table 4.7 shows the number of iterations for the augmented Lagrangian method for the mixed formulation of elliptic equation with respect to different ϵ, where we used

Grid	λ_0								
	10^{-4}	10^{-3}	10^{-2}	10^{-1}	1	10^{1}	10^{2}	10^{3}	10^{4}
9^3	17	16	14	12	11	11	11	11	9
18^3	21	20	18	16	14	14	14	12	12
27^3	22	21	21	17	15	15	14	13	13

Table 4.5. Number of iterations for CG-accelerated AMG on the 3D tetrahedral mesh problem with jump coefficients, using Algorithm 3. λ_0 varies inside $[1/3, 2/3]^3$, and 1 elsewhere, and $\mu \equiv 1$.

Grid	ϵ								
	10^{-4}	10^{-3}	10^{-2}	10^{-1}	1	10^{1}	10^{2}	10^{3}	10^{4}
9^3	6	6	7	9	10	10	9	4	3
18^3	7	7	7	9	10	11	11	7	3
27^3	7	7	7	9	10	11	11	9	4

Table 4.6. Number of iterations for CG-accelerated AMG on the 3D tetrahedral mesh $\mathbf{H}(\mathrm{div})$ problem (4.4.1). ϵ varies from 10^{-4} to 10^{4}.

the AMG $\mathbf{H}(\mathrm{div})$ preconditioner above to solve the nearly singular $\mathbf{H}(\mathrm{div})$ system (4.4.1). The tolerance is 10^{-8}. In particular, according to the theory, the augmented Lagrangian

	ϵ								
Grid	10^{-4}	10^{-3}	10^{-2}	10^{-1}	1	10^{1}	10^{2}	10^{3}	10^{4}
9^3	2	3	3	4	7	16	83	> 100	> 100
18^3	2	3	3	4	7	17	87	> 100	> 100
27^3	2	3	3	5	7	17	88	> 100	> 100

Table 4.7. Number of iterations for the augmented Lagrangian method for mixed method for elliptic equations on the 3D tetrahedral mesh using $\mathbf{H}(\mathrm{div})$ solver. ϵ varies from 10^{-4} to 10^{4}.

method converges faster for smaller ϵ. The convergence rate predicted by Theorem 4.3.1 can be observed in Table 4.7, especially, for the given tolerance if we choose $\epsilon \leq 10^{-8}$ then only one iteration is needed to obtain a solution to (4.3.4). We also observe that the number of iteration grows when ϵ gets larger, as predicted from the theorem.

Chapter 5

Conclusions

In this dissertation, we designed efficient and robust algebraic solvers for the elliptic systems involving gradient, curl, and divergence operators. Our focus was on the applications of robust algorithms for finite element discretizations for problems with strongly discontinuous coefficients. Comprehensive condition number estimates were established for a variety of preconditioners.

For the second order elliptic boundary value problems with strongly discontinuous coefficients, we discussed the eigenvalue distribution of the multilevel and domain decomposition preconditioners. We proved that the preconditioned systems have only a few small eigenvalues due to the large variations of the coefficients. For BPX and multigrid V-cycle preconditioned systems, the effective condition numbers are bounded by $C|\log h|^2$. Therefore, the asymptotic convergence rate of BPX PCG and MGCG algorithms are bounded by $1 - \frac{2}{C|\log h|+1}$. For the two level overlapping domain decomposition preconditioners, the effective condition numbers are bounded by $C|\log H|$. With a mild assumption on the jump subdomains, the effective condition numbers are bounded uniformly which resulting an asymptotically uniformly converge PCG algorithm. Numerical experiments justified our conclusions.

For $\mathbf{H}(\mathbf{curl})$ and $\mathbf{H}(\mathrm{div})$ systems, we gave a comprehensive analysis of HX preconditioners. Based on a framework of auxiliary space preconditioning techniques, the

main theoretical foundations are (discrete) regular decomposition results for vector fields in Hilbert spaces $\mathbf{H}(\mathbf{curl})$ and $\mathbf{H}(\mathrm{div})$. We proved the mesh-independent effectiveness of these preconditioners. Moreover, for the $\mathbf{H}(\mathbf{curl})$ systems with discontinuous coefficients, we developed a theory on (discrete) regular decomposition in weighted norm. According to this theory, we established the nodal auxiliary space preconditioners for the $\mathbf{H}(\mathbf{curl})$ systems with jump coefficients. We proved that the condition number of the preconditioned systems is uniformly bounded with respect to coefficients and mesh.

We also discussed compatible discretization for the H^1, $\mathbf{H}(\mathbf{curl})$ and $\mathbf{H}(\mathrm{div})$ systems. In the light of this general framework, we developed some AMG preconditioners for solving $\mathbf{H}(\mathbf{curl})$ and $\mathbf{H}(\mathrm{div})$ systems. First of all, we reformulated the discrete $\mathbf{H}(\mathbf{curl})$ and $\mathbf{H}(\mathrm{div})$ systems into 2×2 systems, which are equivalent to the original discrete linear system. Then we defined special prolongators to transfer the $(1,1)$ and $(2,2)$ blocks to matrices associated with the standard nodal space. Therefore, these matrices are amenable to some standard AMG solvers for H^1 equations. Numerical experiments showed that the algorithm is very robust even with the presence of large jump coefficients. As an application of the proposed $\mathbf{H}(\mathrm{div})$ solvers, we used the augmented Lagrangian technique to reduce the mixed finite element method to a nearly singular $\mathbf{H}(\mathrm{div})$ system, and solved it by this approach. Numerical experiments also show the efficiency and robustness of the algorithms.

Future Works There are still many open problems that are worthwhile to be studied, both analytically and computationally, in the future. First of all, the analysis in this

dissertation is carried out under the assumption that the finite element grid is quasi-uniform. In practice, a locally adaptive grid may be needed in order to better capture the singularity caused by the discontinuity in the coefficients in the model problems considered in this dissertation, and may also be needed to reduce the overall computation cost. We aim to extend these results to certain locally refined grids obtained by newest bisections in the future. For elliptic equations with discontinuous coefficients, we plan to extend our results to more general cases, such as more general distributed coefficients, and the tensor coefficients case (i.e., anisotropic problems). We are also interested in designing some special multilevel algorithms which converge uniformly for the equations with strongly discontinuous coefficients. For $\mathbf{H}(\mathbf{curl})$ and $\mathbf{H}(\mathrm{div})$ systems, according to numerical experiments, the auxiliary space preconditioners are very robust with respect to the jump coefficients. In some simple cases, this dissertation gave premier results. Based on the results for elliptic equations, we intend to analyze the multilevel methods for $\mathbf{H}(\mathbf{curl})$ and $\mathbf{H}(\mathrm{div})$ systems with more general discontinuous coefficients cases. Also, we would like to combine the adaptivity with the multilevel preconditioners in designing and analyzing the efficient solvers for $\mathbf{H}(\mathbf{curl})$ and $\mathbf{H}(\mathrm{div})$ systems with discontinuous coefficients.

References

[1] R. E. Alcouffe, A. Brandt, J. E. Dendy, and J. W. Painter. The multi-grid methods for the diffusion equation with strongly discontinuous coefficients. *SIAM J. Sci. Statist. Comput.*, 2:430–454, 1981.

[2] A. Alonso and A. Valli. Some remarks on the characterization of the space of tangential traces of $h(rot;\omega)$ and the construction of an extension operator. *manuscripta mathematica*, 89(1):159–178, Dec. 1996.

[3] C. Amrouche, C. Bernardi, M. Dauge, and V. Girault. Vector potentials in three-dimensional non-smooth domains. *Mathematical Methods in the Applied Sciences Math. Meth. Appl. Sci.*, 21(21):823–864, 1998.

[4] D. N. Arnold, R. S. Falk, and R. Winther. Preconditioning in $H(div)$ and applications. *Mathemathics of Computation*, 66:957–984, 1997.

[5] D. N. Arnold, R. S. Falk, and R. Winther. Multigrid in $H(\mathrm{div})$ and $H(\mathrm{curl})$. *Numer. Math.*, 85(85):197C217, 2000.

[6] D. N. Arnold, R. S. Falk, and R. Winther. Multigrid in $H(\mathrm{div})$ and $H(\mathrm{curl})$. *Numer. Math.*, 85(85):197217, 2000.

[7] D. N. Arnold, R. S. Falk, and R. Winther. Finite elment exterior calculus, homological techniques, and applications. *Acta Numerica*, pages 1–155, 2006.

[8] D. N. Arnold, L. R. Scott, and M. Vogelius. Regular inversion of the divergence operator with Dirichlet boundary conditions on a polygon. *Ann. Scuola Norm. Sup. Pisa Cl. Sci. (4)*, 15(2):169–192 (1989), 1988.

[9] O. Axelsson. *Iterative solution methods.* Cambridge University Press, Cambridge, 1994.

[10] O. Axelsson. Iteration number for the conjugate gradient method. *Math. Comput. Simulation*, 61(3-6):421–435, 2003. MODELLING 2001 (Pilsen).

[11] R. Beck. Algebraic multigrid by component splitting for edge elements on simplicial triangulations. Technical Report SC 99-40, ZIB, Berlin, Germany, 1999.

[12] M. S. Birman and M. Z. Solomyak. L^2-theory of the Maxwell operator in arbitrary domains. *Russian Mathematical Surveys*, 42(6):75–96, 1987.

[13] P. Bochev, C. Garasi, J. Hu, A. Robinson, and R. Tuminaro. An improved algebraic multigrid method for solving Maxwell's equations. *SIAM J. Sci. Computing*, 25, 2003.

[14] P. Bochev and J. Hyman. Principles of mimetic discretizations of differential operators. In D. Arnold, P. Bochev, R. Lehoucq, R. Nicolaides, and M. Shashkov, editors, *Compatible Spatial Discretizations*. Springer-Verlag, 2006.

[15] P. Bochev and A. Robinson. Matching algorithms with physics: exact sequences of finite element spaces. In D. Estep and S. Tavener, editors, *Preservation of stability under discretization*, pages 145–165, Philadelphia, 2001. SIAM.

[16] P. B. Bochev, J. J. Hu, C. M. Siefert, and R. S. Tuminaro. An algebraic multigrid approach based on a compatible gauge reformulation of Maxwell's equations. Technical Report SAND2007-1633J, Sandia National Laboratory, 2007.

[17] P. B. Bochev and J. M. Hyman. Principles of mimetic discretizations of differential operators. In *Compatible spatial discretizations*, volume 142 of *IMA Vol. Math. Appl.*, pages 89–119. Springer, New York, 2006.

[18] A. Bossavit. Whitney forms: a class of finite elements for three-dimensional computations in electromagnetism. *Science, Measurement and Technology, IEE Proceedings*, 135(8):493–500, Nov 1988.

[19] A. Bossavit. *Computational electromagnetism*. Electromagnetism. Academic Press Inc., San Diego, CA, 1998. Variational formulations, complementarity, edge elements.

[20] A. Bossavit. Mixed-hybrid methods in magnetostatics: complementarity in one stroke. *Magnetics, IEEE Transactions on*, 39(3):1099 –1102, May 2003.

[21] D. Braess. On the combination of the multigrid method and conjugate gradients. In *Multigrid methods, II (Cologne, 1985)*, volume 1228 of *Lecture Notes in Math.*, pages 52–64. Springer, Berlin, 1986.

[22] J. H. Bramble. *Multigrid Methods*, volume 294 of *Pitman Research Notes in Mathematical Sciences*. Longman Scientific & Technical, Essex, England, 1993.

[23] J. H. Bramble, J. E. Pasciak, and A. H. Schatz. The construction of preconditioners for elliptic problems by substructuring. III. *Math. Comp.*, 51(184):415–430, 1988.

[24] J. H. Bramble, J. E. Pasciak, and A. H. Schatz. The construction of preconditioners for elliptic problems by substructuring. IV. *Math. Comp.*, 53(187):1–24, 1989.

[25] J. H. Bramble, J. E. Pasciak, J. Wang, and J. Xu. Convergence estimates for multigrid algorithms without regularity assumption. *Mahtematics of Computation*, 57(195):23–45, 1991.

[26] J. H. Bramble, J. E. Pasciak, and J. Xu. Parallel multilevel preconditioners. *Mathematics of Computation*, 55(191):1–22, 1990.

[27] J. H. Bramble and J. Xu. Some estimates for a weighted L^2 projection. *Mathematics of Computation*, 56(194):463–476, 1991.

[28] S. C. Brenner and L. R. Scott. *The mathematical theory of finite element methods*, volume 15 of *Texts in Applied Mathematics*. Springer-Verlag, New York, second edition, 2002.

[29] M. Brezina, R. Falgout, S. MacLachlan, T. Manteuffel, S. McCormick, and J. Ruge. Adaptive smoothed aggregation (αSA). *SIAM J. Sci. Comp.*, 25(6):1896–1920, 2004.

[30] F. Brezzi, J. Douglas, Jr., and L. D. Marini. Two families of mixed finite elements for second order elliptic problems. *Numer. Math.*, 47(2):217–235, 1985.

[31] F. Brezzi and M. Fortin. *Mixed and hybrid finite element methods*, volume 15 of *Springer Series in Computational Mathematics*. Springer-Verlag, New York, 1991.

[32] F. Brezzi, J. J. Douglas, R. Durán, and M. Fortin. Mixed finite elements for second order elliptic problems in three variables. *Numer. Math.*, 51(2):237–250, 1987.

[33] W. Briggs, V. Henson, and S. McCormick. *A Multigrid Tutorial*. SIAM Books, Philadelphia, 2000. Second edition.

[34] Z. Q. Cai, C. I. Goldstein, and J. E. Pasciak. Multilevel iteration for mixed finite element systems with penalty. *SIAM J. Sci. Comput.*, 14(5):1072–1088, 1993.

[35] S. Cairns. *Introductory topology*. Ronald Press Co., New York, 1961.

[36] J. M. Cascon, R. H. Nochetto, and K. G. Siebert. Design and convergence of AFEM in $H(\mathrm{div})$. *Mathematical Models and Methods in Applied Sciences*, 17(11):1849C1881, 2007.

[37] T. Chan and W. Wan. Robust multigrid methods for nonsmooth coefficient elliptic linear systems. *J. Comput. Appl. Math.*, 123:323–352, 2000.

[38] T. F. Chan and T. P. Mathew. Domain decomposition algorithms. *Acta Numerica*, 3:61–143, 1994.

[39] Z. Chen, L. Wang, and W. Zheng. An adaptive multilevel method for time-harmonic Maxwell equations with singularities. *SIAM Journal on Scientific Computing*, 29(1):118–138, 2007.

[40] S. Cho, S. V. Nepomnyaschikh, and E.-J. Park. Domain decomposition preconditioning for elliptic problems with jumps in coefficients. Technical Report rep05-22, Radon Institute for Computational and Applied Mathematics (RICAM), 2005.

[41] P. G. Ciarlet. *The finite element method for elliptic problems*, volume 4 of *Studies in Mathematics and its Applications*. North-Holland Publishing Co., Amsterdam-New York-Oxford, 1978.

[42] R. K. Coomer and I. G. Graham. Massively parallel methods for semiconductor device modelling. *Computing*, 56(1):1–27, 1996.

[43] A. Dezin. *Multidimensional analysis and discrete models*. CRC Press, Boca Raton, 1995.

[44] A.-S. B.-B. Dhia, C. Hazard, and S. Lohrengel. A singular field method for the solution of Maxwell's equations in polyhedral domains. *SIAM Journal on Applied Mathematics*, 59(6):2028–2044, 1999.

[45] M. Dryja, M. V. Sarkis, and O. B. Widlund. Multilevel Schwarz methods for elliptic problems with discontinuous coefficients in three dimensions. *Numerische Mathematik*, 72(3):313–348, 1996.

[46] M. Dryja, B. F. Smith, and O. B. Widlund. Schwarz analysis of iterative substructuring algorithms for elliptic problems in three dimensions. *SIAM J. Numer. Anal.*, 31(6):1662–1694, 1994.

[47] M. Dryja and O. B. Widlund. Schwarz methods of neumann-neumann type for three-dimensional elliptic finite element problems. *Communications on Pure and Applied Mathematics*, 48(2):121–155, 1995.

[48] R. E. Ewing and J. Wang. Analysis of mixed finite element methods on locally refined grids. *Numer. Math*, 63:183–194, 1992.

[49] R. E. Ewing and J. Wang. Analysis of multilevel decomposition iterative methods for mixed finite element methods. *M2AN*, 28(4):377–398, 1994.

[50] R. D. Falgout and U. M. Yang. hypre: A library of high performance preconditioners. In *International Conference on Computational Science (3)*, pages 632–641, 2002.

[51] M. Fortin and R. Glowinski. *Augmented Lagrangian methods*, volume 15 of *Studies in Mathematics and its Applications*. North-Holland Publishing Co., Amsterdam, 1983. Applications to the numerical solution of boundary value problems, Translated from the French by B. Hunt and D. C. Spicer.

[52] M. Gee, C. Siefert, J. Hu, R. Tuminaro, and M. Sala. ML 5.0 smoothed aggregation user's guide. Technical Report SAND2006-2649, Sandia National Laboratories, 2006.

[53] V. Girault and P.-A. Raviart. *Finite element methods for Navier-Stokes equations*, volume 5 of *Springer Series in Computational Mathematics*. Springer-Verlag, Berlin, 1986. Theory and algorithms.

[54] G. H. Golub and C. F. Van Loan. *Matrix computations*. Johns Hopkins Studies in the Mathematical Sciences. Johns Hopkins University Press, Baltimore, MD, third edition, 1996.

[55] I. G. Graham and M. J. Hagger. Unstructured additive schwarz-conjugate gradient method for elliptic problems with highly discontinuous coefficients. *SIAM J. SCI. Comput.*, 20:2041–2066, 1999.

[56] W. Hackbusch. *Multigrid Methods and Applications*. Springer–Verlag, Berlin, 1985.

[57] W. Hackbusch. *Iterative solution of large sparse systems of equations*, volume 95 of *Applied Mathematical Sciences*. Springer-Verlag, New York, 1994. Translated and revised from the 1991 German original.

[58] B. Heise and M. Kuhn. Parallel solvers for linear and nonlinear exterior magnetic field problems based upon coupled FE/BE formulations. *Computing*, 56(3):237–258, 1996. International GAMM-Workshop on Multi-level Methods (Meisdorf, 1994).

[59] V. E. Henson and U. M. Yang. BoomerAMG: A parallel algebraic multigrid solver and preconditioner. *Applied Numerical Mathematics*, 41(1):155–177, Apr. 2002.

[60] R. Hiptmair. *Multilevel Preconditioning for Mixed Problems in Three Dimensions*. PhD thesis, Universität Augsburg, 1996.

[61] R. Hiptmair. Multigrid method for $\mathbf{H}(\mathrm{div})$ in three dimensions. *Electron. Trans. Numer. Anal.*, 6(Dec.):133–152, 1997. Special issue on multilevel methods (Copper Mountain, CO, 1997).

[62] R. Hiptmair. Multigrid method for Maxwell's equations. *SIAM Journal on Numerical Analysis*, 36(1):204–225, 1998.

[63] R. Hiptmair. Canonical construction of finite elements. *Math. Comp.*, 68:1325–1346, 1999.

[64] R. Hiptmair. Finite elements in computational electromagnetism. *Acta Numerica*, pages 237–339, 2002.

[65] R. Hiptmair. Analysis of multilevel methods for eddy current problems. *Math. Comp.*, 72(243):1281–1303 (electronic), 2003.

[66] R. Hiptmair and A. Toselli. Overlapping and multilevel Schwarz methods for vector valued elliptic problems in three dimensions. *IMA Volumes in Mathematics and its Applications*, 2000.

[67] R. Hiptmair, G. Widmer, and J. Zou. Auxiliary space preconditioning in $H_0(\mathrm{curl};\ \Omega)$. *Numer. Math.*, 103(3):435–459, 2006.

[68] R. Hiptmair and J. Xu. Nodal auxiliary space preconditioning in $H(\mathrm{curl})$ and $H(\mathrm{div})$ spaces. *SIAM Journal on Numerical Analysis*, 45(6):2483–2509, 2007.

[69] R. Hiptmair and W. Zheng. Local multigrid in $H(\mathrm{curl})$. Technical report, Seminar für Angewandte Mathematik, Eidgenössische Technische Hochschule CH-8092 Zürich, Switzerland, 2007.

[70] V. Howle and S. Vavasis. Preconditioning complex-symmetric layered systems arising in electric power modeling. In T. A. Manteuffel and S. F. McCormick, editors, *Fifth Copper Mountain Conference on Iterative Methods, Copper Mountain, Colorado*, 1998.

[71] Q. Hu and J. Zou. A weighted helmholtz decomposition and application to domain decomposition for saddle-point Maxwell systems. Technical Report 2007-15 (355), CUHK, 2007.

[72] J. Hyman and M. Shashkov. Natural discretizations for the divergence, gradient and curl on logically rectangular grids. *Comput. Math. Appl.*, 33:88–104, 1997.

[73] A. Jüngel, M. C. Mariani, and D. Rial. Local existence of solutions to the transsient quantum hydrodynamic equations. *Mathematical Models and Methods in Applied Sciences*, 12:485–495, 2002.

[74] C. E. Kees, C. T. Miller, E. W. Jenkins, and C. T. Kelley. Versatile two-level Schwarz preconditioners for multiphase flow. *Comput. Geosci.*, 7(2):91–114, 2003.

[75] C. T. Kelley. *Iterative methods for linear and nonlinear equations*, volume 16 of *Frontiers in Applied Mathematics*. Society for Industrial and Applied Mathematics (SIAM), Philadelphia, PA, 1995. With separately available software.

[76] R. Kettler. Analysis and comparison of relaxation schemes in robust multigrid and preconditioned conjugate gradient methods. In *Multigrid methods (Cologne, 1981)*, volume 960 of *Lecture Notes in Math.*, pages 502–534. Springer, Berlin, 1982.

[77] T. Kolev and P. Vassilevski. Some experience with a H^1-based auxiliary space AMG for $H(\mathrm{curl})$ problems. Technical Report 221841, LLNL, 2006.

[78] T. V. Kolev, J. E. Pasciak, and P. S. Vassilevski. $H(\mathrm{curl})$ auxiliary mesh preconditioning. *Numerical Linear Algebra with Applications*, 15(5):455–471, 2008.

[79] T. V. Kolev and P. S. Vassilevski. Parallel H^1-based auxiliary space AMG solver for $H(\mathrm{curl})$ problems. Technical Report UCRL-TR-222763, Lawrence Livermore National Laboratory, July 2006.

[80] P. Le Tallec. Domain decomposition methods in computational mechanics. *Comput. Mech. Adv.*, 1(2):121–220, 1994.

[81] Y.-J. Lee, J. Wu, J. Xu, and L. Zikatanov. Robust subspace correction methods for nearly singular systems. *M3AS*, 17(11):1937–1963, 2007.

[82] B. Liang and K. Zhang. Steady-state solutions and asymptotic limits on the multidimensional semiconductor quantum hydrodynamic model. *Mathematical Models and Methods in Applied Sciences*, 17(2):253–275, 2007.

[83] J. Mandel and M. Brezina. Balancing domain decomposition for problems with large jumps in coefficients. *Math. Comp.*, 65(216):1387–1401, 1996.

[84] J. C. Meza and R. S. Tuminaro. A multigrid preconditioner for the semiconductor equations. *SIAM Journal on Scientific Computing*, 17(1):118–132, 1996.

[85] P. Monk. *Finite element methods for Maxwell's equations*. Numerical Mathematics and Scientific Computation. Oxford University Press, New York, 2003.

[86] J.-C. Nédélec. Mixed finite elements in $\mathbf{R}^3$. *Numer. Math.*, 35(3):315–341, 1980.

[87] J.-C. Nédélec. A new family of mixed finite elements in $\mathbf{R}^3$. *Numer. Math.*, 50(1):57–81, 1986.

[88] S. V. Nepomnyaschikh. Decomposition and fictitious domains methods for elliptic boundary value problems. In *Fifth International Symposium on Domain Decomposition Methods for Partial Differential Equations (Norfolk, VA, 1991)*, pages 62–72. SIAM, Philadelphia, PA, 1992.

[89] S. V. Nepomnyaschikh. Preconditioning operators for elliptic problems with bad parameters. In *Eleventh International Conference on Domain Decomposition Methods (London, 1998)*, pages 82–88 (electronic). DDM.org, Augsburg, 1999.

[90] R. Nicolaides. Direct discretization of planar div-curl problems. *SIAM J. Numer. Anal.*, 29(1):32–56, 1992.

[91] J. Nocedal and S. J. Wright. *Numerical optimization*. Springer Series in Operations Research and Financial Engineering. Springer, New York, second edition, 2006.

[92] P. Oswald. *Multilevel Finite Element Approximation, Theory and Applications*. Teubner Skripten zur Numerik. Teubner Verlag, Stuttgart, 1994.

[93] P. Oswald. On the robustness of the BPX-preconditioner with respect to jumps in the coefficients. *Mathematics of Computation*, 68:633–650, 1999.

[94] J. E. Pasciak and J. Zhao. Overlapping Schwarz methods in $H(\mathrm{curl})$ on polyhedral domains. *J. Numer. Math.*, 10(3):221–234, 2002.

[95] P.-A. Raviart and J. M. Thomas. A mixed finite element method for 2nd order elliptic problems. In *Mathematical aspects of finite element methods (Proc. Conf., Consiglio Naz. delle Ricerche (C.N.R.), Rome, 1975)*, pages 292–315. Lecture Notes in Math., Vol. 606. Springer, Berlin, 1977.

[96] S. Reitzinger and J. Schöberl. An algebraic multigrid method for finite element discretizations with edge elements. *Numerical Linear Algebra with Applications*, 9(3):223–238, 2002.

[97] Y. Saad. *Iterative methods for sparse linear systems*. Society for Industrial and Applied Mathematics, Philadelphia, PA, second edition, 2003.

[98] R. Scott and S. Zhang. Finite element interpolation of nonsmooth functions satisfying boundary conditions. *Mathematics of Computation*, 54:483–493, 1990.

[99] M. Shashkov. *Conservative finite difference methods on general grids*. CRC Press, Boca Raton, FL, 1996.

[100] B. F. Smith. A domain decomposition algorithm for elliptic problems in three dimensions. *Numer. Math.*, 60(2):219–234, 1991.

[101] B. F. Smith, P. E. Bjørstad, and W. D. Gropp. *Domain decomposition*. Cambridge University Press, Cambridge, 1996. Parallel multilevel methods for elliptic partial differential equations.

[102] O. Tatebe. *MGCG method: a robust and highly parallel iterative method*. PhD thesis, the University of Tokyo, 1996.

[103] O. Tatebe and Y. Oyanagi. Efficient implementation of the multigrid preconditioned conjugate gradient method on distributed memory machines. In *Supercomputing*, pages 194–203, 1994.

[104] A. Toselli and O. Widlund. *Domain decomposition methods—algorithms and theory*, volume 34 of *Springer Series in Computational Mathematics*. Springer-Verlag, Berlin, 2005.

[105] J. van Welij. Calculation of eddy currents in terms of H on hexahedra. *IEEE Transactions on Magnetics*, 21(6):2239–2241, 1985.

[106] P. Vaněk, M. Brezina, and J. Mandel. Convergence of algebraic multigrid based on smoothed aggregation. *Numerische Mathematik*, 88(3):559–579, May 2001.

[107] P. Vaněk, J. Mandel, and M. Brezina. Algebraic multigrid by smoothed aggregation for second and fourth order elliptic problems. *Computing*, 56(3):179–196, Sept. 1996.

[108] P. S. Vassilevski and R. D. Lazarov. Preconditioning mixed finite element saddle-point elliptic problems. *Numerical Linear Algebra with Applications*, 3(1):1–20, 1996.

[109] P. S. Vassilevski and J. Wang. Multilevel iterative methods for mixed finite element discretizations of elliptic problems. *Numerische Mathematik*, 63(1):503–520, 1992.

[110] C. Vuik, A. Segal, and J. A. Meijerink. An efficient preconditioned cg method for the solution of a class of layered problems with extreme contrasts in the coefficients. *Journal of Computational Physics*, 152(1):385–403, June 1999.

[111] C. Wang. Fundamental models for fuel cell engineering. *an invited review article for Chemical Reviews*, 104:4727–4766, 2004.

[112] J. Wang. New convergence estimates for multilevel algorithms for finite-element approximations. *Journal of Computational and Applied Mathematics*, 50(1-3):593–604, May 1994.

[113] J. Wang and R. Xie. Domain decomposition for elliptic problems with large jumps in coefficients. In *the Proceedings of Conference on Scientific and Engineering Computing*, pages 74–86. National Defense Industry Press, Beijing, China, 1994.

[114] Z. Wang, C. Wang, and K. Chen. Two phase flow and transport in the air cathode of proton exchange membrane fuel cells. *J.Power Sources*, 94:40–50, 2001.

[115] O. B. Widlund. Some Schwarz methods for symmetric and nonsymmetric elliptic problems. In D. E. Keyes, T. F. Chan, G. A. Meurant, J. S. Scroggs, and R. G. Voigt, editors, *Fifth International Symposium on Domain Decomposition Methods for Partial Differential Equations*, pages 19–36, Philadelphia, 1992. SIAM.

[116] B. I. Wohlmuth, A. Toselli, and O. B. Widlund. An iterative substructuring method for Raviart–Thomas vector fields in three dimensions. *SIAM Journal on Numerical Analysis*, 37(5):1657–1676, 2000.

[117] J. Xu. *Theory of Multilevel Methods.* PhD thesis, Cornell University, 1989.

[118] J. Xu. Counter examples concerning a weighted L^2 projection. *Mathematics of Computation*, 57:563–568, 1991.

[119] J. Xu. Iterative methods by space decomposition and subspace correction. *SIAM Review*, 34:581–613, 1992.

[120] J. Xu. A new class of iterative methods for nonselfadjoint or indefinite problems. *SIAM Journal on Numerical Analysis*, 29:303–319, 1992.

[121] J. Xu. The auxiliary space method and optimal multigrid preconditioning techniques for unstructured grids. *Computing*, 56(3):215–235, Sept. 1996.

[122] J. Xu. An introduction to multigrid convergence theory. In R. Chan, T. Chan, and G. Golub, editors, *Iterative Methods in Scientific Computing.* Springer-Verlag, 1997.

[123] J. Xu. Multilevel finite element theory. Lecture Notes, Penn. State University, 2003.

[124] J. Xu and Y. Zhu. Uniform convergent multigrid methods for elliptic problems with strongly discontinuous coefficients. *M3AS*, 18(1):77–105, January 2008.

[125] J. Xu and L. Zikatanov. The method of alternating projections and the method of subspace corrections in Hilbert space. *Journal of The American Mathematical Society*, 15:573–597, 2002.

[126] J. Xu and J. Zou. Some nonoverlapping domain decomposition methods. *SIAM Rev.*, 40(4):857–914 (electronic), 1998.

[127] H. Yserentant. Hierarchical bases give conjugate gradient type methods a multigrid speed of convergence. *Applied Mathematics and Computation*, 19(1-4):347–358, July 1986.

[128] H. Yserentant. Two preconditioners based on the multi-level splitting of finite element spaces. *Numer. Math.*, 58(2):163–184, 1990.

[129] X. Zhang. Multilevel schwarz methods. *Numerische Mathematik*, 63(1):521–539, Dec. 1992.

[130] Y. Zhu. Domain decomposition preconditioners for elliptic equations with jump coefficients. *Numerical Linear Algebra with Applications*, 15:271–289, 2008.

[131] L. T. Zikatanov. Two-sided bounds on the convergence rate of two-level methods. *Numerical Linear Algebra with Applications*, 15(5):439–454, 2008.

Vita

Yunrong Zhu was born on December 16th, 1978 in Yongkang, Zhejiang Province, P. R. China. He received his B.S. in 2000 and M.S. degree in 2003, in mathematics from Southeast University (Nanjing, China). He enrolled in the Ph.D. program in mathematics at the Pennsylvania State University in Fall 2003.